July 2007
Research Report: UCPRC-RR-2007-05

Reflective Cracking Study: HVS Test Section Forensic Investigation

Authors:
D. Jones, B. Steven, and J. Harvey

Partnered Pavement Research Program (PPRC) Contract Strategic Plan Element 4.10:
Development of Improved Rehabilitation Designs for Reflective Cracking

PREPARED FOR:

California Department of Transportation
Division of Research and Innovation
Office of Roadway Research

PREPARED BY:

University of California
Pavement Research Center
UC Davis, UC Berkeley

DOCUMENT RETRIEVAL PAGE		**Research Report: UCPRC-RR-2007-05**
Title: Reflective Cracking Study: HVS Test Section Forensic Investigation		
Authors: D. Jones, B. Steven and J. Harvey		
Prepared for: Caltrans	**FHWA No:** CA091073I	**Date**: July 2007
Contract No: 65A0172	**Client Reference No:** SPE 4.10	**Status:** Stage 6, Approved Version

Abstract:
This report is one in a series of first-level analysis reports that describe the results of HVS testing on a full-scale experiment being performed at the Richmond Field Station (RFS) to validate Caltrans overlay strategies for the rehabilitation of cracked asphalt concrete. It describes the results of the forensic investigation on the HVS rutting sections (Sections 580RF through 581RF) and HVS reflective cracking testing sections (Sections 586RF through 591RF). The study forms part of Partnered Pavement Research Center Strategic Plan Element 4.10: "Development of Improved Rehabilitation Designs for Reflective Cracking."

Findings and observations based on the data collected during this forensic investigation include:

- There was considerable variation in the thicknesses of the constructed layers of the test road.
- In the rutting experiments, rutting occurred primarily in the underlying DGAC and not in the overlay. In the reflective cracking experiments, rutting occurred in both layers. Very little rutting occurred in the underlying layers.
- Cracks were observed on some of the test pit profiles. In the underlying DGAC layer, cracks were generally clearly visible. However, in the overlays, heat generated from the saw cut operation appeared to seal any cracks and no conclusions could be drawn as to the depth that cracks had reflected into the overlays. Most cracks appeared to have initiated close to the bottom of the underlying DGAC. Some crack initiation was also observed at poorly bonded joints between lifts and overlays in the AR4000-D section.
- Some post-construction cementation of the base material appeared to have occurred. This was substantiated with DCP tests, close inspection of the test pit profile, use of phenolphthalein to determine the pH of the base material, and examination of specimens under optical and scanning electron microscopes. This recementation appears to have contributed to the good performance of the sections.
- Base material density was generally consistent over the section. Nuclear gauge determined wet densities averaged 2,176 kg/m^3, which corresponds with the average of 2,200 kg/m^3 recorded after construction.
- Nuclear gauge-determined base moisture contents averaged 11.1 percent for the 18 test pits, with higher moisture contents in the top 50 mm compared to the remainder of the layer. This is higher than the predetermined optimum (8.9 percent) and the laboratory-determined gravimetric moisture contents (8.7 percent).
- Subgrade densities were not measured. The average subgrade moisture content was 15 percent, considerably higher than the base moisture content. The presence of mottling in the subgrade material indicates that the moisture content probably fluctuated seasonally.
- Air-void contents were lower in the wheelpath after HVS testing compared to before HVS testing, as expected.

The findings of this investigation confirm the conclusions of the other first-level analysis reports on HVS testing. No recommendations as to the use of modified binders in overlay mixes are made at this time.

Keywords:
Reflective cracking, overlay, modified binder, HVS test, MB Road, forensic investigation

Related documents:
UCPRC-RR-2005-03, RR-2006-04, RR-2006-05, RR-2006-06, RR-2006-07, RR-2006-12, RR-2007-04, RR-2007-06

Signatures:

D. Jones 1st Author	J Harvey Technical Review	D. Spinner Editor	J. Harvey Principal Investigator	M Samadian Caltrans Contract Manager

DISCLAIMER

PROJECT OBJECTIVES

The objective of this project is to develop improved rehabilitation designs for reflective cracking for California.

This objective will be met after completion of four tasks identified by the Caltrans/Industry Rubber Asphalt Concrete Task Group (RACTG):

1. Develop improved mechanistic models of reflective cracking in California.
2. Calibrate and verify these models using laboratory and HVS testing.
3. Evaluate the most effective strategies for reflective cracking.
4. Provide recommendations for reflective cracking strategies.

This document is one of a series addressing Tasks 2 and 3.

ACKNOWLEDGEMENTS

The University of California Pavement Research Center acknowledges the assistance of the Rubber Pavements Association, Valero Energy Corporation, and Paramount Petroleum which contributed funds and asphalt binders for the construction of the Heavy Vehicle Simulator test track discussed in this study.

REFLECTIVE CRACKING STUDY REPORTS

The reports prepared during the reflective cracking study document data from construction, Heavy Vehicle Simulator (HVS) tests, laboratory tests, and subsequent analyses. These include a series of first- and second-level analysis reports and two summary reports. On completion of the study this suite of documents will include:

1. Reflective Cracking Study: Summary of Construction Activities, Phase 1 HVS Testing and Overlay Construction (UCPRC-RR-2005-03)
2. Reflective Cracking Study: First-level Report on the HVS Rutting Experiment (UCPRC-RR-2007-06)
3. Reflective Cracking Study: First-level Report on HVS Testing on Section 590RF — 90 mm MB4-G Overlay (UCPRC-RR-2006-04)
4. Reflective Cracking Study: First-level Report on HVS Testing on Section 589RF — 45 mm MB4-G Overlay (UCPRC-RR-2006-05)
5. Reflective Cracking Study: First-level Report on HVS Testing on Section 587RF — 45 mm RAC-G Overlay (UCPRC-RR-2006-06)
6. Reflective Cracking Study: First-level Report on HVS Testing on Section 588RF — 90 mm AR4000-D Overlay (UCPRC-RR-2006-07)
7. Reflective Cracking Study: First-level Report on HVS Testing on Section 586RF — 45 mm MB15-G Overlay (UCPRC-RR-2006-12)
8. Reflective Cracking Study: First-level Report on HVS Testing on Section 591RF — 45 mm MAC15TR-G Overlay (UCPRC-RR-2007-04)
9. Reflective Cracking Study: HVS Test Section Forensic Report (UCPRC-RR-2007-05)
10. Reflective Cracking Study: First-level Report on Laboratory Fatigue Testing (UCPRC-RR-2006-08)
11. Reflective Cracking Study: First-level Report on Laboratory Shear Testing (UCPRC-RR-2006-11)
12. Reflective Cracking Study: Backcalculation of FWD Data from HVS Test Sections (UCPRC-RR-2007-08)
13. Reflective Cracking Study: Second-level Analysis Report (UCPRC-RR-2007-09)
14. Reflective Cracking Study: Summary Report (UCPRC-SR-2007-01): Detailed summary report.
15. Reflective Cracking Study: Summary Report (UCPRC-SR-2007-03): Four-page summary report.

CONVERSION FACTORS

SI* (MODERN METRIC) CONVERSION FACTORS				
APPROXIMATE CONVERSIONS TO SI UNITS				
Symbol	**Convert From**	**Multiply By**	**Convert To**	**Symbol**
LENGTH				
in	inches	25.4	millimeters	mm
ft	feet	0.305	meters	m
AREA				
in^2	square inches	645.2	square millimeters	mm^2
ft^2	square feet	0.093	square meters	m2
VOLUME				
ft^3	cubic feet	0.028	cubic meters	m^3
MASS				
lb	pounds	0.454	kilograms	kg
TEMPERATURE (exact degrees)				
°F	Fahrenheit	5 (F-32)/9 or (F-32)/1.8	Celsius	C
FORCE and PRESSURE or STRESS				
lbf	poundforce	4.45	newtons	N
lbf/in^2	poundforce/square inch	6.89	kilopascals	kPa
APPROXIMATE CONVERSIONS FROM SI UNITS				
Symbol	**Convert From**	**Multiply By**	**Convert To**	**Symbol**
LENGTH				
mm	millimeters	0.039	inches	in
m	meters	3.28	feet	ft
AREA				
mm^2	square millimeters	0.0016	square inches	in^2
m^2	square meters	10.764	square feet	ft^2
VOLUME				
m^3	cubic meters	35.314	cubic feet	ft^3
MASS				
kg	kilograms	2.202	pounds	lb
TEMPERATURE (exact degrees)				
C	Celsius	1.8C+32	Fahrenheit	F
FORCE and PRESSURE or STRESS				
N	newtons	0.225	poundforce	lbf
kPa	kilopascals	0.145	poundforce/square inch	lbf/in^2

*SI is the symbol for the International System of Units. Appropriate rounding should be made to comply with Section 4 of ASTM E380. (Revised March 2003)

EXECUTIVE SUMMARY

This report is one in a series of first-level analysis reports that describe the results of HVS testing on a full-scale experiment being performed at the Richmond Field Station (RFS) to validate Caltrans overlay strategies for the rehabilitation of cracked asphalt concrete. It describes the forensic investigation of the HVS rutting and reflective cracking testing sections, designated 580RF through 591RF, carried out on various modified-binder overlays. The testing forms part of Partnered Pavement Research Center Strategic Plan Element 4.10: "Development of Improved Rehabilitation Designs for Reflective Cracking."

The objective of this project is to develop improved rehabilitation designs for reflective cracking for California. This objective will be met after completion of the following four tasks:

1. Develop improved mechanistic models of reflective cracking in California;
2. Calibrate and verify these models using laboratory and HVS testing;
3. Evaluate the most effective strategies for reflective cracking; and
4. Provide recommendations for reflective cracking strategies.

This report is one of a series addressing Tasks 2 and 3. It consists of three main chapters. Chapter 2 provides information on the experiment layout, pavement design, and HVS test details. Chapter 3 summarizes the forensic investigation procedure, observations and results. Chapter 4 provides a summary and lists key findings.

The underlying pavement was designed following standard Caltrans procedures and it incorporates a 410-mm (16.1 in) Class 2 aggregate base on subgrade with a 90-mm (3.5-in) dense-graded asphalt concrete (DGAC) surface. Design thickness was based on a subgrade R-value of 5 and a Traffic Index of 7 (~121,000 equivalent standard axles, or ESALs). This structure was trafficked with the HVS in 2003 to induce fatigue cracking (Phase 1 HVS testing) then was overlaid with six different treatments to assess their ability to limit reflective cracking. The treatments included:

- Half-thickness (45 mm) MB4 gap-graded overlay (referred to as "45 mm MB4-G" in this report)
- Full-thickness (90 mm) MB4 gap-graded overlay (referred to as "90 mm MB4-G" in this report)
- Half-thickness MB4 gap-graded overlay with minimum 15 percent recycled tire rubber (referred to as "MB15-G" in this report)
- Half-thickness MAC15TR gap-graded overlay with minimum 15 percent recycled tire rubber (referred to as "MAC15-G" in this report)
- Half-thickness rubberized asphalt concrete gap-graded overlay (RAC-G), included as a control for performance comparison purposes (the section discussed in this report)

- Full-thickness (90 mm) AR4000 dense-graded overlay (AR4000-D), included as a control for performance comparison purposes

The thickness for the AR4000-D overlay was determined according to Caltrans Test Method 356. The other overlay thicknesses were either the same or half of the AR4000-D overlay thickness. Details on construction and the first phase of trafficking are provided in an earlier report.

Laboratory fatigue and shear studies are being conducted in parallel with HVS testing. Results of these studies are detailed in separate first-level reports. Comparison of the laboratory and test section performance, including the results of this forensic investigation, will be discussed in a second-level report once all the data from all of the studies has been collected and analyzed.

HVS trafficking on the overlay sections (Phase 2 HVS testing) commenced on September 4, 2003 (Section 580RF), and was completed on June 25, 2007 (Section 591RF). During this period a total of more than 12 million load repetitions (varying from 2,000 repetitions on Section 580RF to 2.55 million on Section 591RF) at loads varying between 60 kN (13,500 lb) and 100 kN (22,500 lb) were applied across the sections, which equates to approximately 366 million ESALs, using the Caltrans conversion of $(\text{axle load}/18{,}000\text{lb})^{4.2}$. A temperature chamber was used to maintain the pavement temperature at 50°C±4°C (122°F±7°F) on the rutting sections, and at 20°C±4°C (68°F±7°F) for the first one million repetitions, then at 15°C±4°C (59°F±7°F) for the remainder of the test on the reflective cracking sections. A dual-tire configuration (720 kPa [104psi] pressure) was used for all experiments. On the rutting tests, channelized unidirectional loading was applied, while on the reflective cracking sections, bidirectional loading with lateral wander was used.

Findings and observations based on the data collected during this forensic investigation include:

- There was considerable variation in the thicknesses of the base, underlying DGAC, and the overlays over the length and width of the test road.
- In the rutting experiments (Sections 580RF through 585RF), rutting occurred primarily in the underlying DGAC and not in the overlay. On the reflective cracking experiments (Sections 586RF through 591RF), rutting occurred in both layers. Rutting from the Phase 1 trafficking was clearly visible on most test pit profiles. Very little rutting occurred in the base and no rutting was recorded in the subgrade. This corresponds to the Multi-Depth Deflectometer permanent deformation analyses discussed in the first-level reports on each section.
- Cracks were observed on some of the test pit profiles. In the underlying DGAC layer, cracks were generally clearly visible. However, in the overlays, heat generated from the saw cut

operation appeared to seal any cracks and no conclusions could be drawn as to the depth that cracks had reflected into the overlays. Most cracks appeared to have initiated close to the bottom of the underlying DGAC. Some crack initiation was also observed at poorly bonded joints between lifts and overlays in the AR4000-D section (Section 588RF). No additional information was gathered from an assessment of cores. No cracking was observed in the base.

- Some post-construction cementation of the base material appeared to have occurred. This was substantiated with Dynamic Cone Penetrometer (DCP) tests, close inspection of the test pit profile, the use of phenolphthalein to determine the pH of the base material, and examination of specimens under optical and scanning electron microscopes. This recementation appears to have contributed to the good performance of the sections.
- Densities were generally consistent throughout the section. Nuclear gauge determined wet densities averaged 2,176 kg/m^3 (standard deviation of 34 kg/m^3 [135.8 pcf, standard deviation of 2.1 pcf), which corresponds with the average wet density of 2,200 kg/m^3 (137.3 pcf) for the road base recorded after construction.
- Nuclear gauge determined moisture contents averaged 11.1 percent (standard deviation of 1.1 percent) for the eighteen test pits. In most test pits, the moisture content in the upper 50 mm (2 in) was on the order of one percent higher than in the material between 150 mm (6 in) and 200 mm (8 in). The optimum moisture content of the Class 2 aggregate base material, determined prior to construction, was 8.9 percent, somewhat lower than the average recorded with the nuclear gauge. Laboratory-determined gravimetric moisture contents averaged 8.7 percent, which was closer to the optimum moisture content.
- Subgrade densities were not measured. The average subgrade moisture content was 15 percent (lowest of 12.9 percent and highest of 18.0 percent), considerably higher than the base moisture content. The presence of mottling in the subgrade material indicates that the moisture content probably fluctuated seasonally.
- The air-void contents of cores removed from the wheelpaths in the reflective cracking sections after HVS testing were lower compared to those determined from cores removed from outside the sections prior to HVS testing, as expected.

The findings of this investigation confirm the conclusions drawn from analyses of data collected from the instrumentation during HVS testing and documented in the first-level analysis reports.

No recommendations as to the use of modified binders in overlay mixes are made at this time. These recommendations will be included in the second-level analysis report, which will be prepared and submitted on completion of all data analysis.

TABLE OF CONTENTS

LIST OF TABLES

LIST OF FIGURES

1. INTRODUCTION

1.1. Objectives

The first-level analysis presented in this report is part of Partnered Pavement Research Center Strategic Plan Element 4.10 (PPRC SPE 4.10) being undertaken for the California Department of Transportation (Caltrans) by the University of California Pavement Research Center (UCPRC). The objective of the study is to evaluate the reflective cracking performance of asphalt binder mixes used in overlays for rehabilitating cracked asphalt concrete pavements in California. The study includes mixes modified with rubber and polymers, and it will develop tests, analysis methods, and design procedures for mitigating reflective cracking in overlays. This work is part of a larger study on modified binder (MB) mixes being carried out under the guidance of the Caltrans Pavement Standards Team (PST) (1), which includes laboratory and accelerated pavement testing using the Heavy Vehicle Simulator (carried out by the UCPRC), and the construction and monitoring of field test sections (carried out by Caltrans).

1.2. Overall Project Organization

This UCPRC project is a comprehensive study, carried out in three phases, involving the following primary elements (2):

- Phase 1
  - The construction of a test pavement and subsequent overlays;
  - Six separate Heavy Vehicle Simulator (HVS) tests to crack the pavement structure;
  - Placing of six different overlays on the cracked pavement;
- Phase 2
  - Six HVS tests to assess the susceptibility of the overlays to high-temperature rutting (Phase 2a);
  - Six HVS tests to determine the low-temperature reflective cracking performance of the overlays (Phase 2b);
  - Laboratory shear and fatigue testing of the various hot-mix asphalts (Phase 2c);
  - Falling Weight Deflectometer (FWD) testing of the test pavement before and after construction and before and after each HVS test;
  - Forensic evaluation of each HVS test section;
- Phase 3
  - Performance modeling and simulation of the various mixes using models calibrated with data from the primary elements listed above.

Phase 1

In this phase, a conventional dense-graded asphalt concrete (DGAC) test pavement was constructed at the Richmond Field Station (RFS) in the summer of 2001. The pavement was divided into six cells, and within each cell a section of the pavement was trafficked with the HVS until the pavement failed by either fatigue (2.5 m/m^2 [0.76 ft/ft^2]) or rutting (12.5 mm [0.5 in]). This period of testing began in the summer of 2001 and was concluded in the spring of 2003. In June 2003 each test cell was overlaid with either conventional DGAC or asphalt concrete with modified binders as follows:

- Full-thickness (90 mm) AR4000-D dense-graded asphalt concrete overlay, included as a control for performance comparison purposes (AR-4000 is approximately equivalent to a PG64-16 performance grade binder);
- Full-thickness (90 mm) MB4-G gap-graded overlay;
- Half-thickness (45 mm) rubberized asphalt concrete gap-graded overlay (RAC-G), included as a control for performance comparison purposes;
- Half-thickness (45 mm) MB4-G gap-graded overlay;
- Half-thickness (45 mm) MB4-G gap-graded overlay with minimum 15 percent recycled tire rubber (MB15-G), and
- Half-thickness (45 mm) MAC15-G gap-graded overlay with minimum 15 percent recycled tire rubber.

The conventional overlay was designed using the current (2003) Caltrans overlay design process. The various modified overlays were either full (90 mm) or half thickness (45 mm). Mixes were designed by Caltrans. The overlays were constructed in one day.

Phase 2

Phase 2 included high-temperature rutting and low-temperature reflective cracking testing with the HVS as well as laboratory shear and fatigue testing. The rutting tests were started and completed in the fall of 2003. For these tests, the HVS was placed above a section of the underlying pavement that had not been trafficked during Phase 1. A reflective cracking test was next conducted on each overlay from the winter of 2003-2004 to the summer of 2007. For these tests, the HVS was positioned precisely on top of the sections of failed pavement from the Phase 1 HVS tests to investigate the extent and rate of crack propagation through the overlay.

In conjunction with Phase 2 HVS testing, a full suite of laboratory testing, including shear and fatigue testing, was carried out on field-mixed, field-compacted; field-mixed, laboratory-compacted; and laboratory-mixed, laboratory-compacted specimens.

Phase 3

Phase 3 entailed a second-level analysis carried out on completion of HVS and laboratory testing (the focus of this report). This included extensive analysis and characterization of the mix fatigue and mix shear data, backcalculation of the FWD data, performance modeling of each HVS test, and a detailed series of pavement simulations carried out using the combined data.

An overview of the project timeline is shown in Figure 1.1.

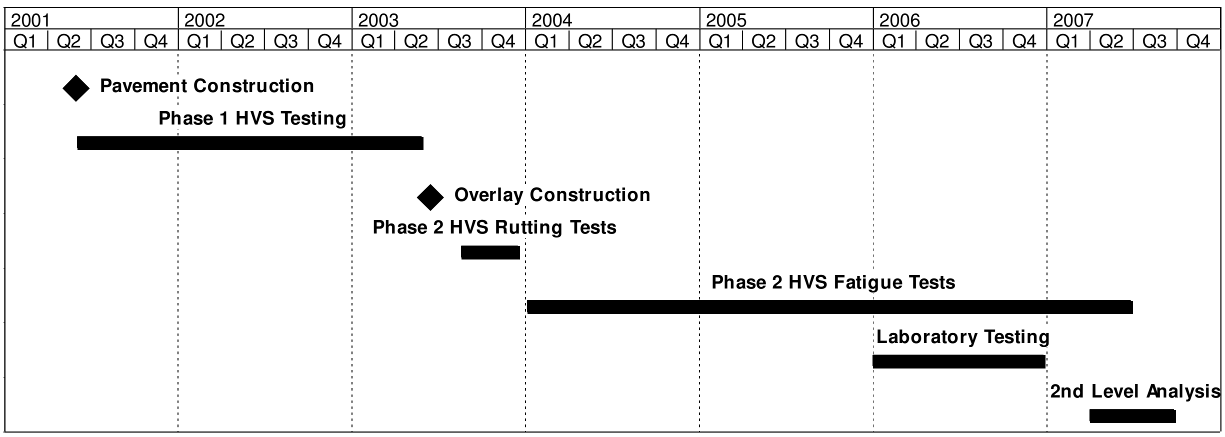

Figure 1.1: Timeline for the Reflective Cracking Study.

Reports

The reports prepared during the reflective cracking study document data from construction, HVS tests, laboratory tests, and subsequent analyses. These include a series of first- and second-level analysis reports and two summary reports. On completion of the study this suite of documents will include:

- One first-level report covering the initial pavement construction, the six initial HVS tests, and the overlay construction (Phase 1);
- One first-level report covering the six Phase 2 rutting tests (but offering no detailed explanations or conclusions on the performance of the pavements);
- Six first-level reports, each of which covers a single Phase 2 reflective cracking test (containing summaries and trends of the measured environmental conditions, pavement responses, and pavement performance but offering no detailed explanations or conclusions on the performance of the pavement);
- One first-level report covering laboratory shear testing;
- One first-level report covering laboratory fatigue testing;
- One report summarizing the HVS test section forensic investigation;
- One report summarizing the backcalculation analysis of deflection tests,

- One second-level analysis report detailing the characterization of shear and fatigue data, pavement modeling analysis, comparisons of the various overlays, and simulations using various scenarios (Phase 3), and
- One four-page summary report capturing the conclusions and one longer, more detailed summary report that covers the findings and conclusions from the research conducted by the UCPRC.

1.3. Structure and Content of This Report

This report presents the results of a forensic investigation on HVS test sections 580RF through 591RF and is organized as follows:

- Chapter 2 contains a description of the HVS test program.
- Chapter 3 presents a summary of the forensic investigation procedure and discussion of the observations and test results collected.
- Chapter 4 contains a summary of the results together with conclusions and observations.

A second-level analysis report will be prepared upon completion of all the testing and data analysis exercises and will include a comparison of the performance of the various sections and a comparison of those results with laboratory test data, as well as simulations with different climate, traffic and pavement structures.

1.4. Measurement Units

Metric units have always been used in the design and layout of HVS test tracks, and for all the measurements, data storage, analysis, and reporting at the eight HVS facilities worldwide (as well as all other international accelerated pavement testing facilities). Continued use of the metric system facilitates consistency in analysis, reporting, and data sharing.

In this report, metric and English units are provided in the Executive Summary, Chapters 1 and 2, and the Conclusion. In keeping with convention, only metric units are used in Chapter 3. A conversion table is provided on Page iv at the beginning of this report.

2. TEST DETAILS

2.1. Experiment Layout

Six overlays were constructed as part of the second phase of the study as follows, each with a rutting test section and a reflective cracking test section. These sections and the corresponding Phase 1 fatigue test sections are shown in Figure 2.1.

1. Sections 580RF and 586RF: Half-thickness (45 mm) MB4 gap-graded overlay with minimum 15 percent recycled tire rubber (referred to as "MB15-G" in this report);
2. Sections 581RF and 587RF: Half-thickness (45 mm) rubberized asphalt concrete gap-graded (RAC-G) overlay;
3. Sections 582RF and 588RF: Full-thickness (90 mm) AR4000 dense-graded asphalt concrete overlay (designed using CTM356 and referred to as "AR4000-D" in this report);
4. Sections 583RF and 589RF: Half-thickness (45 mm) MB4 gap-graded overlay (referred to as "45 mm MB4-G" in this report);
5. Sections 584RF and 590RF: Full-thickness (90 mm) MB4 gap-graded overlay (referred to as "90 mm MB4-G" in this report), and
6. Sections 585RF and 591RF: Half-thickness (45 mm) MAC15TR gap-graded overlay with minimum 15 percent recycled tire rubber (referred to as "MAC15-G" in this report).

2.2. Test Section Layout

The general test section layout for each section is shown in Figure 2.2. Station numbers refer to fixed points on the test section and are used for measurements and as a reference for discussing performance.

2.3. Underlying Pavement Design

The pavement for the first phase of HVS trafficking was designed according to the Caltrans Highway Design Manual Chapter 600 using the computer program *NEWCON90*. Design thickness was based on a tested subgrade R-value of 5 and a Traffic Index of 7 (~121,000 ESALs) (3).

The pavement design for the test road and as-built pavement structure for the overlay sections (580RF through 591RF), determined from cores removed from the edge of the sections, are illustrated in Figure 2.3.

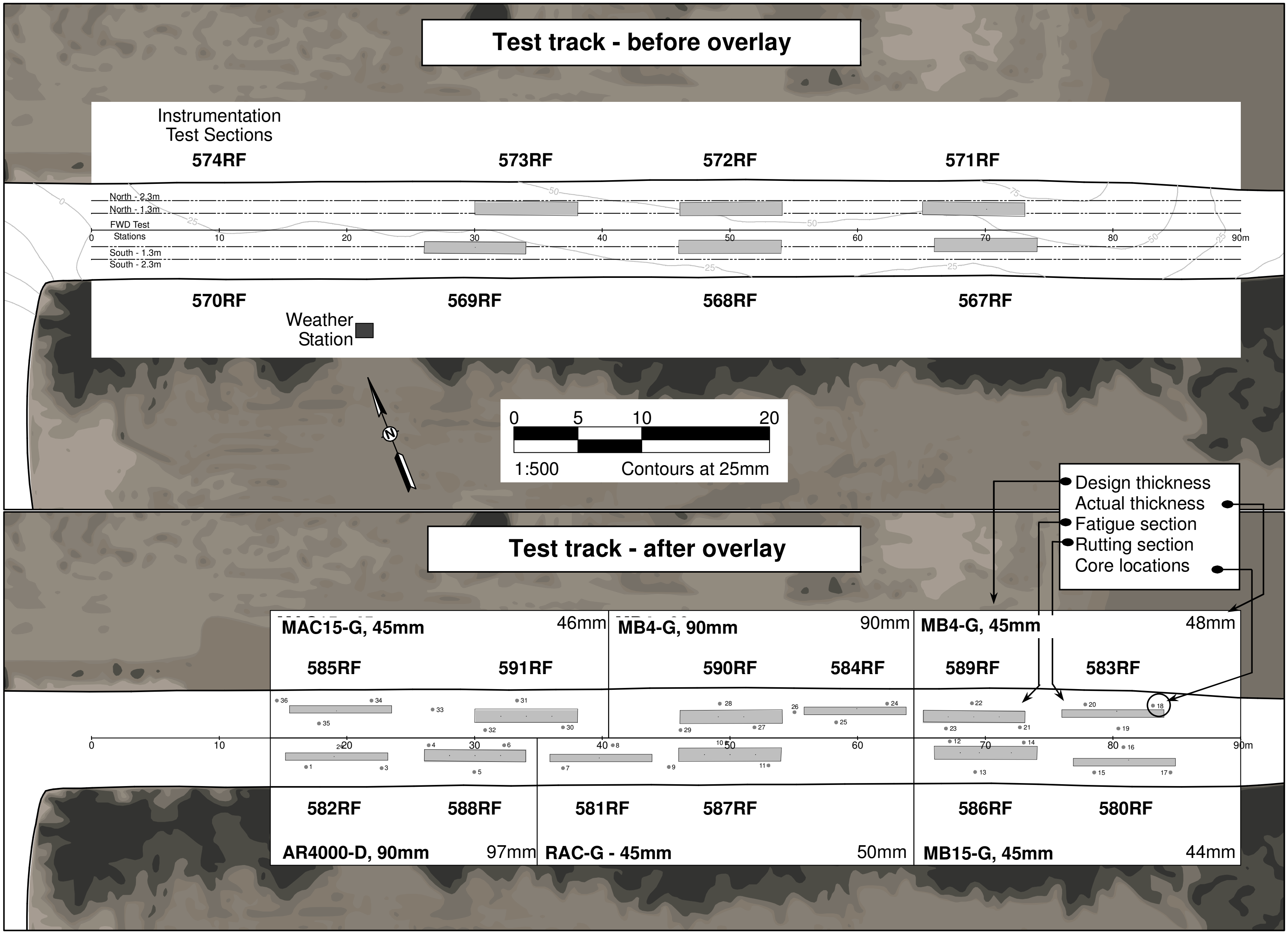

Figure 2.1: Layout of Reflective Cracking Study project.

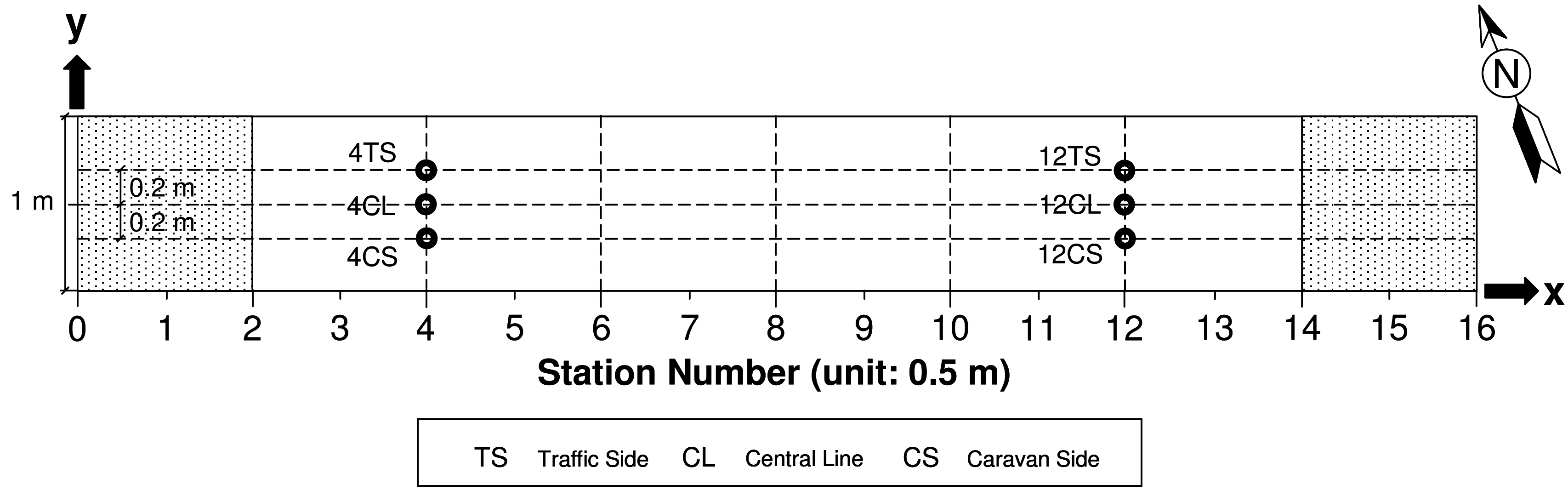

Figure 2.2: Test section layout.

Design	580RF/586RF	581RF/587RF	582RF/588RF	583RF/589RF	584RF/590RF	585RF/591RF
Overlay (45 or 90 mm)	MB15-G (46 mm)	RAC-G (50 mm)	AR4000-D (94 mm)	MB4-G (48 mm)	MB4-G (91 mm)	MAC15-G (45 mm)
DGAC (90 mm)	DGAC (81 mm)	DGAC (81 mm)	DGAC (93 mm)	DGAC (77 mm)	DGAC (88 mm)	DGAC (110 mm)
Class 2 Aggregate Base (410 mm)	Class 2 Aggregate Base (398 mm)	Class 2 Aggregate Base (398 mm)	Class 2 Aggregate Base (369 mm)	Class 2 Aggregate Base (372 mm)	Class 2 Aggregate Base (352 mm)	Class 2 Aggregate Base (411 mm)
Clay subgrade (semi-infinite)	Clay subgrade (semi-infinite)	Clay subgrade (semi-infinite)	Clay subgrade (semi-infinite)	Clay subgrade (semi-infinite)	Clay subgrade (semi-infinite)	Clay subgrade (semi-infinite)

Figure 2.3: Pavement design for Reflective Cracking Study experiment (design and actual).

The existing subgrade was ripped and reworked to a depth of 200 mm (8 in) so that the optimum moisture content and the maximum wet density met the specification per Caltrans Test Method CTM 216. The average maximum wet density of the subgrade was 2,180 kg/m^3 (136 pcf). The average relative compaction of the subgrade was 97 percent (3).

The aggregate base was constructed to meet the Caltrans compaction requirements for aggregate base Class 2 using CTM 231 nuclear density testing. The maximum wet density of the base determined according to CTM 216 was 2,200 kg/m^3 (137 pcf). The average relative compaction was 98 percent.

The DGAC layer consisted of a dense-graded asphalt concrete (DGAC) with AR-4000 binder and aggregate gradation limits following Caltrans 19-mm (0.75 in) maximum size coarse gradation (3). The target asphalt content was 5.0 percent by mass of aggregate, while actual contents varied between 4.34 and 5.69 percent. Nuclear density measurements and extracted cores were used to determine a preliminary as-built mean air-void content of 9.1 percent with a standard deviation of 1.8 percent. The based was primed before placing the asphalt concrete.

2.4. Summary of Testing on the Underlying Layer

Phase 1 trafficking took place between December 21, 2001, and March 25, 2003, and is summarized in Table 2.1. Figure 2.4 presents the final cracking patterns of each section after testing.

Table 2.1: Summary of Testing on the Underlying DGAC Layer

Section	Start date	End date	Repetitions	Wheel Load (kN)	Wheel	Tire Pressure (kPa)	Direction
567RF	12/21/01	01/07/02	78,500	60[1]	Dual	720[2]	Bi
568RF	01/14/02	02/12/02	377,556	60	Dual	720	Bi
569RF	03/25/03	04/11/03	217,116	60	Dual	720	Bi
571RF	07/12/02	10/02/02	1,101,553	60	Dual	720	Bi
572RF	01/23/03	03/12/03	537,074	60	Dual	720	Bi
573RF	03/18/02	03/08/02	983,982	60	Dual	720	Bi

[1] - 13,500 lb [2] - 104 psi

567RF 78,500 repetitions	568RF 377,556 repetitions	569RF 217,116 repetitions	571RF 1,101,553 repetitions	572RF 537,074 repetitions	573RF 983,982RF

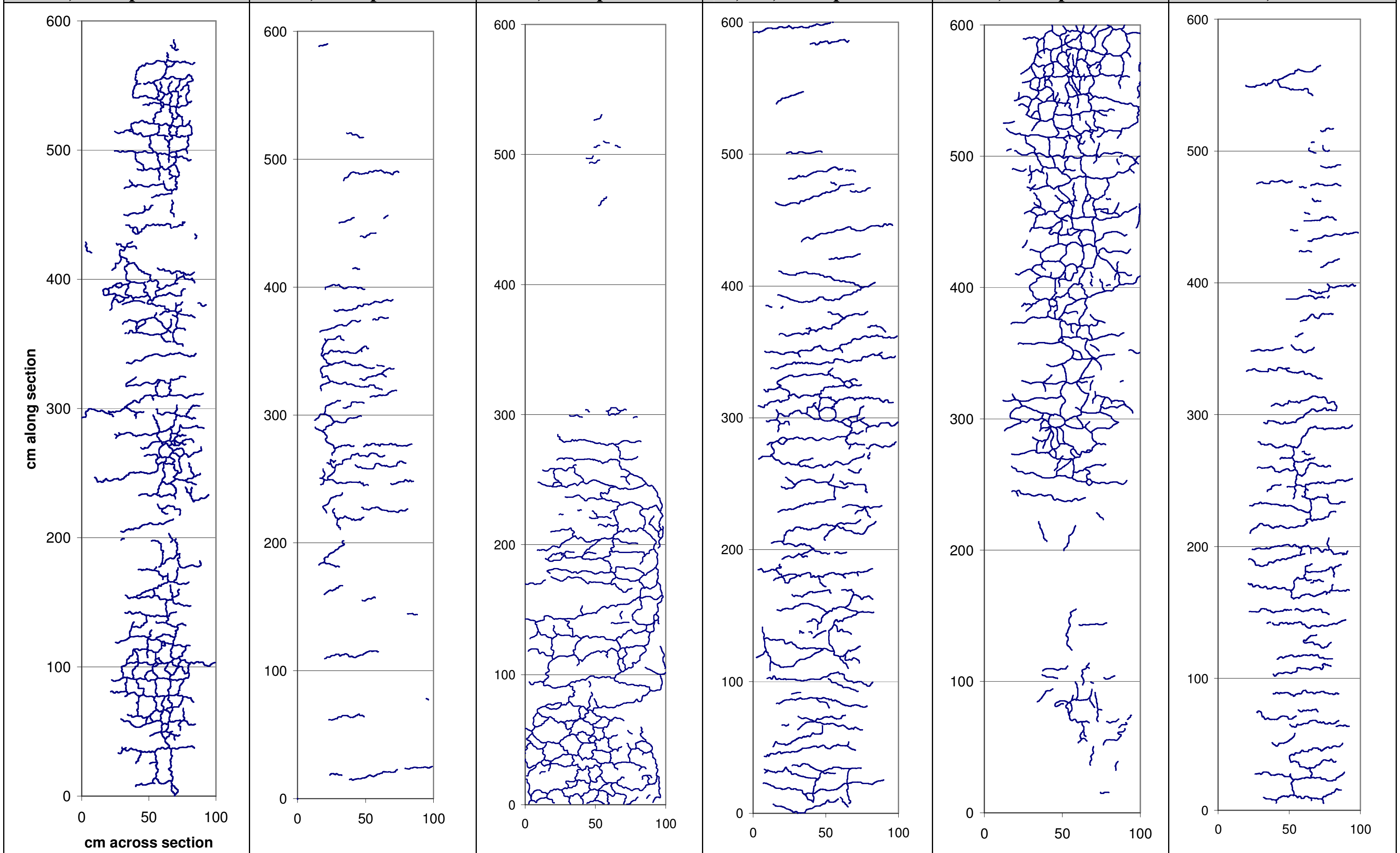

Average Maximum Rut depths					
15.7 mm (0.62 in)	13.9 mm (0.55 in)	6.3 mm (0.25 in)	14.3 mm (0.56 in)	16.4 mm (0.65 in)	14.6 mm (0.57 in)

Figure 2.4: Cracking patterns and rut depths on Sections 569RF through 573RF after Phase 1.

2.5. Overlay Design

The overlay thickness for the experiment was determined according to Caltrans Test Method CTM 356 using Falling Weight Deflectometer data from the Phase 1 experiment.

Laboratory testing was carried out by Caltrans and UCPRC on samples collected during construction to determine actual binder properties, binder content, aggregate gradation, and air-void content. The binders met requirements, based on testing performed by Caltrans. The average ignition-extracted binder contents of the various layers, corrected for aggregate ignition and compared to the design binder content are listed in Table 2.2. For each section, actual binder contents were higher than design contents. It is not clear whether this is a function of the test or contractor error.

Table 2.2: Design versus Actual Binder Contents

Section	Mix	Binder content (%)	
		Design	Actual
580RF and 586RF	MB15-G	7.1	7.52
581RF and 587RF	RAC-G	8.0	8.49
582RF and 588RF	AR4000-D	5.0	6.13
583RF and 589RF	MB4-G (45mm)	7.2	7.77
584RF and 590RF	MB4-G (90mm)	7.2	7.77
585RF and 591RF	MAC15-G	7.4	7.55

The aggregate gradations for the dense- and gap-graded mixes generally met Caltrans specifications for 19.0 mm (0.75 in.) maximum size coarse and gap gradations respectively, with specifics for each section detailed below. Gradations are illustrated in Figures 2.5 (AR4000-D) and 2.6 (modified binders).

- 580RF and 586RF: Material passing the 6.35 mm (1/4 in), 9.5 mm (3/8 mm), 12.5 mm (1/2 in) and 19.0 mm (3/4 in) sieves was on the lower envelope limit (Figure 2.6).
- 581RF and 587RF: Material passing the 0.3 mm (#50), 0.6 mm (#30) and 2.36 mm (#8) sieves was on the upper envelope limit (Figure 2.6).
- 582RF and 588RF: Material passing the 0.6 mm (#30), 2.36 mm (#8) and 4.75 mm (#4) sieves was on the upper envelope limit (Figure 2.5).
- 583RF and 589RF: Material passing the 6.35 mm (1/4 in) and 9.5 mm (3/8 in) sieves was on the lower envelope limit (Figure 2.6).
- 584RF and 590RF: Material passing the 6.35 mm (1/4 in) and 9.5 mm (3/8 in) sieves was on the lower envelope limit (Figure 2.6).
- 585RF and 591RF: Material passing the 0.6 mm (#30), 9.5 mm (3/8 in), 12.5 mm (1/2 in) and 19.0 mm (3/4 in) sieves was on the upper envelope limit, while material passing the 2.36 mm (#8), 4.75 mm (#4) and 6.35 mm (1/4 in) sieves was outside the upper limit (Figure 2.6).

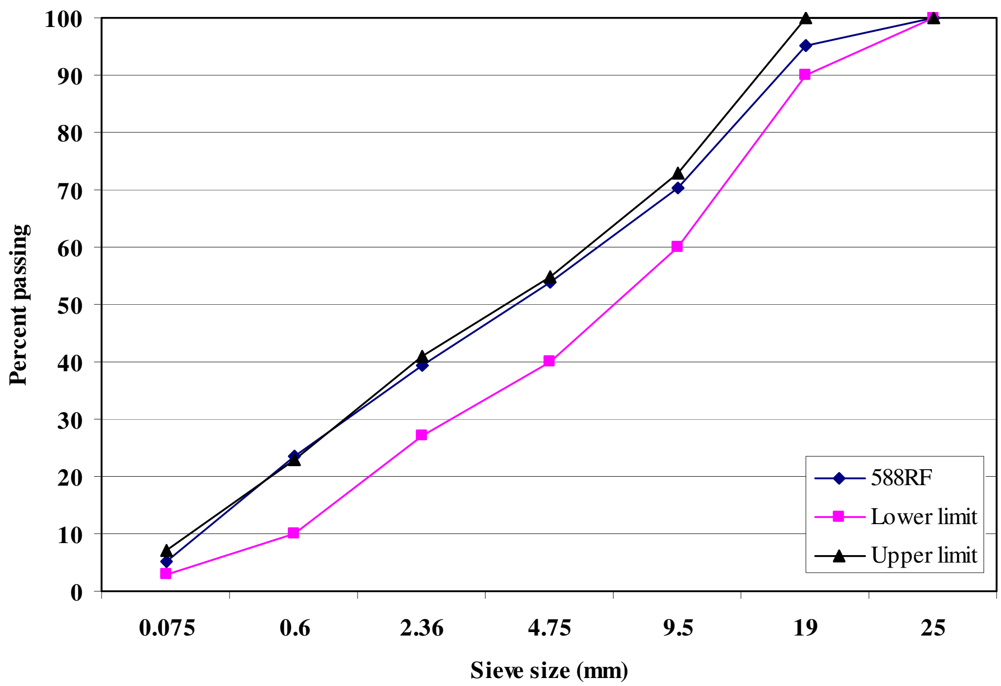

Figure 2.5: Gradation for AR4000-D overlay.

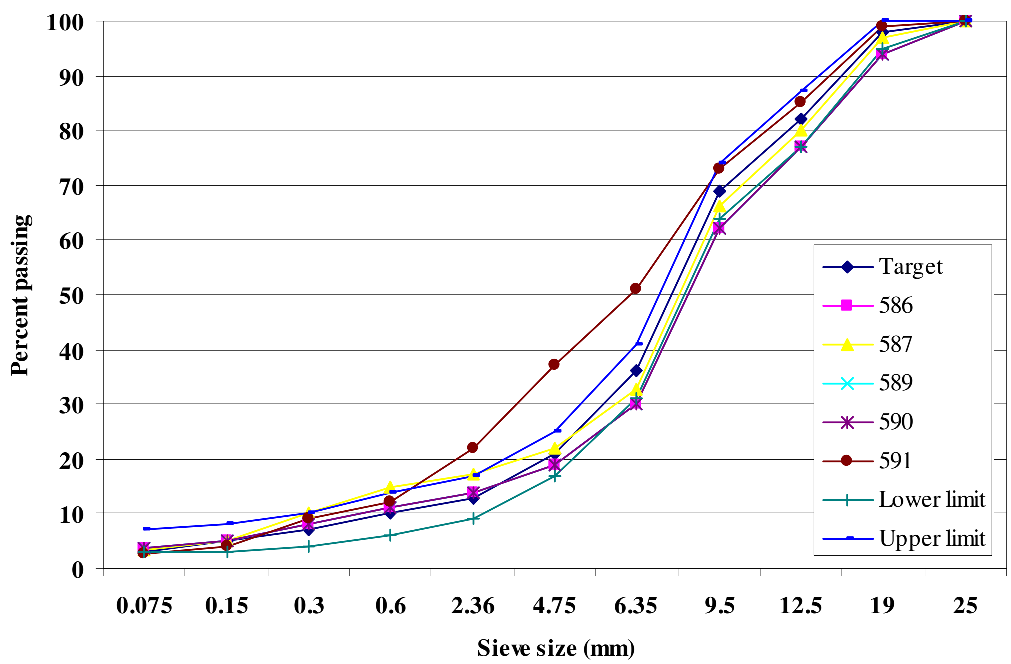

Figure 2.6: Gradation for modified binder overlays.

The overlays were placed on the same day, within a few hours of each other. A tack coat was applied prior to placement. The 90 mm layers were placed in two lifts of 45 mm and a tack coat was applied between lifts. The preliminary as-built air-void contents for each section, based on cores taken outside of the HVS sections prior to HVS testing are listed in Table 2.3.

Table 2.3: Air void Contents

Section	Mix	Air void content (%)	
		Average for section	Standard deviation
580RF and 586RF	MB15-G	5.1	1.7
581RF and 587RF	RAC-G	8.8	1.3
582RF and 588RF	AR4000-D	7.1	1.5
583RF and 589RF	MB4-G (45mm)	6.5	0.6
584RF and 590RF	MB4-G (90mm)	6.5	0.6
585RF and 591RF	MAC15-G	4.9	1.0

2.6. Summary of HVS Testing

Phase 2 HVS testing is discussed in a series of first-level analysis reports (4-10).

2.6.1 Test Section Failure Criteria

Failure criteria for HVS testing were set as follows:

- Rutting study:
  - Maximum surface rut depth of 12.5 mm (0.5 in) or more
- Reflective cracking study:
  - Cracking density of 2.5 m/m^2 (0.76 ft/ft^2) or more, and/or
  - Maximum surface rut depth of 12.5 mm (0.5 in) or more.

2.6.2 Environmental Conditions

In the rutting study, the pavement surface temperature was maintained at 50°C±4°C (122°F±7°F) in order to assess the susceptibility of the mixes to early rutting under typical pavement temperatures. In the reflective cracking study, the pavement surface temperature was maintained at 20°C±4°C (68°F±7°F) for the first one million repetitions to minimize rutting in the asphalt concrete and to accelerate fatigue damage. Thereafter, the pavement surface temperature was reduced to 15°C±4°C (59°F±7°F) to further accelerate fatigue damage. A temperature control chamber (11) was used to maintain the test temperatures.

The pavement surface received no direct rainfall as it was protected by the temperature control chamber. The sections were tested during both wet and dry seasons and hence water infiltration into the pavement from the side drains and through the raised groundwater table was possible at certain stages of the testing.

2.6.3 Test Duration

HVS trafficking on each section was initiated and completed as shown in Table 2.4.

Table 2.4: Test duration for Phase 2 HVS testing

Phase	Section	Mix	Start Date	Finish Date	Repetitions
Rutting	580RF	MB15-G	09/29/03	10/01/03	2,000
	581RF	RAC-G	09/15/03	09/19/03	7,600
	582RF	AR4000-D	09/04/03	09/09/03	18,564
	583RF	MB4-G (45mm)	12/08/03	12/16/03	15,000
	584RF	MB4-G (90mm)	11/13/03	11/26/03	34,800
	585RF	MAC15-G	10/10/03	10/20/03	3,000
Reflective cracking	586RF	MB15-G	05/25/06	11/21/06	2,492,387
	587RF	RAC-G	03/15/05	10/10/05	2,024,793
	588RF	AR4000-D	11/02/05	04/11/06	1,410,000
	589RF	MB4-G (45mm)	06/23/04	02/08/05	2,086,004
	590RF	MB4-G (90mm)	01/13/04	06/16/04	1,981,365
	591RF	MAC15-G	01/10/07	06/25/07	2,554,335

2.6.4 Loading Program

The HVS loading program for each section is summarized in Table 2.5. Test configurations were as follows:

- In the rutting tests, all trafficking was carried out with a dual-wheel configuration, using radial truck tires (Goodyear G159 - 11R22.5- steel belt radial) inflated to a pressure of 720 kPa, in a channelized, uni-directional loading mode.
- In the reflective cracking tests, all trafficking was carried out with a dual-wheel configuration, using radial truck tires (Goodyear G159 - 11R22.5- steel belt radial) inflated to a pressure of 720 kPa, in a bi-directional loading mode. Lateral wander over the one-meter width of the test section was programmed to simulate traffic wander on a typical highway lane.

Table 2.5: Summary of HVS Loading Program

Phase	Section	Start repetition	Total repetitions	Wheel load (kN)		ESALs	Traffic index
				Planned	Actual*		
Rutting	580RF	Full test	2,000	40	60	11,000	N/A
	581RF		7,600			42,000	N/A
	582RF		18,564			102,000	N/A
	583RF		15,000			83,000	N/A
	584RF		34,800			191,000	N/A
	585RF		3,000			17,000	N/A

* The loading program differs from the original test plan due to an incorrect hydraulic control system setup on loads less than 65 kN in the Phase 1 experiment. The loading pattern from the Phase 1 experiment was thus retained to facilitate comparisons of performance between all tests in the Reflective Cracking Study.

40 kN - 9,000 lb   60 kN - 13,500 lb

Table 2.5: Summary of Load History (cont)

Phase	Section	Start repetition	Total repetitions	Wheel load (kN) Planned	Wheel load (kN) Actual*	ESALs	Traffic index
Reflective cracking	586RF (MB15-G)	0 215,000 410,000 1,000,001	2,492,387	40 60 80 100	60 90 80 100	88 million	15
	587RF (RAC-G)	0 215,000 410,000 1,000,001	2,024,793	40 60 80 100	60 90 80 100	66 million	15
	588RF (AR4000-D)	0 215,000 410,000 1,000,001	1,410,000	40 60 80 100	60 90 80 100	37 million	14
	589RF (45mm MB4-G)	0 215,000 407,197 1,002,000	2,086,004	40 60 80 100	60 90 80 100	69 million	15
	590RF** (90mm MB4-G)	0 1,071,004 1,439,898 1,629,058	1,981,365	40 60 80 100	60 90 80 100	37 million	14
	591RF (MAC15-G)	0 215,000 410,000 1,000,001	2,554,335	40 60 80 100	60 90 80 100	91 million	15

* The loading program differs from the original test plan due to an incorrect hydraulic control system setup on loads less than 65 kN in the Phase 1 experiment. The loading pattern from the Phase 1 experiment was thus retained to facilitate comparisons of performance between all tests in the Reflective Cracking Study.

** 590RF was the first HVS test on the overlays, and the 60 kN loading pattern was retained for an extended period to prevent excessive initial deformation (rutting) of the newly constructed overlay.

40 kN - 9,000 lb | 60 kN - 13,500 lb | 80 kN - 18,000 lb | 90 kN - 20,200 lb | 100 kN - 22,500 lb

3. FORENSIC INVESTIGATION SUMMARY

This chapter provides a summary of the observations and measurements recorded during the forensic investigation of Phase 2 of the Reflective Cracking study. Interpretation of the data in terms of pavement performance will be discussed in a separate second-level analysis report.

3.1. Forensic Investigation Procedure

The forensic investigation included the following components:

- Test pit demarcation and excavation
- Test pit profile (Section 3.2)
- Test pit description and photographs (Section 3.3 [Rutting study] and Section 3.4 [Fatigue study])
- Density and moisture content determination (Section 3.4)
- Dynamic Cone Penetrometer (DCP) measurements (Section 3.5)
- Visual assessment of the slab and cores removed from the slab (Section 3.6)
- Scanning Electron Microscope assessment of base materials (Section 3.7)

A total of 18 test pits were excavated for the study, one test pit on each rutting section (between Stations 6 and 8 [see Figure 2.2]) and two test pits on each reflective cracking section (between Stations 4 and 6 and between Stations 10 and 12). The pits were excavated approximately 200 mm into the subgrade below the base. The order of the investigation tasks was as follows:

1. Demarcate the pit;
2. Saw the asphalt concrete;
3. Remove the slab;
4. Determine the wet density of the base (nuclear density gauge);
5. Determine the in situ strength of the base and subgrade (Dynamic Cone Penetrometer);
6. Remove the base material and top 200 mm of the subgrade;
7. Sample material from the top 150 mm and bottom 150 mm of the base, and from the subgrade for moisture content determination
8. Measure layer thicknesses;
9. Describe the profile;
10. Photograph the profile;
11. Sample additional material from the profile if required, and
12. Reinstate the pit.

The following additional information is relevant to the investigation:

- The procedures for HVS test section forensic investigations, detailed in the document entitled *Quality Management System for Site Establishment, Daily Operations, Instrumentation, Data Collection and Data Storage for APT Experiments* (12) were followed.
- The saw cuts were made at least 50 mm into the base to ensure that the slab could be removed from the pit without it breaking.
- Nuclear density measurements were taken between the test section centerline and inside (traffic side) edge of the test section. Two readings were taken, the first with the gauge aligned with the direction of trafficking and the second at 90° to the first measurement (Figure 3.1).
- DCP measurements were taken between the test section centerline and inside (traffic side) edge of the test section, and between the edge of the test section and the edge of the test pit on the traffic side (Figure 3.1). A third DCP measurement was taken if inconsistent readings were obtained.
- Layer thicknesses were measured from a leveled reference straightedge above the pit. This allowed the camber of the section to be included in the profile. Measurements were taken across the pit at 50-mm intervals.

3.2. Test Pit Profiles

Test pit profile illustrations are provided in Appendix A. Average measurements from the profile are listed in Tables 3.1 and 3.2.

Table 3.1: Average Layer Thicknesses from Rutting Study Test Pit Profiles

	Section	Layer	Average (mm)	Std. Deviation (mm)	Minimum (mm)	Maximum (mm)
Rutting Study	580RF	MB15-G	37	3	31	43
		DGAC	86	8	72	102
		Base	387	26	357	428
	581RF	RAC-G	56	3	51	61
		DGAC	79	6	67	89
		Base	257	11	239	273
		Selected	116	7	100	124
	582RF	AR4000-D	101	3	95	104
		DGAC	97	4	89	108
		Base	394	6	385	400
	583RF	MB4-G	45	3	39	51
		DGAC	77	11	61	103
		Base	361	17	330	387
	584RF	MB4-G	94	4	88	100
		DGAC	102	5	92	110
		Base	332	11	310	347
	585RF	MAC15-G	45	2	35	50
		DGAC	110	8	101	127
		Base	411	4	404	422

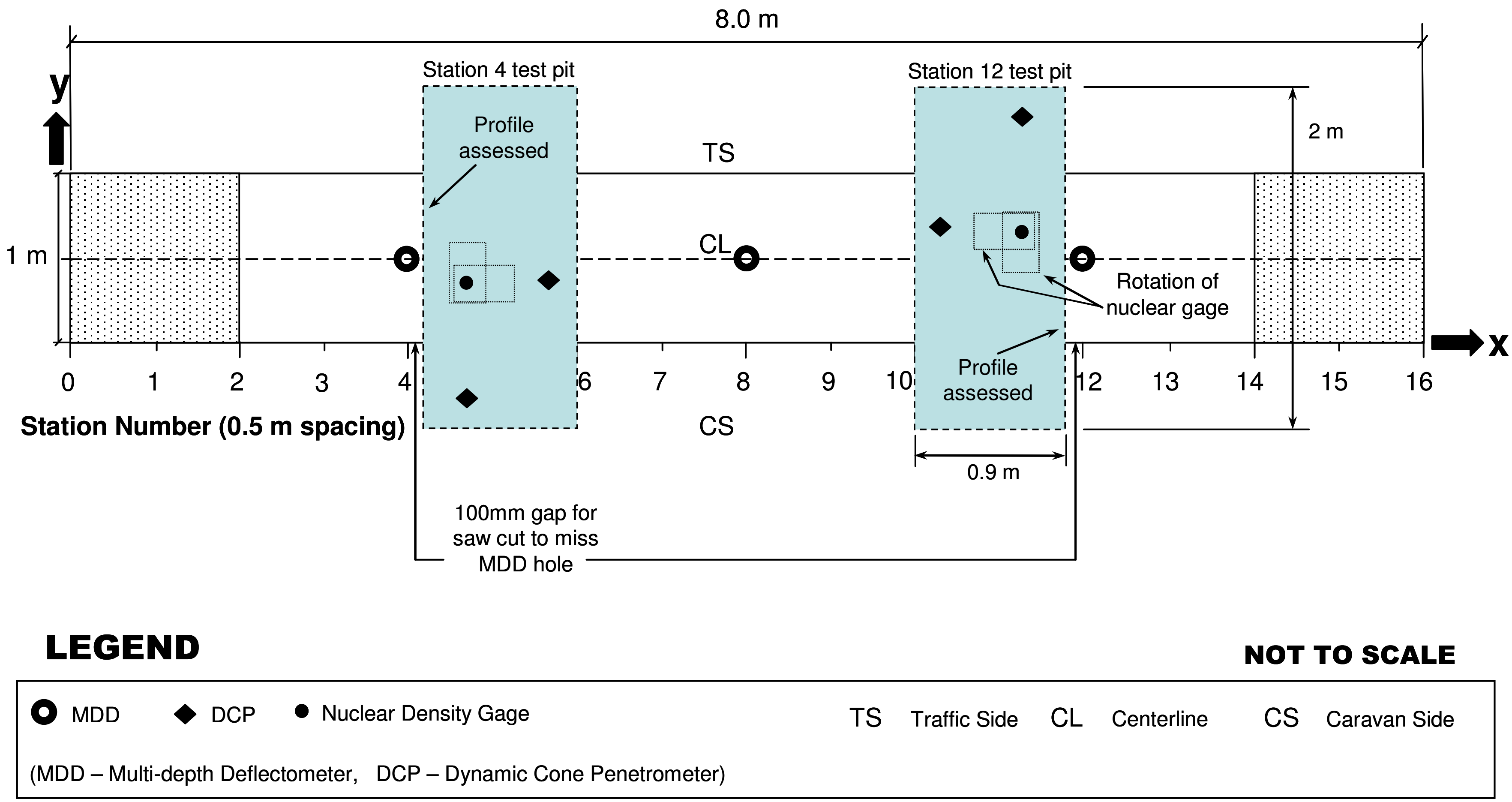

Figure 3.1: Typical cracking section test pit layout.

Table 3.2: Average Layer Thicknesses from Reflective Cracking Study Test Pit Profiles

	Section and Test Pit Station	Layer	Average (mm)	Std. Deviation (mm)	Minimum (mm)	Maximum (mm)
Reflective Cracking Study	586RF#4	MB15-G	52	4	48	62
		DGAC	76	6	64	85
		Base	400	7	387	415
	586RF#12	MB15-G	45	5	36	54
		DGAC	81	5	72	89
		Base	406	8	394	425
	587RF#4	RAC-G	47	4	40	52
		DGAC	81	6	73	94
		Base	325	10	313	344
		Selected	82	6	65	85
	587RF#12	RAC-G	46	5	37	52
		DGAC	83	3	77	89
		Base	332	13	318	356
		Selected	82	1	82	82
	588RF#4	AR4000-D	89	4	83	95
		DGAC	92	5	85	103
		Base	364	25	325	405
	588RF#12	AR4000-D	93	5	82	109
		DGAC	89	6	75	100
		Base	348	11	335	366
	589RF#4	MB4-G	50	3	44	56
		DGAC	84	4	76	91
		Base	385	6	378	400
	589RF#12	MB4-G	48	6	35	67
		DGAC	75	16	56	116
		Base	362	11	34	390
	590RF#4	MB4-G	86	3	82	93
		DGAC	81	3	77	87
		Base	366	4	354	372
	590RF#12	MB4-G	94	5	87	103
		DGAC	81	9	68	99
		Base	359	11	339	371
	591RF#4	MAC15-G	51	4	45	57
		DGAC	77	3	65	76
		Base	333	6	322	343
	591RF#12	MAC15-G	49	2	45	52
		DGAC	80	4	75	92
		Base	325	8	312	338

3.3. Rutting Study Test Pit Observations

3.3.1 Section 580RF: 45 mm MB15-G

Observations from the Section 580RF test pit (Figure 3.2) include:

- The overlay thickness was considerably less than the design (average 37 mm), while the average thickness of the underlying DGAC was marginally less (86 mm) than the design.

- Some densification (approximately 3 to 4 mm) was noted in the overlay in the trafficked area. Most of the rutting occurred in the underlying DGAC layer (Figure 3.3). No rutting was noted in the base and subgrade. Some displacement was recorded on either side of the trafficked area.
- The overlay was well bonded to the DGAC, which was well bonded to the aggregate base.
- Apart from rutting, no other distresses were noted in the asphalt layers.
- The base under the trafficked area was thinner than the design (average 387 mm), but met the design requirements (410 mm) on the shoulder side of the section. The base material was dark grey-brown and consisted primarily of non-plastic recycled construction rubble, which included various types of natural aggregate (including andesite, granite, quartz, and quartzite pebbles) and small quantities of glass, fabric, and organic matter. The structure was generally homogenous. Grain size varied from fine to coarse with maximum particle size typically between 19 mm and 25 mm. Consistency was rated as hard in the top 70 mm, very hard between 70 mm and 250 mm, and firm to hard below as moisture content increased (Figures 3.4 and 3.5).
- Recementation of the base material was visibly apparent. A cement odor was present and strong effervescence was noted when dilute hydrochloric acid was sprayed onto the base material, indicating the presence of old cement (Figure 3.6). When phenolphthalein was sprayed onto the base material, the sprayed area turned red, signifying a pH greater than 10, which is indicative of uncarbonated cemented material (Figures 3.6 and 3.7). These tests, together with the DCP measurements discussed in Section 3.6 indicate some recementation of the recycled concrete base material occurred after construction. This is discussed in more detail in Section 3.7.
- Moisture content in the base was rated as dry-to-moist. The material appeared drier than the pits on the other sections.
- The layer definition between the base and subgrade was clear. No punching of the base into the in situ material was noted.
- The subgrade was moist, dark brown clay with medium to high plasticity. Mottling was evident. Consistency was rated as hard and structure as slickensided. Some organic matter was noted. No hydrochloric acid or phenolphthalein reaction was recorded.

Figure 3.2: 580RF test pit location.

Figure 3.3: 580RF test pit profile. (1)

Figure 3.4: 580RF test pit profile. (2)

Figure 3.5: 580RF test pit profile. (3)

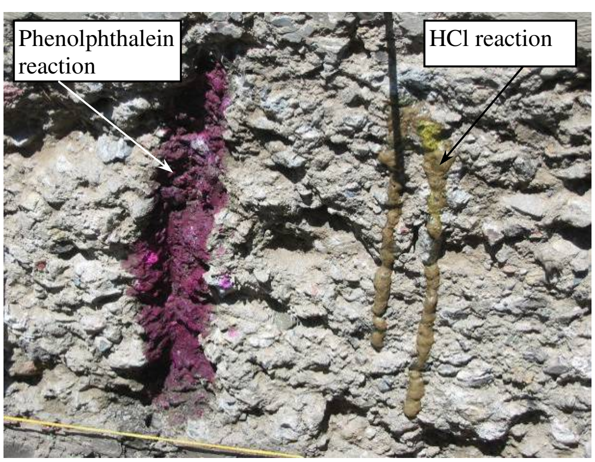

Figure 3.6: 580RF phenolphthalein and hydrochloric acid reaction on base material.

Figure 3.7: 580RF phenolphthalein reaction.

3.3.2 Section 581RF: 45 mm RAC-G

Observations from the Section 581RF test pit (Figure 3.8) include:

- The overlay was considerably thicker than the design (average 56 mm), while the average thickness of the underlying DGAC was less than the design (average 79 mm).
- Some densification (approximately 2 to 3 mm) was noted in the overlay in the trafficked area. Most of the rutting occurred in the DGAC layer (Figure 3.9). No rutting was recorded in the base and subgrade. Some displacement was recorded on either side of the trafficked area.
- The overlay was well bonded to the DGAC in the trafficked area, but some debonding was noted on the edge of the pit. Poor bonding was also noted between the two lifts in the DGAC in some areas. Water from the saw cutting operation was still clearly visible in these poorly bonded areas after the rest of the profile had dried (Figure 3.10). The DGAC was well bonded to the aggregate base.
- Some segregation was noted in the DGAC layer on the traffic side of the section (Figure 3.10). Apart from this and the rutting, no other distresses were noted in the asphalt layers.
- The base under the trafficked area was thinner than the design (average 373 mm). Two distinct layers were noted in the base and although the material appeared to be from the same source, the lower layer was far wetter and appeared to have a weaker structure (Figure 3.11). This layer was designated as a selected layer in the profile assessment. The material in the two layers was dark grey-brown and consisted primarily of non-plastic recycled construction rubble, which included various types of natural aggregate (including andesite, chert, phyllite, quartz, and quartzite pebbles) and small quantities of glass, fabric, metal, and organic matter. The structure was generally homogenous. Grain size varied from fine to coarse with maximum particle size typically between 19 mm and 25 mm. Consistency was rated as hard in the top 50 mm, very hard between 50 and 250 mm, and hard to firm in the selected layer as moisture content increased and structure changed (Figures 3.12 and 3.13).
- Recementation of the base material was visibly apparent. A cement odor was present and strong hydrochloric acid and phenolphthalein reactions were noted.
- Moisture content in the base and selected layer was rated as moist and moist-to-wet, respectively.
- The layer definition between the base, selected layer, and subgrade was clear. No punching of the selected layer into the in situ material was noted.
- The subgrade was moist, dark brown clay with medium to high plasticity. Some mottling was observed. Consistency was rated as hard and structure as slickensided. Some organic matter was noted. No hydrochloric acid or phenolphthalein reaction was recorded.

Figure 3.8: 581RF test pit location.

Figure 3.9: 581RF test pit profile (1).

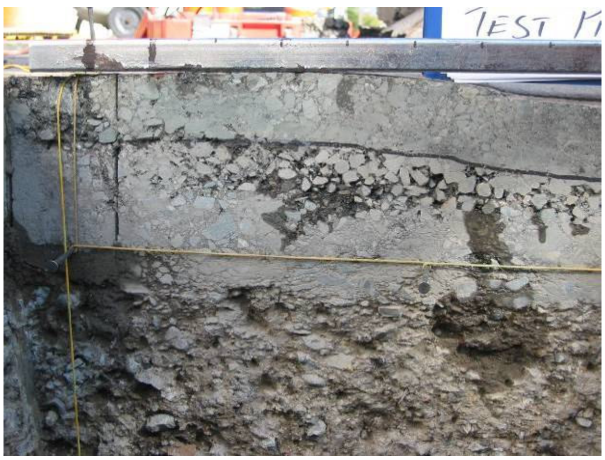

Figure 3.10: 581RF segregation in DGAC layer.

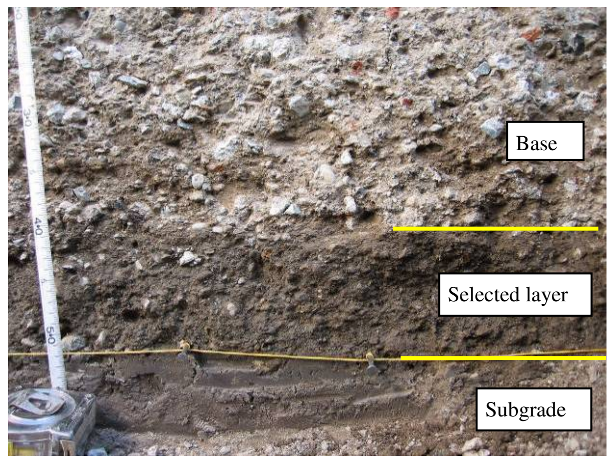

Figure 3.11: 581RF selected layer.

Figure 3.12: 581RF test pit profile. (2)

Figure 3.13: 581RF test pit profile. (3)

3.3.3 Section 582RF: 90 mm AR4000-D

Observations from the Section 582RF test pit (Figure 3.14) include:

- The average thicknesses of the overlay (101 mm) and underlying DGAC (97 mm) were greater than the design.
- Rutting was noted in both the overlay and the underlying layer (Figure 3.15). No rutting was noted in the base and subgrade. Slight displacement was recorded on either side of the trafficked area.
- The overlay was generally poorly bonded to the underlying layer. Bonding between lifts was also unsatisfactory. Water from the saw cutting operation was still clearly visible in these poorly bonded areas after the rest of the profile had dried (Figure 3.16). The DGAC was well bonded to the aggregate base.
- Some segregation was noted in the underlying DGAC layer on the traffic side of the section (Figure 3.16). Apart from this and the rutting, no other distresses were noted in the asphalt layers.
- The base under the trafficked area was marginally thinner (average 394 mm) than the design. The material was dark grey-brown and consisted primarily of non-plastic recycled construction rubble, which included various types of natural aggregate (including chert, quartzite pebbles, and basalt) and small quantities of glass, fabric, metal wire, and organic matter. The structure was generally homogenous. Grain size varied from fine to coarse with maximum particle size typically between 19 mm and 25 mm. Consistency was rated as hard in the top 100 mm, very hard between 100 and 300 mm, and hard below 300 mm (Figure 3.17).
- Recementation of the base material was visibly apparent. A cement odor was present and strong hydrochloric acid and phenolphthalein reactions were noted.
- Moisture content in the base was rated as moist.
- The layer definition between the base and subgrade was clear. Some punching of the base material into the in situ material was noted.
- The subgrade was moist, dark brown clay with medium to high plasticity. Mottling was noted. Consistency was rated as hard and structure as slickensided. Some organic matter was present. No hydrochloric acid or phenolphthalein reaction was recorded on the subgrade material.

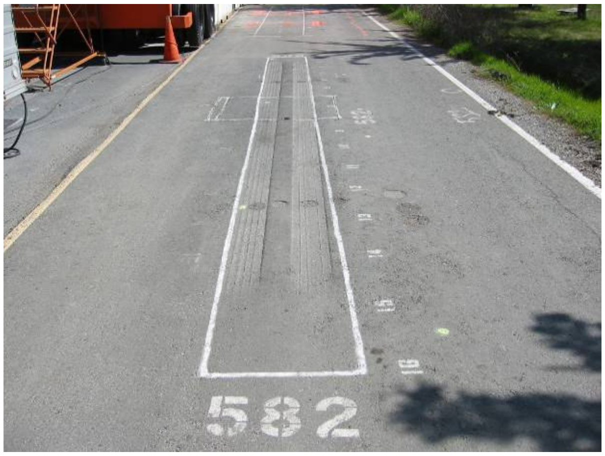

Figure 3.14: 582RF test pit location.

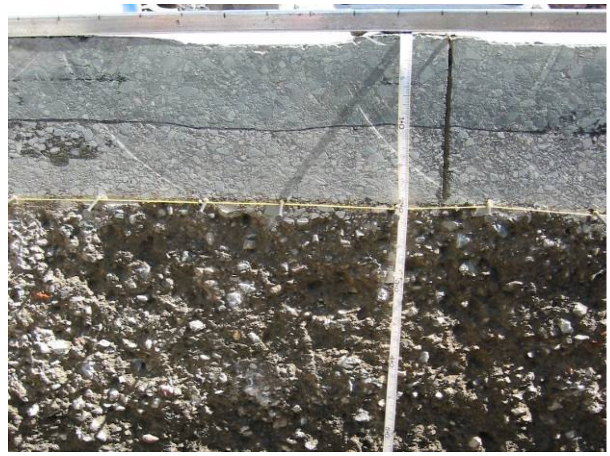

Figure 3.15: 582RF test pit profile (1).

Figure 3.16: 582RF moisture in asphalt concrete layer bonds.

Figure 3.17: 582RF test pit profile. (2)

3.3.4 Section 583RF: 45 mm MB4-G

Observations from the Section 583RF test pit (Figure 3.18) include:

- The average thickness of the overlay matched the design thickness, although measurements indicated that thickness tapered over the width of the test pit (51 mm to 39 mm). The average thickness of the underlying DGAC was considerably less (77 mm) than the design and also tapered from one side of the pit to the other (103 mm to 61 mm).
- Some densification (approximately 4 to 5 mm) was noted in the wheelpaths in the overlay. Most of the rutting occurred in the DGAC layer (Figure 3.19). No rutting was noted in the base and subgrade. Severe displacement was recorded on the shoulder side of the trafficked area and in between the wheelpaths (Figure 3.19).
- The overlay was well bonded to the DGAC although some shearing was noted on the bond between the overlay and DGAC in the severely heaved areas. The DGAC was well bonded to the aggregate base.

- Apart from rutting, no other distresses were noted in the asphalt layers.
- The base was thinner (average 361 mm) than the design across the full width of the test pit. The base material was dark grey-brown and consisted primarily of non-plastic, recycled construction rubble, which included various types of natural aggregate (including quartz, quartzite pebbles, phyllite, and andesite) and small quantities of glass, fabric, and organic matter. The structure was generally homogenous. Grain size varied from fine to coarse with maximum particle size typically between 19 mm and 25 mm. Consistency was rated as very hard in the top 220 mm, and hard to firm below as moisture content increased (Figures 3.20 and 3.21).
- Recementation of the base material was visibly apparent. A cement odor was present and strong hydrochloric acid and phenolphthalein reactions were noted.
- Moisture content in the base was rated as moist.
- The layer definition between the base and subgrade was clear. No punching of the base into the in situ material was noted.
- The subgrade was moist, dark brown clay with medium to high plasticity. Some mottling was observed. Consistency was rated as hard and structure as slickensided. Some organic matter was noted. No hydrochloric acid or phenolphthalein reaction was recorded on the subgrade material.

Figure 3.18: 583RF test pit location.

Figure 3.19: 583RF test pit profile. (1)

Figure 3.20: 583RF test pit profile. (2)

Figure 3.21: 583RF test pit profile. (3)

3.3.5 Section 584RF: 90 mm MB4-G

Observations from the Section 584RF test pit (Figure 3.22) include:

- The average thickness of the overlay was marginally greater (94 mm) than the design thickness, while the average thickness of the underlying DGAC was considerably thicker (102 mm).
- Some densification (approximately 4 to 5 mm) was noted in the overlay in the wheelpaths, but most of the rutting occurred in the DGAC layer (Figure 3.23). No rutting was noted in the base and subgrade. Some displacement was recorded on either side of the trafficked area.
- The overlay was well bonded to the DGAC, which was well bonded to the aggregate base.
- Apart from rutting, no other distresses were noted in the asphalt layers.
- The base under the trafficked area was significantly thinner (average 332 mm) than the design. The base material was dark grey-brown and consisted primarily of non-plastic, recycled construction rubble, which included various types of natural aggregate (including quartz, quartzite pebbles, phyllite, granite, and andesite) and small quantities of glass, fabric, metal (nails and wire), and some organic matter. The structure was generally homogenous. Grain size varied from fine to coarse with maximum particle size typically between 19 mm and 25 mm. Consistency was rated as very hard in the top 200 to 250 mm, and hard to firm below that as moisture content increased (Figures 3.24 and 3.25).
- Recementation of the base material was visibly apparent. A cement odor was present and strong hydrochloric acid and phenolphthalein reactions were noted.
- Moisture content in the base was rated as moist.
- The layer definition between the base and subgrade was clear but rather uneven. Some punching of the base into the in situ material was also noted.

- The subgrade was moist, dark brown clay with medium to high plasticity. Mottling was observed. Consistency was rated as hard and structure as slickensided. Some organic matter was present. No hydrochloric acid or phenolphthalein reaction was recorded on the subgrade material.

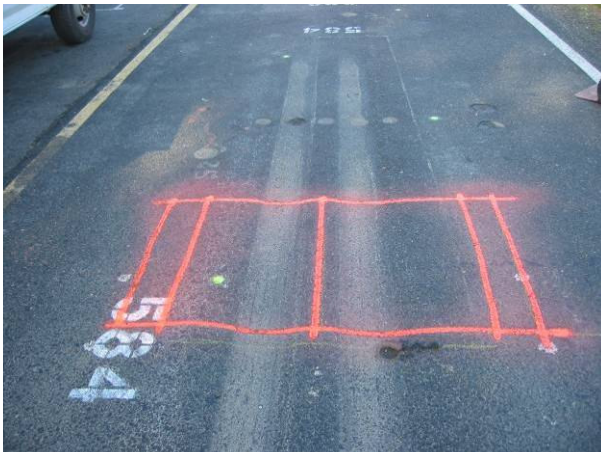

Figure 3.22: 584RF test pit location.

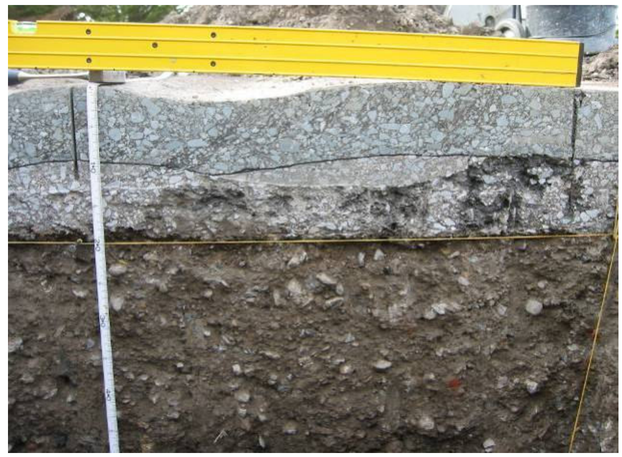

Figure 3.23: 584RF test pit profile. (1)

Figure 3.24: 584RF test pit profile. (2)

Figure 3.25: 584RF test pit profile. (3)

3.3.6 Section 585RF: 45 mm MAC15-G

Observations from the Section 585RF test pit (Figure 3.26) include:

- The average thickness of the overlay matched the design thickness, although measurements indicated that thickness tapered over the width of the test pit (35 mm to 50 mm). The average thickness of the underlying DGAC was considerably thicker (110 mm) than the design and also tapered from one side of the pit to the other (101 mm to 127 mm).
- Minor densification (approximately 1 to 2 mm) was noted in the overlay in the wheelpaths, with most of the rutting occurring in the DGAC layer (Figure 3.27). No rutting was noted in the base and subgrade. Some displacement was recorded on either side of the trafficked area.

- The overlay was well bonded to the DGAC, which was well bonded to the aggregate base.
- Apart from rutting, no other distresses were noted in the asphalt layers.
- The base under the trafficked area met the design thickness. The base material was dark grey-brown and consisted primarily of non-plastic recycled construction rubble, which included various types of natural aggregate (including quartz, quartzite pebbles, andesite, and granite) and small quantities of glass, fabric, metal (nails and wire), and some organic matter. The structure was generally homogenous. Grain size varied from fine to coarse with maximum particle size typically between 19 mm and 25 mm. Consistency was rated as very hard in the top 250 mm, and hard to firm below that as moisture content increased (Figures 3.28 and 3.29).
- Recementation of the base material was visibly apparent. A cement odor was present and strong hydrochloric acid and phenolphthalein reactions were noted.
- Moisture content in the base was rated as moist.
- The layer definition between the base and subgrade was clear and no punching of the base into the in situ material was noted.
- The subgrade was moist, to wet dark brown clay with medium to high plasticity. Some mottling was noted. Consistency was rated as hard and structure as slickensided. Some organic matter was present. No hydrochloric acid or phenolphthalein reaction was recorded on the subgrade material.

Figure 3.24: 585RF test pit location.

Figure 3.25: 585RF test pit profile. (1)

Figure 3.26: 585RF test pit profile. (2)

Figure 3.27: 585RF test pit profile. (3)

3.4. Reflective Cracking Study Test Pit Observations

3.4.1 Section 586RF: 45 mm MB15-G

Observations from the Section 586RF test pits (Figure 3.28) include:

- The average thickness of the overlay equaled or exceeded the design thickness (45 mm at Station 12 and 52 mm at Station 4), while the average thickness of the underlying DGAC was less than the design (76 mm and 81 mm at Stations 4 and 12, respectively).
- Very little rutting/densification was evident in the overlay. Rutting in the underlying DGAC from the Phase 1 trafficking was noted in both test pits (Figures 3.29 and 3.30). No rutting was noted in the base and subgrade. No displacement was recorded on either side of the trafficked area.
- The overlay was well bonded to the DGAC, which was well bonded to the aggregate base (Figure 3.31).
- Bottom-up cracking was noted in the DGAC layer in both test pits (Figure 3.32). No propagation of the cracks into the overlay was observed, however, this could be attributed to resealing of any cracks when the overlay was heated during sawing and excavation of the test pit. No other distresses were noted in the asphalt concrete layers.
- The average thickness of the base was marginally less than the design (average 400 mm to 406 mm), but exceeded the design requirements on the shoulder side of the section (415 mm to 425 mm). The base material was dark grey-brown and consisted primarily of non-plastic recycled construction rubble, which included various types of natural aggregate (predominantly quartz and quartzite pebbles) and small quantities of brick, glass, fabric, and organic matter. The structure was generally homogenous. Grain size varied from fine to coarse with maximum particle size typically between 19 mm and 25 mm. Consistency was rated as hard in the top 180 mm, very hard

between 180 mm and 290 mm, and firm to hard below as moisture content increased (Figure 3.33). The DCP did not penetrate the trafficked area of the test pit at Station 12.

- Recementation of the base material was visibly apparent. A cement odor was present and strong hydrochloric acid and phenolphthalein reactions were noted.
- Moisture content in the base was rated as moist.
- The layer definition between the base and subgrade was clear. No punching of the base into the in situ material was noted.
- The subgrade was moist, dark brown clay with medium to high plasticity. Mottling was evident. Consistency was rated as hard and structure as slickensided. Some organic matter was noted. No hydrochloric acid or phenolphthalein reaction was recorded.

Figure 3.28: 586RF test pit location.

Figure 3.29: 586RF#4 test pit profile.

Figure 3.30: 586RF#12 test pit profile.

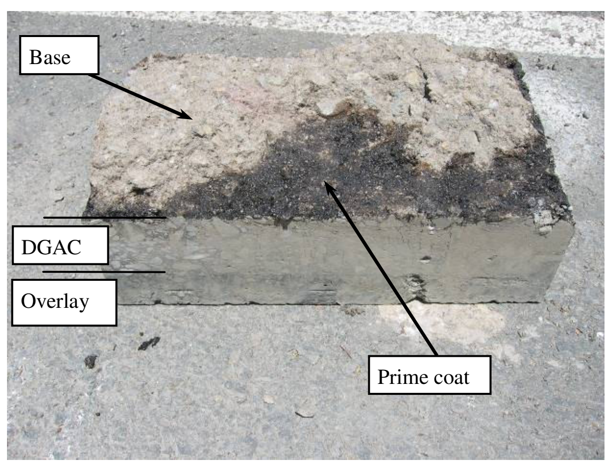

Figure 3.31: 586RF bond between DGAC and base.

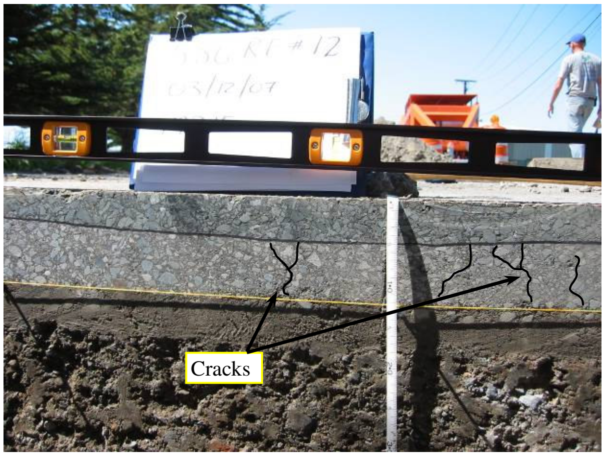

Figure 3.32: 586RF cracks in underlying DGAC.

Figure 3.33: 586RF strongly cemented base.

3.4.2 Section 587RF: 45 mm RAC-G

Observations from the Section 587RF test pits (Figure 3.34) include:

- The average thickness of the overlay in both test pits equaled the design thickness, while the average thickness of the underlying DGAC was less than the design (81 mm and 83 mm at Stations 4 and 12 respectively).
- Although a rut was measured on the surface, very little rutting/densification was evident in the overlay in either test pit. Most rutting occurred in the underlying DGAC. The rut resulting from Phase 1 HVS trafficking (see Section 1.2) could not be distinguished from that resulting from Phase 2 trafficking at Station 4 (Figure 3.35). However, at Station 12, where less rutting was recorded during Phase 2 HVS testing, the rut from earlier trafficking was observed (Figure 3.36). A small rut (2 mm to 4 mm) was measured in the base across the width of the trafficked section in both test pits. No rutting was observed in the subgrade. Some displacement was recorded on both sides of the trafficked area.
- The overlay was well bonded to the DGAC in the trafficked area, but some debonding was noted on the edge of the test pit at Station 4. Poor bonding was also noted between the two lifts in the DGAC in some areas. The DGAC was well bonded to the aggregate base.
- Bottom-up cracking was noted in the DGAC and overlay in the test pit at Station 4 (Figure 3.37). No cracks were observed in the asphalt concrete at Station 12 (Figure 3.38). No other distresses were noted in the asphalt concrete.
- The average thickness of the base was considerably less than the design (average 325 mm to 332 mm). As noted in the Section 581RF test pit, two distinct layers were observed in the base with the material in the lower layer appearing wetter and weaker than the upper layer. The base material was dark grey-brown and consisted primarily of non-plastic recycled construction rubble, which included various types of natural aggregate (including quartz, quartzite pebbles, phyllite,

and granite) and small quantities of brick, glass, fabric, wood chips, and other organic matter. The structure was generally homogenous. Grain size varied from fine to coarse with maximum particle size typically between 19 mm and 25 mm. At Station 4, consistency was rated as hard in the top 200 mm and hard to firm below (Figure 3.33), with the DCP penetrating the layer relatively easily. At Station 12, DCP penetration was slower with consistency rated as hard in the top 40 mm of material, very hard between 40 mm and 240 mm, and hard to firm towards the subgrade.

- Recementation of the base material was visibly apparent in both test pits, although bond strengths appeared weaker in the test pit at Station 4. On this pit face, a strong hydrochloric acid reaction, and a moderate phenolphthalein reaction were recorded (with pink indicating a pH of between 8.4 and 10 [attributed to possible carbonation of the cemented layer or to weak cementation]). At Station 12, strong hydrochloric acid and phenolphthalein reactions were recorded.
- Moisture content in the base was rated as moist.
- The layer definition between the base and subgrade was clear. No punching of the base into the in situ material was noted.
- The subgrade was moist, to wet dark brown clay with medium to high plasticity. Mottling was evident. Consistency was rated as hard and structure as slickensided. Some organic matter was noted. No hydrochloric acid or phenolphthalein reaction was recorded.

Figure 3.34: 587RF test pit location.

Figure 3.35: 587RF#4 test pit profile.

Figure 3.36: 587RF#12 test pit profile.

Figure 3.37: 587RF#4 cracks in overlay and underlying DGAC.

Figure 3.38: 587RF#4 cracks in underlying DGAC.

Figure 3.39: 587RF#12 absence of visible cracks.

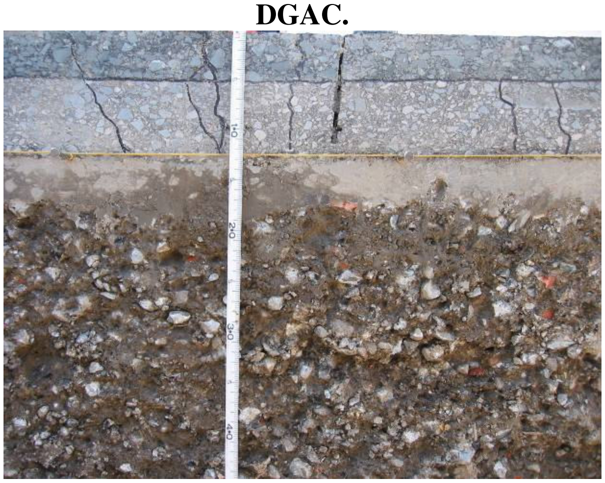

Figure 3.40: 587RF#4 weaker cemented base material.

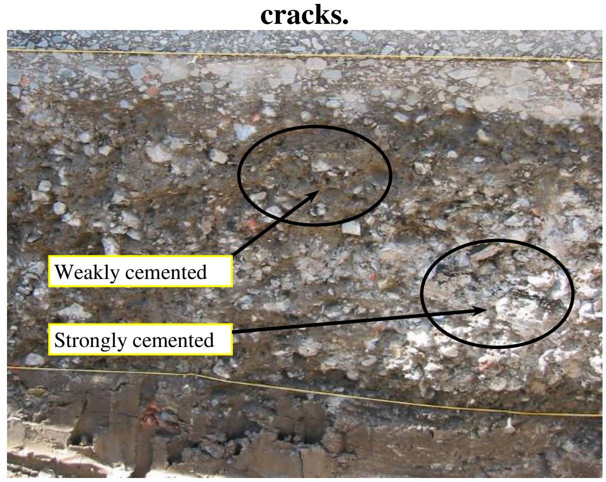

Figure 3.41: 587RF#12 areas of strong and weak base cementation.

3.4.3 Section 588RF: 90 mm AR4000-D

Observations from the Section 588RF test pits (Figure 3.42) include:

- The average thicknesses of the overlay and underlying DGAC in both test pits were close to the design thickness (89 mm and 93 mm for the overlay and 92 mm and 89 mm for the underlying layer).
- Rutting was noted in both the overlay and the underlying layer (Figures 3.43 and 3.44). Some rutting was also measured at the top of the base in the test pit at Station 12. No rutting was observed in the subgrade. Displacement was recorded on either side of the trafficked area. The rut resulting from Phase 1 trafficking could not be clearly distinguished from that resulting from Phase 2 trafficking.
- The overlay was generally poorly bonded to the underlying layer (Figure 3.45). Bonding between lifts was also unsatisfactory (Figure 3.46). Water from the saw cutting operation was still clearly visible in these poorly bonded areas after the rest of the profile had dried. The DGAC was well bonded to the aggregate base.
- Bottom-up cracking was noted in the underlying DGAC and in the overlay in both test pits. Some of the cracks originated at the bottom of the underlying DGAC and continued all the way to the surface (Figure 3.44), while some appeared to have stopped at the bond between the two lifts of the overlay. A few bottom-up cracks originating from the weak bond between the overlay and the underlying layer and between the overlay lifts were also noted (Figure 3.47). Some segregation was noted in the underlying DGAC layer (Figure 3.46).
- The average thickness of the base was considerably less (364 mm and 348 mm for the two test pits) than the design. The base material was dark grey-brown and consisted primarily of non-plastic recycled construction rubble, which included various types of natural aggregate (including quartz, quartzite pebbles, phyllite, basalt, and granite) and small quantities of brick, glass, fabric, wood chips and other organic matter. The structure was generally homogenous. Grain size varied from fine to coarse with maximum particle size typically between 19 mm and 25 mm. At Station 4, consistency was rated as hard in the top 100 mm, as very hard between 100 mm and 200 mm, as hard between 200 and 260 mm, and as hard to firm below 260 mm. At Station 12, consistency was rated as hard in the top 60 mm of material, very hard between 60 mm and 250 mm, and hard to firm below.
- Recementation of the base material was visibly apparent in both test pits, although bond strengths appeared weaker in the test pit at Station 12 (Figure 3.48) compared to the material at Station 4 (Figure 3.49). Relatively strong hydrochloric acid and phenolphthalein reactions were recorded in both test pits.
- Moisture content in the base was rated as moist.

- The layer definition between the base and subgrade was clear. Some punching of the base into the in situ material was noted.
- The subgrade was moist, to wet dark brown clay with medium to high plasticity. Mottling was evident. Consistency was rated as hard and structure as slickensided. Some organic matter was noted. No hydrochloric acid or phenolphthalein reaction was recorded.

Figure 3.42: 588RF test pit location.

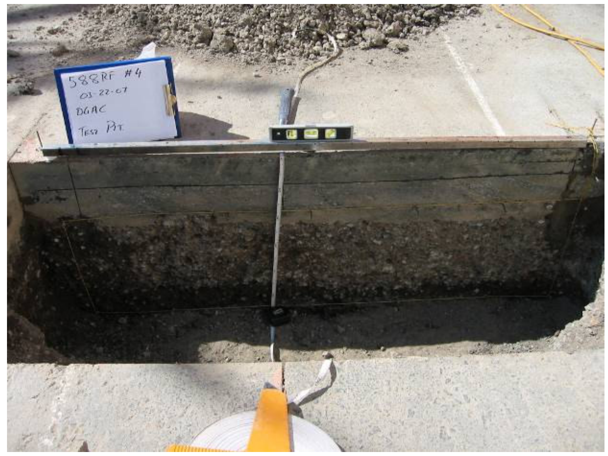

Figure 3.43: 588RF#4 test pit profile.

Figure 3.44: 588RF#12 test pit profile.

Figure 3.45: 588RF debonding between overlay and underlying layer.

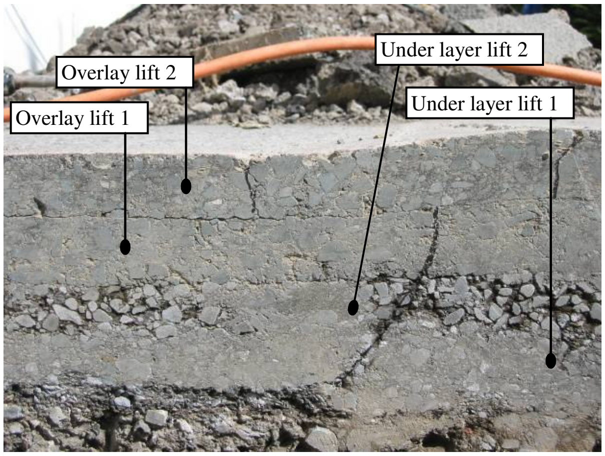

Figure 3.46: 588RF poor bonding between layers.

Figure 3.47: 588RF cracks in overlay and underlying DGAC.

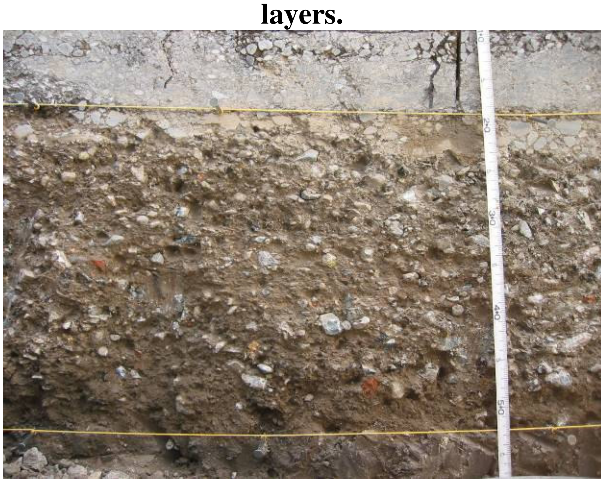

Figure 3.48: 588RF#12 weaker cemented base material.

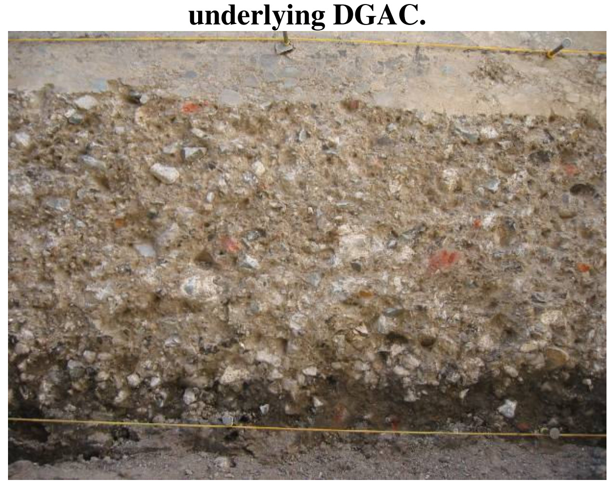

Figure 3.49: 588RF#4 areas of strong base cementation.

3.4.4 Section 589RF: 45 mm MB4-G

Observations from the Section 589RF test pits (Figure 3.50) include:

- The average thickness of the overlay generally equaled the design thickness, while the average thickness of the underlying DGAC was considerably less than the design (84 mm and 75 mm at Stations 4 and 12 respectively).
- Very little rutting/densification was evident in the overlay. Rutting in the underlying DGAC from the Phase 1 trafficking was noted in the Station 4 profile (Figure 3.51), but no rutting was noted in the base and subgrade on this profile. At Station 12, the severe rutting observed occurred predominantly in the underlying DGAC layer, with some rutting in the base and only minor densification in the overlay (Figure 3.52). No rutting was recorded in the subgrade. Severe displacement was recorded on either side of the trafficked area at the Station 12 test pit (Figure 3.53).
- The overlay was well bonded to the DGAC, which was well bonded to the aggregate base.

- Bottom-up cracking was noted in the DGAC layer in both test pits. No propagation of the cracks into the overlay was observed. However, this could be attributed to resealing of any cracks when the overlay was heated during sawing and excavation of the test pit. No other distresses were noted in the asphalt concrete layers.
- The average thickness of the base was less than the design (average 362 mm to 385 mm). The base material was dark grey-brown and consisted primarily of non-plastic recycled construction rubble, which included various types of natural aggregate (predominantly basalt, andesite, quartz and quartzite pebbles) and small quantities of brick, glass, fabric, and organic matter. The structure was generally homogenous. Grain size varied from fine to coarse with maximum particle size typically between 19 mm and 25 mm. The material from the test pit at Station 12 appeared coarser than in other pits (Figures 3.54 and 3.55). Consistency was rated as very hard in the top 250 mm, hard between 250 mm and 290 mm, and hard to firm below as moisture content increased.
- Recementation of the base material was visibly apparent. A cement odor was present and moderate hydrochloric acid and phenolphthalein reactions were noted in some areas.
- Moisture content in the base was rated as moist.
- The layer definition between the base and subgrade was clear. Some punching of the base material into the subgrade was observed.
- The subgrade was moist, dark brown clay with medium to high plasticity. Mottling was evident. Consistency was rated as hard and structure as slickensided. Some organic matter was noted. No hydrochloric acid or phenolphthalein reaction was recorded.

Figure 3.50: 589RF test pit location.

Figure 3.51: 589RF#4 test pit profile.

Figure 3.52: 589RF#12 test pit profile.

Figure 3.53: 589RF#12 severe displacement on edge of rut.

Figure 3.54: 589RF#4 base material.

Figure 3.55: 589RF#12 base material (coarser than other pits).

3.4.5 Section 590RF: 90 mm MB4-G

Observations from the Section 590RF test pits (Figure 3.56) include:

- The average thickness of the overlay varied between 86 mm (Station 4) and 94 mm (Station 12). The average thickness of the underlying DGAC was considerably less than the design (average of 81 mm in both test pits).
- Very little rutting/densification was recorded on the section, with most occurring in the underlying DGAC (Figures 3.57 and 3.58). Rutting in the underlying DGAC from the Phase 1 trafficking was noted in the Station 12 profile (Figure 3.58). No significant displacement was measured and no rutting was noted in the base and subgrade.
- The overlay was well bonded to the DGAC, which was well bonded to the aggregate base.
- Bottom-up cracking was noted in the DGAC layer in both test pits (Figure 3.59). No propagation of the cracks into the overlay was observed, however, this could be attributed to resealing of any

cracks when the overlay was heated during sawing and excavation of the test pit. No other distresses were noted in the asphalt concrete layers.

- The average thickness of the base was less than the design (average 359 mm to 366 mm). The base material was dark grey-brown and consisted primarily of non-plastic recycled construction rubble, which included various types of natural aggregate (predominantly basalt, andesite, quartz and quartzite pebbles) and small quantities of brick, glass, fabric, and organic matter (Figures 3.60 and 3.61). The structure was generally homogenous. Grain size varied from fine to coarse with maximum particle size typically between 19 mm and 25 mm. Consistency was rated as very hard in the top 200 mm, as hard between 200 mm and 220 mm, and as firm below.
- Recementation of the base material was visibly apparent. A cement odor was present and moderate hydrochloric acid and phenolphthalein reactions were noted in some areas.
- Moisture content in the base was rated as moist.
- The layer definition between the base and subgrade was clear. Some punching of the base material into the subgrade was observed.
- The subgrade was moist, dark brown clay with medium to high plasticity. Mottling was evident. Consistency was rated as hard and structure as slickensided. Some organic matter was noted. No hydrochloric acid or phenolphthalein reaction was recorded.

Figure 3.56: 590RF test pit location.

Figure 3.57: 590RF#4 test pit profile.

Figure 3.58: 590RF#12 test pit profile.

Figure 3.59: 590RF cracks in DGAC layer.

Figure 3.60: 590RF#4 base material.

Figure 3.61: 590RF#12 base material.

3.4.6 Section 591RF: 45 mm MAC15-G

Observations from the Section 591RF test pits (Figure 3.62) include:

- The average thickness of the overlay was slightly thicker than the design (51 mm at Station 4 and 49 mm at Station 12), while the average thickness of the underlying DGAC was considerably less than the design (72 mm and 80 mm at Stations 4 and 12 respectively).
- Very little rutting/densification was evident in the overlay. Rutting in the underlying DGAC from Phase 1 trafficking was noted in both test pits (Figures 3.63 to 3.65). Some rutting, attributed to Phase 1 trafficking, was noted at the top of the base in both test pits. No rutting was observed in the subgrade and no displacement was recorded on either side of the trafficked area.
- The overlay was well bonded to the DGAC, which was well bonded to the aggregate base.

- Bottom-up cracking was noted in the DGAC layer in both test pits (Figure 3.66). No propagation of the cracks into the overlay was observed. However, this could be attributed to resealing of any cracks when the overlay was heated during sawing and excavation of the test pit. No other distresses were noted in the asphalt concrete layers.
- The average thickness of the base was considerably less than the design (average 325 mm and 333 mm for the two test pits, respectively). The base material was dark grey-brown and consisted primarily of non-plastic recycled construction rubble, which included various types of natural aggregate (including andesite, phyllite, quartz and quartzite pebbles) and small quantities of brick, glass, wire, fabric, and organic matter (Figure 3.67). The structure was generally homogenous. Grain size varied from fine to coarse with maximum particle size typically between 19 mm and 25 mm. Consistency was rated as hard to very hard in the top 200 mm, and hard below that (Figure 3.68).
- Recementation of the base material was visibly apparent. A cement odor was present and strong hydrochloric acid and phenolphthalein reactions were noted.
- Moisture content in the base was rated as moist.
- The layer definition between the base and subgrade was clear. Some punching of the base into the in situ material was noted (Figure 3.68).
- The subgrade was moist, dark brown clay with medium to high plasticity. Some punching of aggregate from the base was recorded (Figure 3.69). Mottling was evident. Consistency was rated as hard and structure as slickensided. Some organic matter was noted. No hydrochloric acid or phenolphthalein reaction was recorded.

Figure 3.62: 591RF test pit location.

Figure 3.63: 591RF#4 test pit profile.

Figure 3.64: 591RF#4 rutting from Phase 1 trafficking.

Figure 3.65: 591RF test pit profile.

Figure 3.66: 591RF cracks in underlying DGAC.

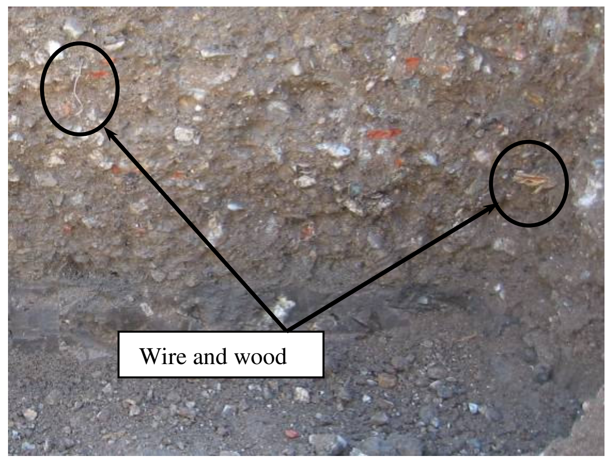

Figure 3.67: 591RF wire and wood in base material.

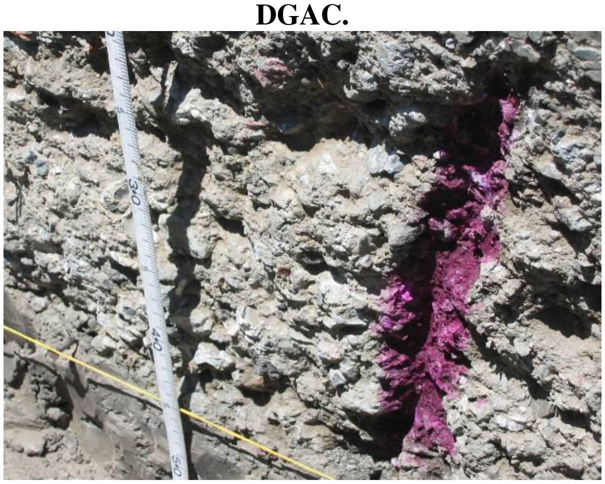

Figure 3.68: 591RF strongly cemented base.

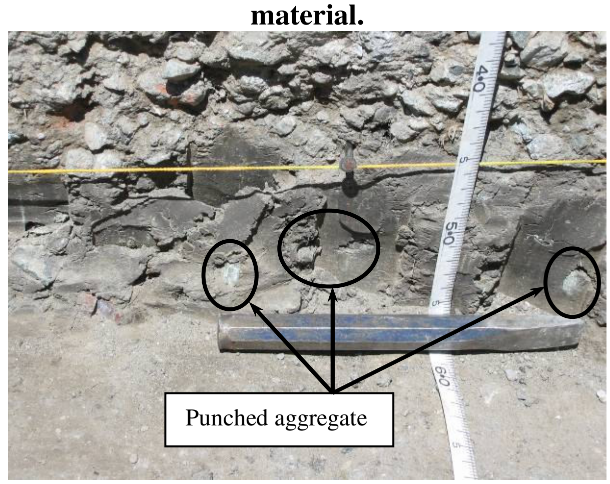

Figure 3.69: 591RF aggregate punched into subgrade.

3.5. Density and Moisture Content

Table 3.3 (rutting study) and Table 3.4 (reflective cracking study) summarize the density and moisture content measurements on each section. The tables include wet and dry density and moisture content of the base as measured with a nuclear gauge, the laboratory determined gravimetric moisture content of the base (average of two samples from the top and bottom of the excavated base), the subgrade laboratory determined gravimetric moisture content (sample removed from the bottom of the test pit, approximately 200 mm below the bottom of the base), and the recalculated dry density of the base (using the gravimetric moisture content). The gauge measurements are an average of two readings taken in the pit (see Figure 3.1).

Table 3.3: Rutting Study Density and Moisture Content Measurements

	Section and Test Pit Station	Depth	Nuclear Gauge			Laboratory		
			Wet density (kg/m^3)	Moisture (%)	Dry Density (kg/m^3)	Base Moisture (%)	Dry Density* (kg/m^3)	Subgrade Moisture (%)
Rutting	580RF (MB15-G)	50	2,123	9.2	1,947	6.9	2,031	15.1
		100	2,174	8.7	2,001			
		150	2,199	9.0	2,019			
		200	2,189	9.0	2,010			
	581RF (RAC-G)	50	2,160	10.7	1,952	8.2	2,040	12.9
		100	2,197	10.9	1,981			
		150	2,240	10.8	2,023			
		200	2,232	10.4	2,022			
	582RF (AR4000-D)	50	2,292	11.8	1,783	8.6	1,988	17.3
		100	2,033	10.6	1,839			
		150	2,131	11.1	1,919			
		200	2,182	10.5	1,975			
	583RF (45mm MB4-G)	50	2,095	10.2	1,900	8.8	1,998	14.7
		100	2,173	9.6	1,983			
		150	2,215	9.6	2,022			
		200	2,212	9.5	2,019			
	584RF (90mm MB4-G)	50	2,146	12.8	1,816	9.2	1,964	15.6
		100	2,097	12.2	1,870			
		150	2,150	12.4	1,921			
		200	2,190	11.6	1,963			
	585RF (MAC15-G)	50	2,114	11.3	1,900	8.3	2,015	14.4
		100	2,178	11.1	1,962			
		150	2,212	10.9	1,995			
		200	2,225	10.7	2,009			

* Recalculated dry density using gauge wet density and laboratory gravimetric moisture content.

Table 3.4: Reflective Cracking Study Density and Moisture Content Measurements

	Section and Test Pit Station	Depth	Nuclear Gauge			Laboratory		
			Wet Density (kg/m^3)	Moisture (%)	Dry Density (kg/m^3)	Base Moisture (%)	Dry Density* (kg/m^3)	Subgrade Moisture (%)
Reflective Cracking	586RF#4 (MB15-G)	50	2,146	11.0	1,935	8.6	2,037	15.7
		100	2,234	11.2	2,014			
		150	2,232	10.9	2,013			
		200	2,237	10.7	2,022			
	586RF#12 (MB15-G)	50	2,073	9.9	1,887	8.5	1,998	14.0
		100	2,147	9.9	1,954			
		150	2,202	9.5	2,012			
		200	2,249	8.9	2,064			
	587RF#4 (RAC-G)	50	2,070	12.5	1,841	8.8	1,980	17.1
		100	2,146	12.0	1,917			
		150	2,193	11.4	1,968			
		200	2,212	11.7	1,981			
	587RF#12 (RAC-G)	50	2,203	11.3	1,981	8.9	2,057	18.0
		100	2,249	11.0	2,027			
		150	2,257	10.9	2,035			
		200	2,254	11.3	2,025			
	588RF#4 (AR4000-D)	50	2,084	11.5	1,870	9.2	1,974	14.0
		100	2,147	11.7	1,924			
		150	2,183	11.4	1,962			
		200	2,212	11.3	1,989			
	588RF#12 (AR4000-D)	50	2,163	12.1	1,929	9.0	2,033	14.1
		100	2,216	12.0	1,980			
		150	2,237	11.8	2,003			
		200	2,250	11.4	2,020			
	589RF#4 (45mm MB4-G)	50	2,012	11.0	1,809	8.9	1,938	14.6
		100	2,111	10.6	1,910			
		150	2,135	10.6	1,931			
		200	2,185	10.1	1,984			
	589RF#12 (45mm MB4-G)	50	2,159	11.6	1,936	8.6	2,222	15.5
		100	2,207	10.7	1,994			
		150	2,262	11.3	2,003			
		200	2,261	11.1	2,036			
	590RF#4 (90mm MB4-G)	50	2,041	13.4	1,802	9.1	1,947	15.1
		100	2,115	13.7	1,862			
		150	2,149	14.4	1,905			
		200	2,196	12.6	1,952			
	590RF#12 (90mm MB4-G)	50	2,107	13.1	1,864	9.2	1,972	15.2
		100	2,144	12.3	1,911			
		150	2,170	11.8	1,941			
		200	2,193	11.7	1,964			
	591RF#4 (MAC15-G)	50	2,114	11.5	1,897	8.8	2,006	15.0
		100	2,160	11.1	1,945			
		150	2,218	11.2	1,997			
		200	2,240	10.5	2,028			
	591RF#12 (MAC15-G)	50	2,131	11.1	1,919	8.0	2,034	15.6
		100	2,186	10.8	1,974			
		150	2,227	10.6	2,014			
		200	2,242	10.5	2,030			

* Recalculated dry density using gauge wet density and laboratory gravimetric moisture content.

Densities were generally consistent throughout the section. Nuclear gauge determined wet densities ranged between 2,111 kg/m^3 and 2,241 kg/m^3 for the 18 test pits (average 2,176 kg/m^3, standard deviation 34 kg/m^3). This corresponds with the average wet density of 2,200 kg/m^3 for the road base recorded after construction. The average nuclear gauge determined dry density was 1,956 kg/m^3 with a standard deviation of 44 kg/m^3. The lowest dry density recorded was 1,879 kg/m^3 (582RF) and the highest was 2,017 kg/m^3 (587RF).

Nuclear gauge determined moisture contents, measured at four intervals in the top 200 mm of the base, averaged 11.1 percent (standard deviation of 1.1 percent) for the 18 test pits. The highest moisture content measured was 14.4 percent (590RF, Station 4 at 150 mm depth), while the lowest was 8.7 percent (580RF, at 100 mm depth). In most test pits, the moisture content in the upper 50 mm was on the order of one percent higher than in the material between 150 mm and 200 mm. The optimum moisture content of the Class II aggregate base material, determined prior to construction, was 8.9 percent, somewhat lower than the average recorded with the nuclear gauge.

Laboratory-determined gravimetric moisture contents varied between 6.9 percent and 9.2 percent, with an average of 8.7 percent. The laboratory-determined moisture contents were on average 2.0 percent lower (between 0.9 and 4.4 percent) than that recorded by the nuclear gauge, and were therefore more consistent with the optimum moisture content of the material. The higher moisture contents determined with the nuclear gauge could be associated with the presence of some excess moisture from the saw cutting operation during pit excavation. Recalculated dry densities, determined using the gauge wet density and gravimetric moisture content, were therefore higher than the gauge determined dry densities.

Subgrade densities were not measured. The average subgrade moisture content was 15 percent (lowest of 12.9 percent, and highest of 18.0 percent), considerably higher than the base moisture content. The presence of mottling in the subgrade material indicates that the moisture content probably fluctuated seasonally.

3.6. Dynamic Cone Penetrometer

Dynamic Cone Penetrometer (DCP) analysis plots for the trafficked and untrafficked areas from each test pit are provided in Appendix B. A summary of the results is provided in Tables 3.5 and 3.6.

Table 3.5: Rutting Study Dynamic Cone Penetrometer Summary

	Section	Trafficked					Untrafficked				
		DSN*	Redefined Layers	Penetration (mm/blow)	DCP-Derived Strengths		DSN*	Redefined Layers	Penetration (mm/blow)	DCP-Derived Strengths	
					UCS (kPa)	E-Modulus (MPa)				UCS (kPa)	E-Modulus (MPa)
Rutting	580RF (MB15-G)	281	0–70 70–193 193–249 249–295 295–450 450–800	1.80 0.95 1.43 3.13 10.54 16.67	1487 2340 1780 835 215 129	599 1182 763 332 92 56	271	0–90 90–152 152–202 202–290 290–640 640–800	1.33 0.64 1.46 3.81 14.14 24.97	1882 2791 1757 669 155 82	825 1793 749 269 67 37
	581RF (RAC-G)	157	0–44 44–136 136–288 288–438 438–800	3.19 1.49 2.89 11.28 56.39	816 1724 913 199 33	325 730 362 85 15	188	0–44 44–110 110–245 245–316 316–800	2.95 1.90 1.46 3.81 26.20	892 1425 1750 669 78	354 564 745 269 35
	582RF (AR4000-D)	175	0–95 5–211 211–328 328–800	3.61 1.50 3.60 16.12	711 1720 713 134	285 728 286 58	213	0–95 95–124 124–181 181–297 297–398 398–800	3.22 1.98 1.17 1.62 4.49 24.09	809 1388 2063 1612 558 85	323 542 948 667 227 38
	583RF (45mm MB4-G)	190	0–65 65–226 26–300 300–800	2.24 1.17 3.27 26.86	1210 1745 794 76	473 742 317 34	229	0–90 90–145 145–221 221–290 290–800	1.42 0.94 1.51 4.75 17.69	1789 2348 1709 524 120	768 1190 722 213 53
	584RF (90mm MB4-G)	156	0–99 99–238 238–800	1.65 2.94 14.41	1590 894 151	655 355 66	149	0–184 184–246 246–800	1.79 4.50 23.98	1489 556 86	600 226 38
	585RF (MAC15-G)	208	0–32 32–187 187–252 252–800	2.14 1.26 2.78 14.68	1279 1952 954 148	498 870 377 64	181	0–266 266–335 335–800	1.97 4.92 22.03	1389 503 94	542 206 42

Table 3.6: Reflective Cracking Study Dynamic Cone Penetrometer Summary

	Section	Trafficked					Untrafficked				
		DSN[1]	Redefined Layers	Penetration (mm/blow)	DCP-Derived Strengths UCS[2] (kPa)	DCP-Derived Strengths E-Modulus[3] (MPa)	DSN	Redefined Layers	Penetration (mm/blow)	DCP-Derived Strengths UCS (kPa)	DCP-Derived Strengths E-Modulus (MPa)
Reflective Cracking	586RF#4 (MB15-G)	337	0–181	1.65	1594	658	295	0–91	3.09	847	337
			181–291	0.81	2533	1396		91–304	1.07	2175	1035
			291–336	2.40	1122	440		304–363	2.57	1041	410
			336–800	15.01	145	63		363–800	13.08	169	73
	586RF#12 (MB15-G)	DCP did not penetrate					298	0–47	3.45	748	300
								47–147	1.12	2112	985
								147–229	0.83	2510	1368
								229–305	2.24	1213	474
								305–718	12.00	186	80
								718–800	31.00	64	29
	587RF#4 (RAC-G)	217	0–241	1.49	1725	731	193	0–284	2.03	1351	525
			241–298	3.86	660	266		284–408	9.66	237	100
			298–800	23.32	88	39		408–800	22.72	91	41
	587RF#12 (RAC-G)	234	0–47	2.46	1094	430	239	0–31	2.08	1318	513
			47–237	1.33	1880	824		31–180	1.14	2088	967
			237–307	3.10	843	335		180–230	1.72	1536	626
			307–800	15.53	139	61		230–290	3.50	736	295
								290–800	17.54	122	53
	588RF#4 (AR4000-D)	163	0–105	2.60	1026	404	186	0–79	3.98	638	257
			105–210	1.49	1722	729		79–271	1.68	1570	645
			210–264	3.80	673	271		271–393	5.96	406	168
			264–800	21.50	97	43		393–800	26.34	78	35
	588RF#12 (AR4000-D)	138	0–276	2.69	988	390	223	0–68	4.56	548	223
			276–385	7.81	300	126		68–259	1.41	1804	777
			385–800	31.30	64	29		259–348	7.80	301	126
								348–800	20.82	100	44
	589RF#4 (45mm MB4-G)	232	0–244	1.45	1765	754	217	0–228	1.40	1809	780
			244–292	3.39	764	306		228–280	3.84	664	267
			292–800	13.80	159	69		280–800	16.51	130	57
	589RF#12 (45mm MB4-G)	175	0–268	1.95	1399	548	185	0–69	1.61	1620	672
			268–800	18.16	117	51		69–112	0.88	2432	1278
								112–194	1.67	1577	648
								194–254	4.13	612	247
								254–800	22.89	90	40

[1] DCP Structure Number (number of blows to 800 mm) [2] Unconfined compressive strength [3] Elastic modulus

Table 3.6: Reflective Cracking Study Dynamic Cone Penetrometer Summary (cont)

	Section	Trafficked					Untrafficked				
		DSN*	Redefined Layers	Penetration (mm/blow)	DCP derived strengths		DSN*	Redefined Layers	Penetration (mm/blow)	DCP-Derived Strengths	
					UCS (kPa)	E-Modulus (MPa)				UCS (kPa)	E-Modulus (MPa)
Reflective Cracking	590RF#4 (90mm MB4-G)	153	0–64	2.59	1032	407	174	0–92	1.92	1416	558
			64–102	1.92	1416	559		92–161	1.17	2056	943
			102–155	1.22	2004	906		161–228	2.93	900	357
			155–204	3.57	721	289		228–800	15.26	142	62
			204–560	14.42	151	66					
			560–800	10.38	219	93					
	590RF#12 (90mm MB4-G)	153	0–190	2.01	1368	531	220	0–35	1.84	1458	582
			190–800	12.53	177	76		35–150	0.92	2380	1222
								150–210	2.56	1046	412
								210–800	17.72	120	53
	591RF#4 (MAC15-G)	178	0–191	1.47	1740	739	234	0–42	1.27	1941	863
			191–244	4.01	632	255		42–137	0.76	2603	1489
			244–524	18.78	113	50		137–215	3.20	816	325
			524–800	33.09	60	27		215–620	19.45	108	48
								620–800	10.65	212	91
	591RF#12 (MAC15-G)	169	0–270	0.76	1229	480	183	0–198	1.49	1727	732
			270–800	4.48	88	39		198–275	5.84	416	171
								275–800	29.45	68	31

[1] DCP Structure Number (number of blows to 800 mm) [2] Unconfined compressive strength [3] Elastic modulus

The DCP Structure Number (DSN_{800}) is the total number of blows needed to penetrate 800 mm into the pavement structure and is used as a quick indicator of the overall pavement strength. A summary of this parameter from the 18 test pits is provided in Table 3.7.

Table 3.7: Summary of DSN800 Analysis

Sample	DCP Location	Average	Standard Deviation	Lowest	Highest
All pits	All	212	50	138	337
All pits	Trafficked Untrafficked	205 219	56 44	138 149	337 298
Pits on rutting sections	All	200	43	149	281
Pits on cracking sections	All	222	54	138	337
Pits on rutting sections	Trafficked Untrafficked	195 205	47 42	156 149	281 271
Pits on cracking sections	Trafficked Untrafficked	214 230	66 45	138 135	337 298

The summary results indicate that the trafficked areas were marginally stronger than the untrafficked areas and that the reflective cracking sections were marginally stronger than the rutting sections. This is probably attributed to the higher number of load repetitions on the sections and the associated densification of the material. It is interesting to note that the weakest section (588RF at Station 12) was also the area with the most cracking on completion of testing.

Further analysis of the results indicate the presence of a weaker area at the top of the base (upper 30 to 90 mm) and an even weaker area at the bottom of the base. This is consistent with observations in the pits. The weak upper layer could be attributed to poor compaction, to crushing under HVS loading, or a combination of the two. It is not attributed to carbonation of the recemented layer, based on the results of phenolphthalein tests in the pits. The weak area at the bottom of the base is attributed to poor compaction associated with the poor support provided by the relatively weak subgrade.

The DCP-derived Unconfined Compressive Strength (UCS) and elastic modulus are consistent with measurements on highways around the state.

3.7. Assessment of Cores

3.7.1 Visual Assessment

Up to 20 cores were sampled from the trafficked area on each section, including eight cores from each test pit slab. These cores were obtained to gain a better understanding of where the crack initiated, the crack path, where the crack it terminated, and how far cracks continued into the overlays. Each core was cleaned and then scrutinized for cracks. Photographs of the cores from each section are shown in Figures 3.70 to 3.76. Cracks have been highlighted. If no cracks were observed on the sides or bottom and top faces, the core was split in a similar manner to an indirect tensile test to determine whether it would break on a weak plane caused by the presence of a crack.

Figure 3.70: MB15-G: Cracks on core.

Figure 3.71: RAC-G: Cracks on core.

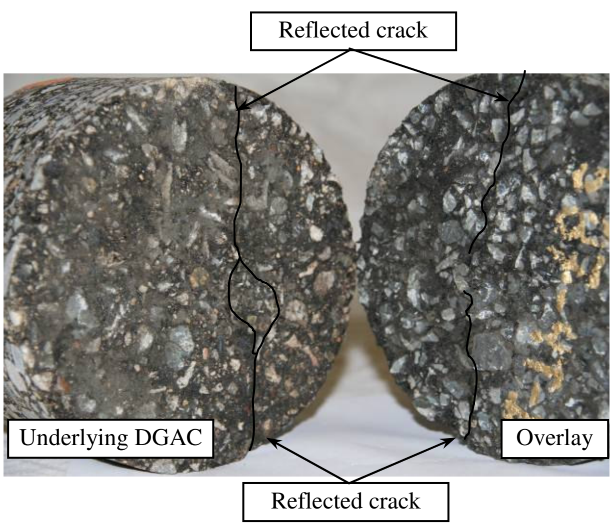

Figure 3.72: RAC-G: Highlighted reflected crack through both layers.

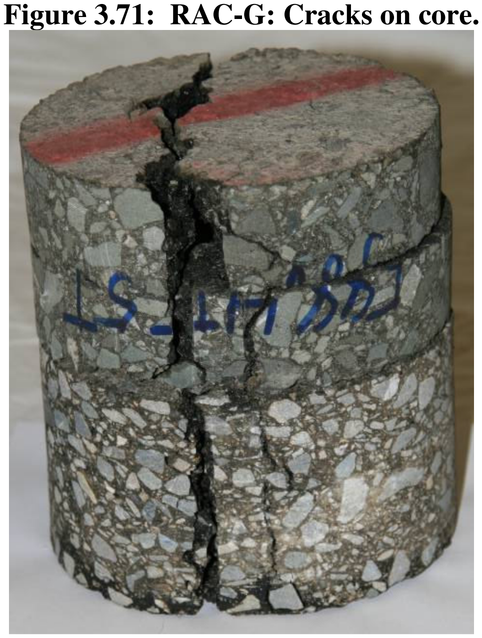

Figure 3.73: AR4000-D: Cracks on core.

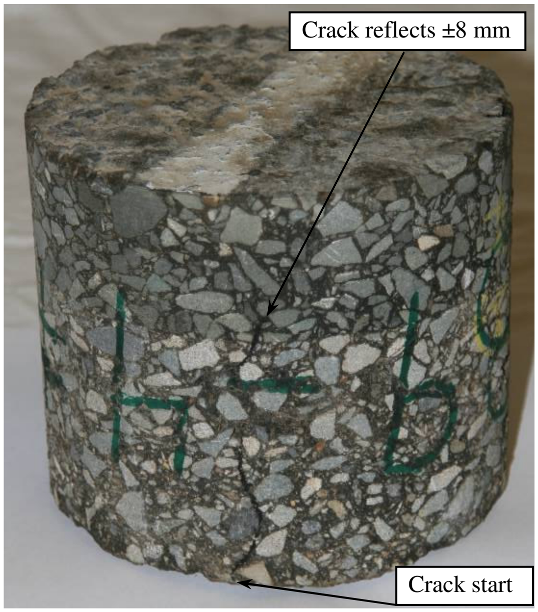

Figure 3.74: 45 mm MB4-G: Cracks on core.

Figure 3.75: 90 mm MB4-G: Cracks on core..

Figure 3.76: MAC15-G: Cracks on core.

Very little information on cracking patterns was obtained from this assessment. This was attributed to a number of factors including the sealing of cracks with melted rubber during the coring process. Reflected cracks were only clearly distinguishable on the AR4000-D and RAC-G cores. These cracks all appeared to have initiated close to the bottom of the underlying DGAC layer and then propagated through to the surface (Figures 3.71 to 3.73). No cores were retrieved from the severely cracked area of Section 588RF (AR4000-D), because the test pit slab disintegrated when it was handled. No conclusions could be drawn regarding the depth (if any) that cracks had reflected through into those overlays that did not crack after HVS testing (i.e., MB4-G, MB15-G and MAC15-G).

3.7.2 Final Air-Void Content

The air-void contents of the trafficked reflective cracking sections were determined from cores removed from each section during the forensic investigation. Results are summarized in Table 3.8.

Table 3.8: Summary of Air-Void Contents after HVS Testing

Section	Overlay	Number of Cores	Air-Void content (%)					
			Average		Std. Dev		Lowest	Highest
			After	(Before)[1]	After	(Before)[1]		
586RF	MB15-G	16	3.8	(5.1)	1.5	(1.7)	2.2	6.8
587RF	RAC-G	13	4.0	(8.8)	1.6	(1.3)	2.3	7.0
588RF	AR4000-D	21	6.5	(7.1)	1.6	(1.5)	3.3	9.4
589RF	45 mm MB4-G	10	2.9	(6.5)	1.2	(0.6)	1.5	5.2
590RF	90 mm MB4-G	15	1.9	(6.5)	0.7	(0.6)	0.8	3.6
591RF	MAC15-G	12	2.7	(4.9)	1.5	(1.0)	3.2	8.0

[1] Before HVS testing, included for comparison. Cores taken outside HVS section.

The results show that the air-void content decreased after HVS trafficking on all sections except Section 591RF. It is not clear why the air-void content on Section 591RF increased, although it could be attributed to the first set of cores being taken from outside of the section (closer to the edge of the road), which may have had a slightly higher compaction. The largest change was recorded on Section 590RF and the smallest on Section 588RF. Variability along and across the section was relatively high, this being attributed to the programmed wander pattern of the HVS, which applies more passes in the center portion of the section compared to the edges.

3.8. Microscope Study

3.8.1 Background and Objectives

Samples removed from the test pits in Section 591RF were assessed using optical and scanning electron (SEM) microscopes in an attempt to determine whether the cementation of the base material resulting from vestigial cement generated during breaking up and processing had occurred. No additional cement was added during construction of the test track. It should be noted that this was only a very brief investigation and that a more thorough exercise on a wider spectrum of samples might reveal additional information.

Various components of the pavement were investigated using a number of samples. Two samples are discussed below:

- Sample 1: Intact base material matrix, and
- Sample 2: Intact base material matrix after exposure to atmospheric air for 10 days.

3.8.2 Observations

Sample 1

This material was the essentially uncarbonated matrix material. Figure 3.77 shows the overall view at a magnification of about 60 times.

Figure 3.77: General SEM view of Sample 1 at ±60x magnification.

The material was generally intact and showed mostly particles of about 100 µm diameter within a cemented matrix. At a greater magnification (Figure 3.78 [optical microscope with ±200x magnification] and Figure 3.79 [SEM with ±600x magnification]), definite interlocking needle-like crystals can be identified in fragments of the original stabilized material. These are typical of the cementitious products in old, well-stabilized road materials. Closer examination showed that some subsequent (i.e. after construction) crystal development had also occurred.

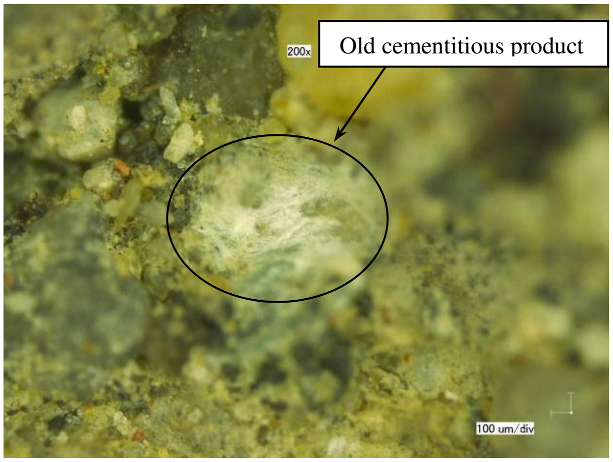

Figure 3.78: Optical microscope view (±200x) of Sample 1.

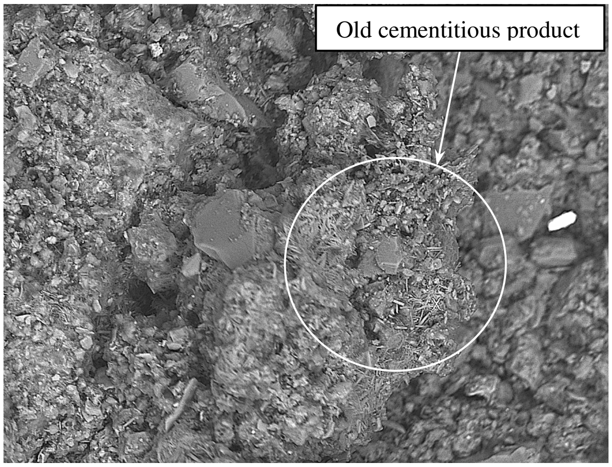

Figure 3.79: SEM view (±600x) of Sample 1.

Sample 2

Sample 2 was exactly the same as Sample 1 except that the specimen was exposed to atmospheric carbon dioxide prior to preparation for the microscope studies. The overall effect is shown in Figure 3.80 (optical microscope at ±100x magnification) and Figure 3.81 (SEM at ±55x magnification), in which significant cracking is visible. This is the typical result of carbonation where the development of calcite (calcium carbonate, $CaCO_3$) from lime (calcium hydroxide, $Ca(OH)_2$) in the material results in expansion and cracking of the material. Such cracking is unlikely to result from drying as it was not seen in the uncarbonated specimen, which was also dried, albeit under slightly different conditions. Figure 3.82 (optical microscope at ±100x magnification), Figure 3.83 (optical microscope at ±200x magnification), and Figure 3.84 (SEM at ±140x magnification) show the presence of calcite crystals associated with the cracking in the carbonated sample, none of which were evident in the uncarbonated material. The well-crystallized nature of the material is indicative of recent formation (during the week before examination). There was also a conspicuous absence of calcium hydroxide, indicating severe carbonation.

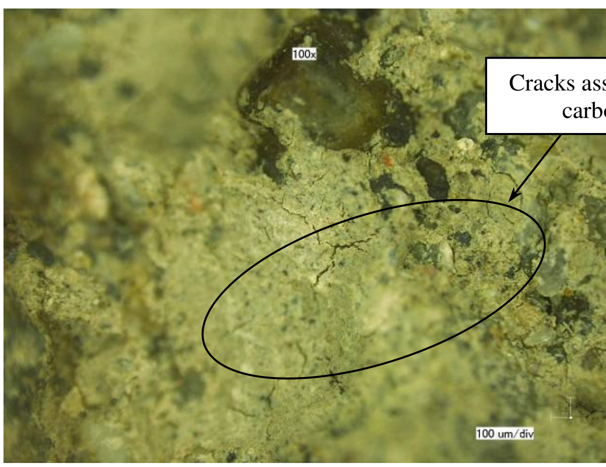

Figure 3.80: Optical microscope view (±100x) of Sample 2.

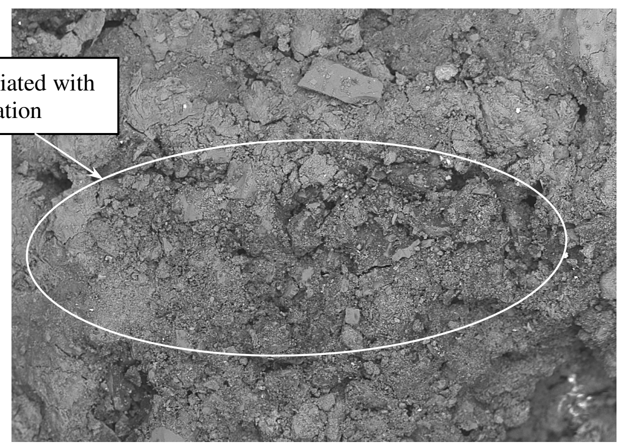

Figure 3.81: SEM view (±55x) of Sample 2.

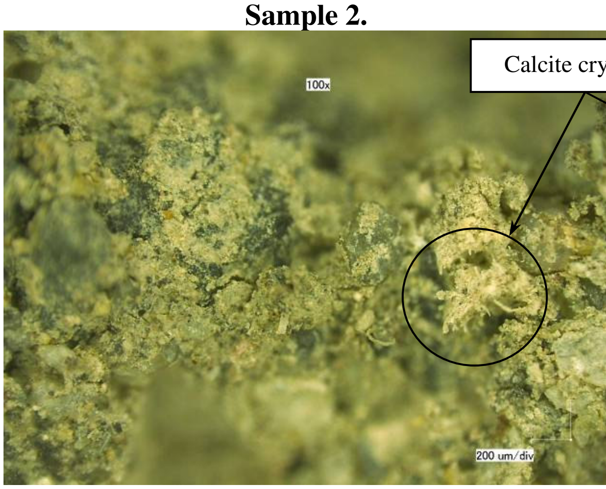

Figure 3.82: Optical microscope view (±100x) of calcite crystal development associated with cracks.

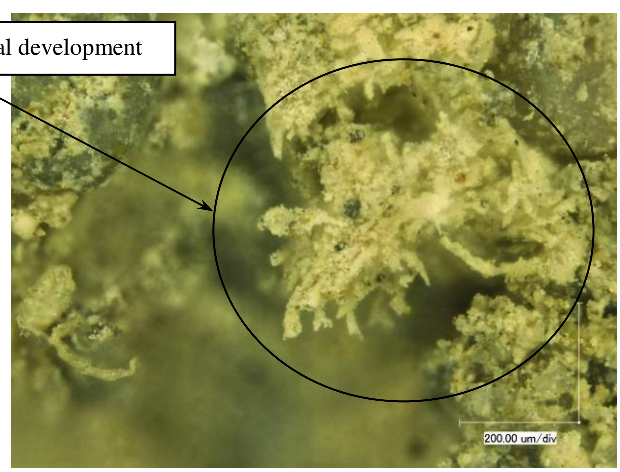

Figure 3.83: Optical microscope view (±200x) of calcite crystal development associated with cracks.

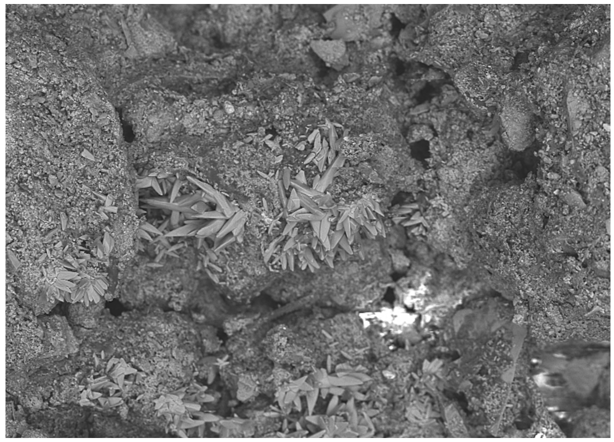

Figure 3.84: SEM view (±140x) of calcite crystal development associated with cracks.

3.9. Second-Level Analysis

A second-level analysis report will be prepared on completion of all HVS testing, laboratory testing, and data analysis. This report will include:

- Comparison of performance between test sections;
- Comparisons of HVS test results with laboratory test results;
- Predicted (mechanistic-empirical) versus actual performance;
- Performance comparison of the overlays with the same underlying support conditions, and
- Simulations using various pavement structures, climatic conditions, traffic volumes, and traffic speeds.

4. CONCLUSIONS

This report follows seven first-level reports that detail the results of HVS testing performed to validate Caltrans overlay strategies for the rehabilitation of cracked asphalt concrete. It describes the findings and observations of the forensic investigation, which included the excavation and assessment of 18 test pits (one on each rutting section and two on each reflective cracking section), nuclear density measurements, Dynamic Cone Penetrometer (DCP) assessments, and a visual assessment of cores. A microscope study was also undertaken to investigate apparent recementation of the base material. Laboratory fatigue and shear studies were conducted in parallel with HVS testing and those results are detailed in separate reports. Comparison of the laboratory and test section performance is discussed in a separate second-level report.

The pavement was designed according to the Caltrans Highway Design Manual Chapter 600 using the computer program *NEWCON90*. Design thickness was based on a subgrade R-value of 5 and a Traffic Index of 7 (~121,000 ESALs). The overlay thickness was determined according to Caltrans Test Method (CTM) 356 using Falling Weight Deflectometer (FWD) deflections.

Findings and observations based on the data collected during this forensic investigation include:

- There was considerable variation in the thicknesses of the base, underlying DGAC, and the overlays over the length and width of the test road.
- In the rutting experiments (Sections 580RF through 585RF), rutting occurred primarily in the underlying DGAC and not in the overlay. In the reflective cracking experiments (Sections 586RF through 591RF), rutting occurred in both layers. Rutting from the Phase 1 trafficking was clearly visible on most test pit profiles. Very little rutting occurred in the base and no rutting was recorded in the subgrade. This corresponds to the Multi-depth Deflectometer permanent deformation analyses discussed in the first-level reports on each section.
- Cracks were observed on some of the test pit profiles. In the underlying DGAC layer, cracks were generally clearly visible. However, in the overlays, heat generated from the saw cut operation appeared to seal any cracks and no conclusions could be drawn as to the depth that cracks had reflected into the overlays. Most cracks appeared to have initiated close to the bottom of the underlying DGAC. Some crack initiation was also observed at poorly bonded joints between lifts and overlays in the AR4000-D section (Section 588RF). No additional information was gathered from an assessment of cores. No cracking was observed in the base.
- Some post-construction cementation of the base material appeared to have occurred. This was substantiated with DCP tests, close inspection of the test pit profile, the use of phenolphthalein to

determine the pH of the base material, and examination of specimens under optical and scanning electron microscopes. This recementation appears to have contributed to the good performance of the sections.

- Densities were generally consistent throughout the section. Nuclear gauge determined wet densities averaged 2,176 kg/m^3 (standard deviation of 34 kg/m^3 [135.8 pcf, standard deviation of 2.1 pcf), which corresponds with the average wet density of 2,200 kg/m^3 (137.3 pcf) for the road base recorded after construction.
- Nuclear gauge determined moisture contents averaged 11.1 percent (standard deviation of 1.1 percent) for the 18 test pits. In most test pits, the moisture content in the upper 50 mm (2 in) was on the order of one percent higher than in the material between 150 mm (6 in) and 200 mm (8 in). The optimum moisture content of the Class II aggregate base material, determined prior to construction, was 8.9 percent, somewhat lower than the average recorded with the nuclear gauge. Laboratory-determined gravimetric moisture contents averaged 8.7 percent, which was closer to the optimum moisture content.
- Subgrade densities were not measured. The average subgrade moisture content was 15 percent (lowest of 12.9 percent, and highest of 18.0 percent), considerably higher than the base moisture content. The presence of mottling in the subgrade material indicates that the moisture content probably fluctuated seasonally.
- The air-void contents of cores removed from the reflective cracking sections after HVS testing were lower compared to those determined from cores removed from outside the sections prior to HVS testing, as expected.

The findings of this investigation confirm the conclusions drawn from analyses of data collected from the instrumentation during HVS testing and documented in the first-level analysis reports.

No recommendations as to the use of the modified binders in overlay mixes are made at this time. These recommendations will be included in the second-level analysis report, which will be prepared and submitted on completion of all HVS and laboratory testing.

5. REFERENCES

1. **Generic experimental design for product/strategy evaluation — crumb rubber modified materials.** 2005. Sacramento, CA: Caltrans.
2. **Reflective Cracking Study: Workplan for the Comparison of MB, RAC-G, and DGAC Mixes Under HVS and Laboratory Testing.** 2003. Davis and Berkeley, CA: University of California Pavement Research Center. (UCPRC-WP-2003-01).
3. BEJARANO, M., Jones, D., Morton, B., and Scheffy, C. 2005. **Reflective Cracking Study: Summary of Construction Activities, Phase 1 HVS Testing, and Overlay Construction**. Davis and Berkeley, CA: University of California Pavement Research Center. (UCPRC-RR-2005-03).
4. JONES, D. Tsai, B.W., and Harvey, J. 2006. **Reflective Cracking Study: First-level Report on HVS Testing on Section 590RF — 90 mm MB4-G Overlay.** Davis and Berkeley, CA: University of California Pavement Research Center. (UCPRC-RR-2006-04)
5. JONES, D., Wu, R., Lea, J., and Harvey, J. 2006. **Reflective Cracking Study: First-level Report on HVS Testing on Section 589RF — 45 mm MB4-G Overlay.** Davis and Berkeley, CA: University of California Pavement Research Center. (UCPRC-RR-2006-05)
6. WU, R., Jones, D., and Harvey, J. 2006. **Reflective Cracking Study: First-level Report on HVS Testing on Section 587RF — 45 mm RAC-G Overlay.** Davis and Berkeley, CA: University of California Pavement Research Center. (UCPRC-RR-2006-06)
7. JONES, D., Wu, R., and Harvey, J. 2006. **Reflective Cracking Study: First-level Report on HVS Testing on Section 588RF — 90 mm DGAC Overlay.** Davis and Berkeley, CA: University of California Pavement Research Center. (UCPRC-RR-2006-07)
8. JONES, D., Wu, R., and Harvey, J. 2006. **Reflective Cracking Study: First-level Report on HVS Testing on Section 586RF — 45 mm MB15-G Overlay.** Davis and Berkeley, CA: University of California Pavement Research Center. (UCPRC-RR-2006-12)
9. JONES, D., Wu, R., and Harvey, J. 2007. **Reflective Cracking Study: First-level Report on HVS Testing on Section 591RF — 45 mm MAC15-G Overlay.** Davis and Berkeley, CA: University of California Pavement Research Center. (UCPRC-RR-2007-04)
10. STEVEN, B., Jones, D., and Harvey, J. 2007). **Reflective Cracking Study: First-level Report on the HVS Rutting Experiment.** Davis and Berkeley, CA: University of California Pavement Research Center. (UCPRC-RR-2007-06)
11. HARVEY, J., Du Plessis, L., Long, F., Deacon, J., Guada, I., Hung, D., and Scheffy, C. 1997. **CAL/APT Program: Test Results from Accelerated Pavement Test on Pavement Structure**

Containing Untreated Base – Section 501RF. Davis and Berkeley, CA: University of California Pavement Research Center. (UCPRC-RR-1997-03 and RTA-65W4845-3)

12. JONES, D. 2005. **Quality management system for site establishment, daily operations, instrumentation, data collection and data storage for APT experiments.** Pretoria, South Africa: CSIR Transportek. Contract Report CR-2004/67-v2.

APPENDIX A: TEST PIT PROFILES

Test pit profiles for each test pit are provided on the following page. The vertical scale on each profile has been exaggerated in relation to the horizontal scale to better illustrate variation in layer thicknesses and in rutting patterns.

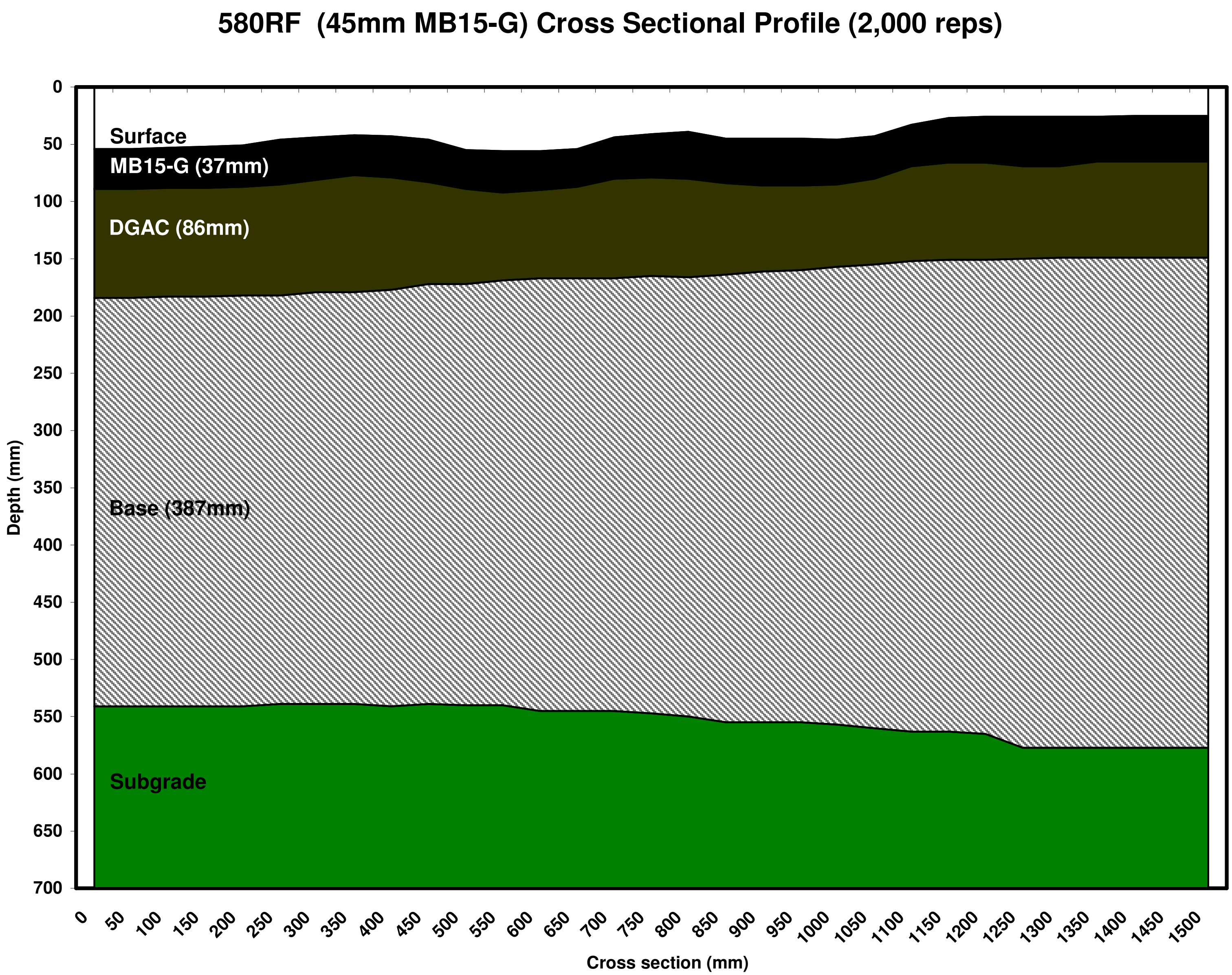

580RF (45mm MB15-G) Cross Sectional Profile (2,000 reps)
Surface
MB15-G (37mm)
DGAC (86mm)
Base (387mm)
Subgrade
Depth (mm)
Cross section (mm)
0
50
100
150
200
250
300
350
400
450
500
550
600
650
700
750
800
850
900
950
1000
1050
1100
1150
1200
1250
1300
1350
1400
1450
1500

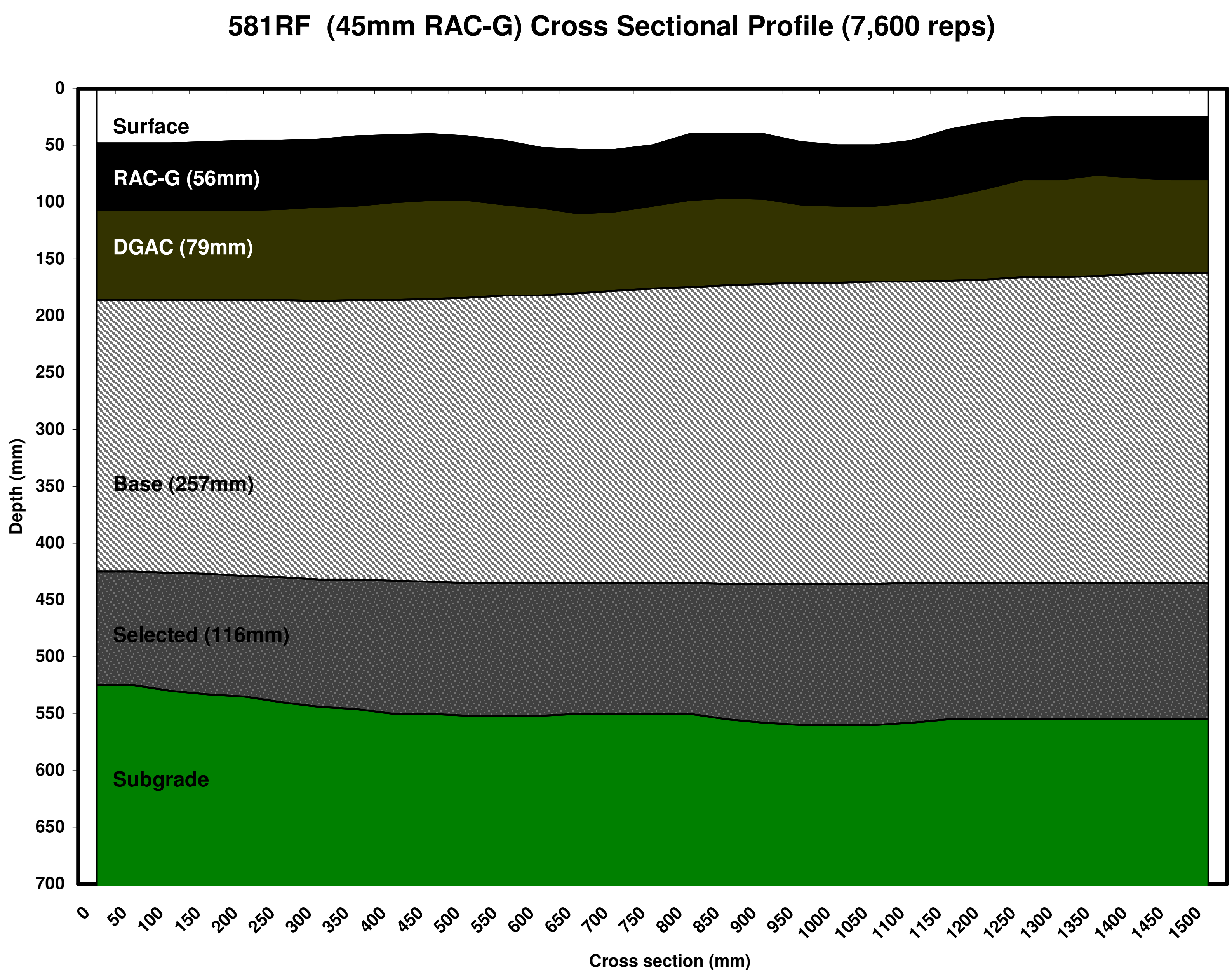

581RF (45mm RAC-G) Cross Sectional Profile (7,600 reps)
Surface
RAC-G (56mm)
DGAC (79mm)
Base (257mm)
Selected (116mm)
Subgrade
Depth (mm)
0
50
100
150
200
250
300
350
400
450
500
550
600
650
700
Cross section (mm)
0
50
100
150
200
250
300
350
400
450
500
550
600
650
700
750
800
850
900
950
1000
1050
1100
1150
1200
1250
1300
1350
1400
1450
1500

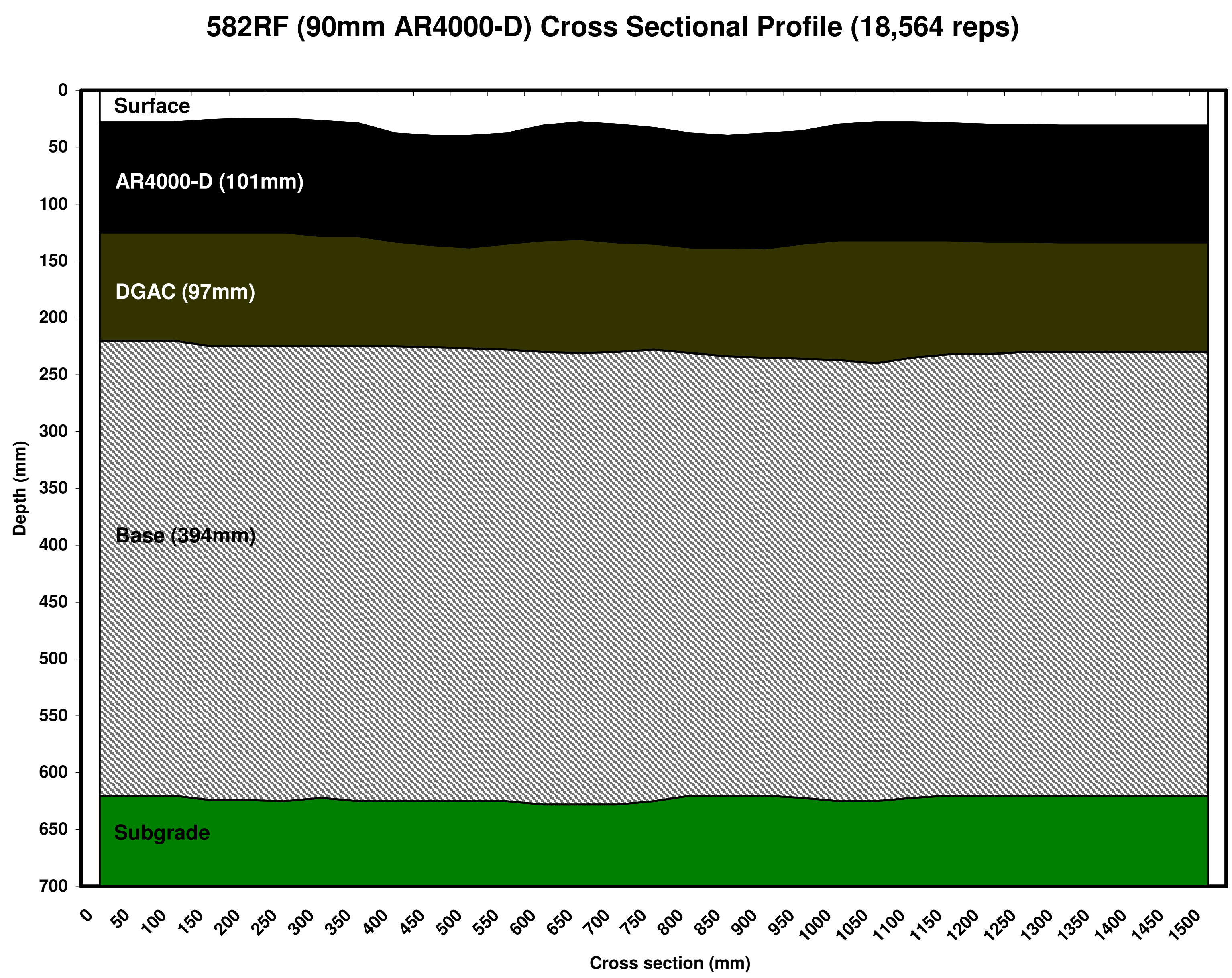
582RF (90mm AR4000-D) Cross Sectional Profile (18,564 reps)
Surface
AR4000-D (101mm)
DGAC (97mm)
Base (394mm)
Subgrade
Depth (mm)
Cross section (mm)
0
50
100
150
200
250
300
350
400
450
500
550
600
650
700
750
800
850
900
950
1000
1050
1100
1150
1200
1250
1300
1350
1400
1450
1500

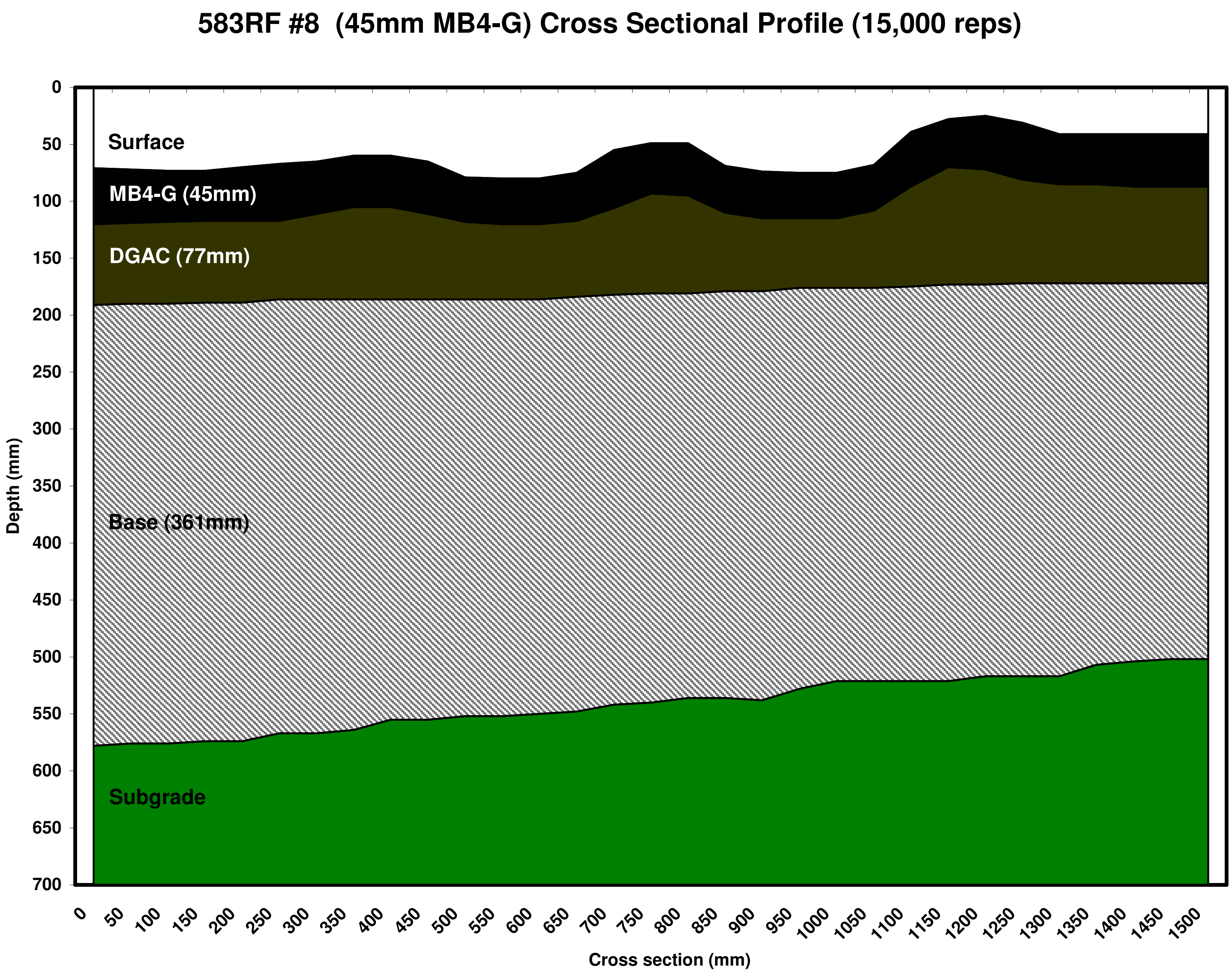
583RF #8 (45mm MB4-G) Cross Sectional Profile (15,000 reps)
Surface
MB4-G (45mm)
DGAC (77mm)
Base (361mm)
Subgrade
Depth (mm)
Cross section (mm)
0
50
100
150
200
250
300
350
400
450
500
550
600
650
700
750
800
850
900
950
1000
1050
1100
1150
1200
1250
1300
1350
1400
1450
1500

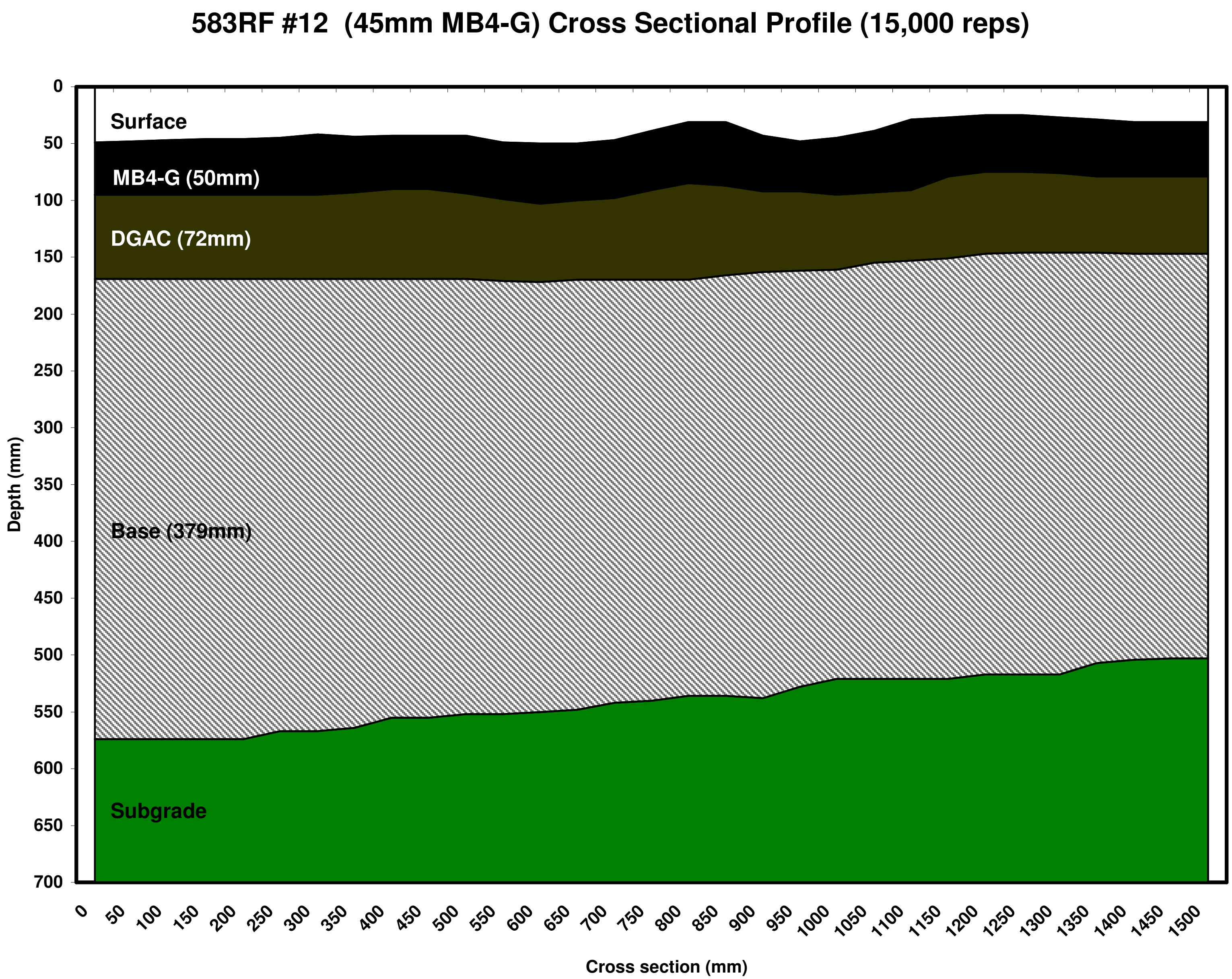
583RF #12 (45mm MB4-G) Cross Sectional Profile (15,000 reps)
Surface
MB4-G (50mm)
DGAC (72mm)
Base (379mm)
Subgrade
Depth (mm)
0
50
100
150
200
250
300
350
400
450
500
550
600
650
700
Cross section (mm)
0 50 100 150 200 250 300 350 400 450 500 550 600 650 700 750 800 850 900 950 1000 1050 1100 1150 1200 1250 1300 1350 1400 1450 1500

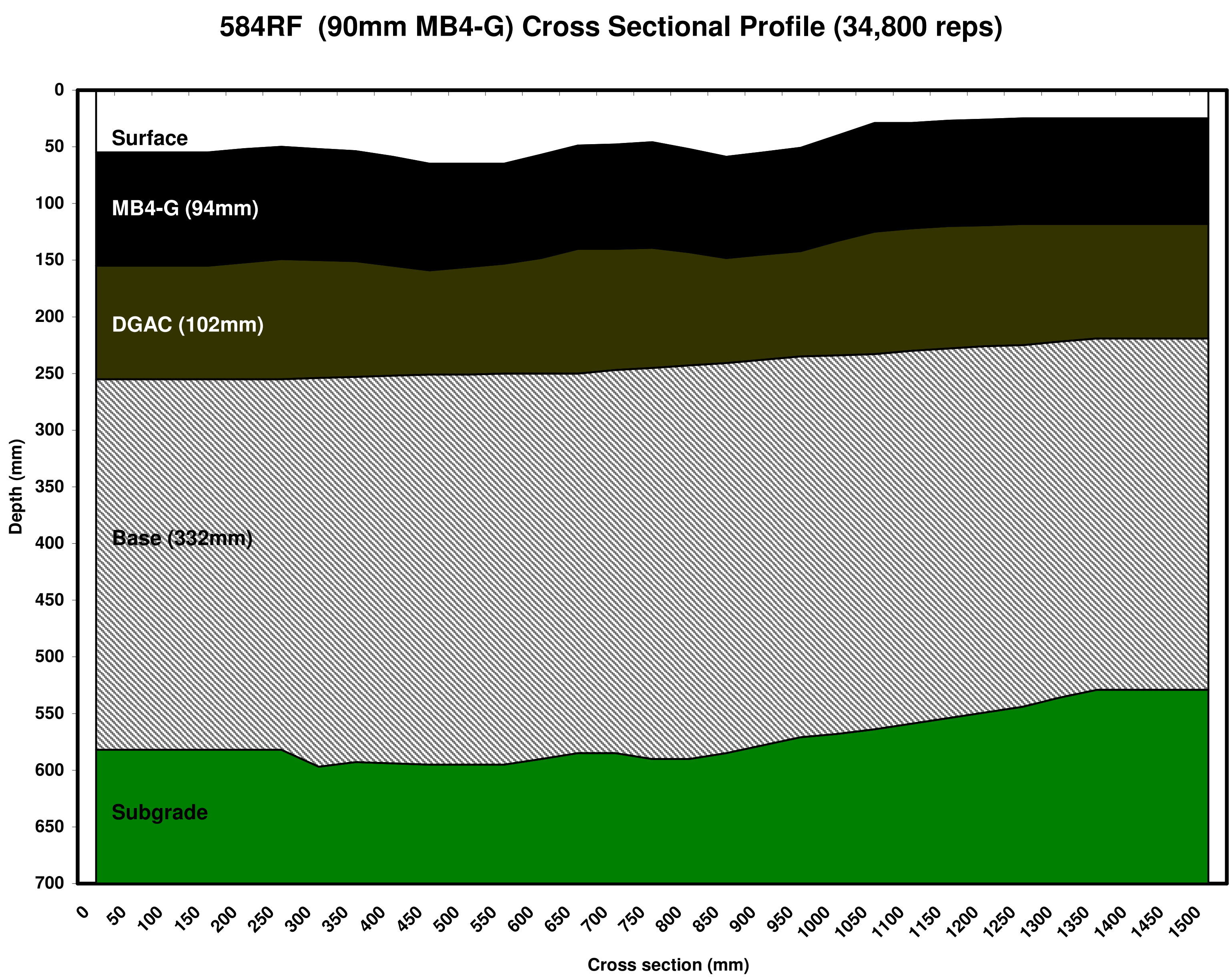
584RF (90mm MB4-G) Cross Sectional Profile (34,800 reps)
Surface
MB4-G (94mm)
DGAC (102mm)
Base (332mm)
Subgrade
Depth (mm)
0
50
100
150
200
250
300
350
400
450
500
550
600
650
700
Cross section (mm)
0
50
100
150
200
250
300
350
400
450
500
550
600
650
700
750
800
850
900
950
1000
1050
1100
1150
1200
1250
1300
1350
1400
1450
1500

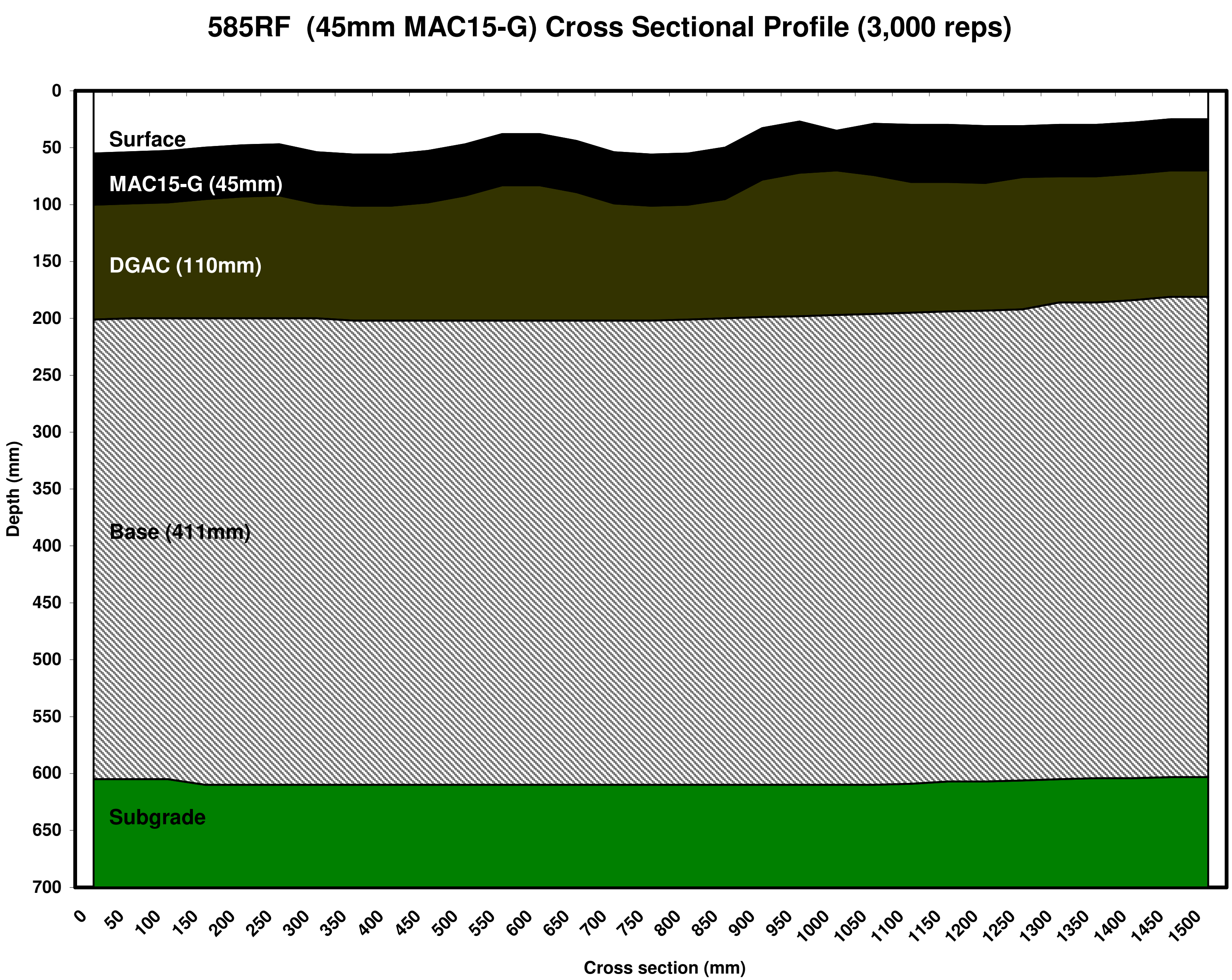
585RF (45mm MAC15-G) Cross Sectional Profile (3,000 reps)
Surface
MAC15-G (45mm)
DGAC (110mm)
Base (411mm)
Subgrade
Depth (mm)
Cross section (mm)
0
50
100
150
200
250
300
350
400
450
500
550
600
650
700
0
50
100
150
200
250
300
350
400
450
500
550
600
650
700
750
800
850
900
950
1000
1050
1100
1150
1200
1250
1300
1350
1400
1450
1500

586RF #4 (45mm MB15-G) Cross Sectional Profile (2,492,387 reps)

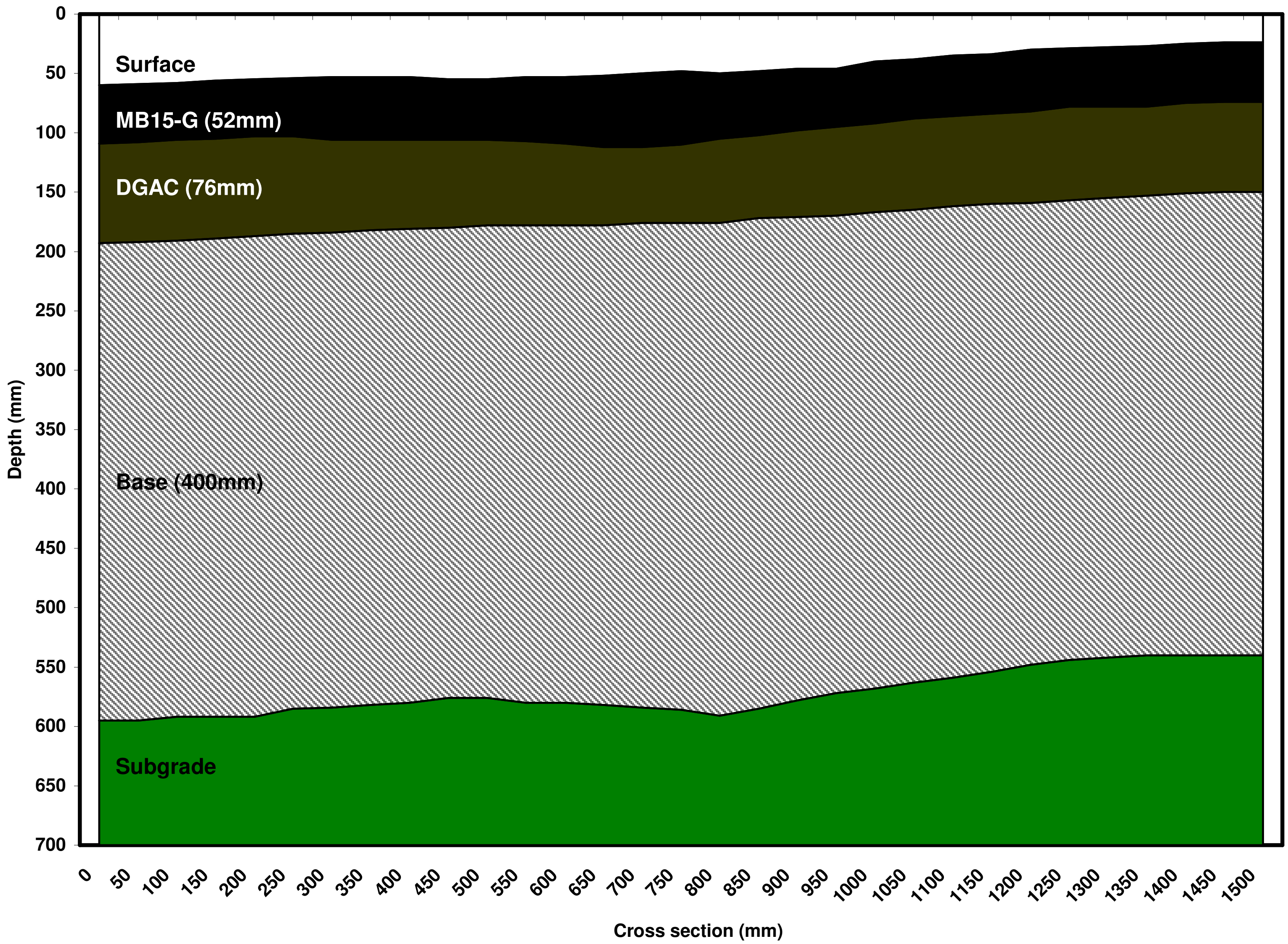

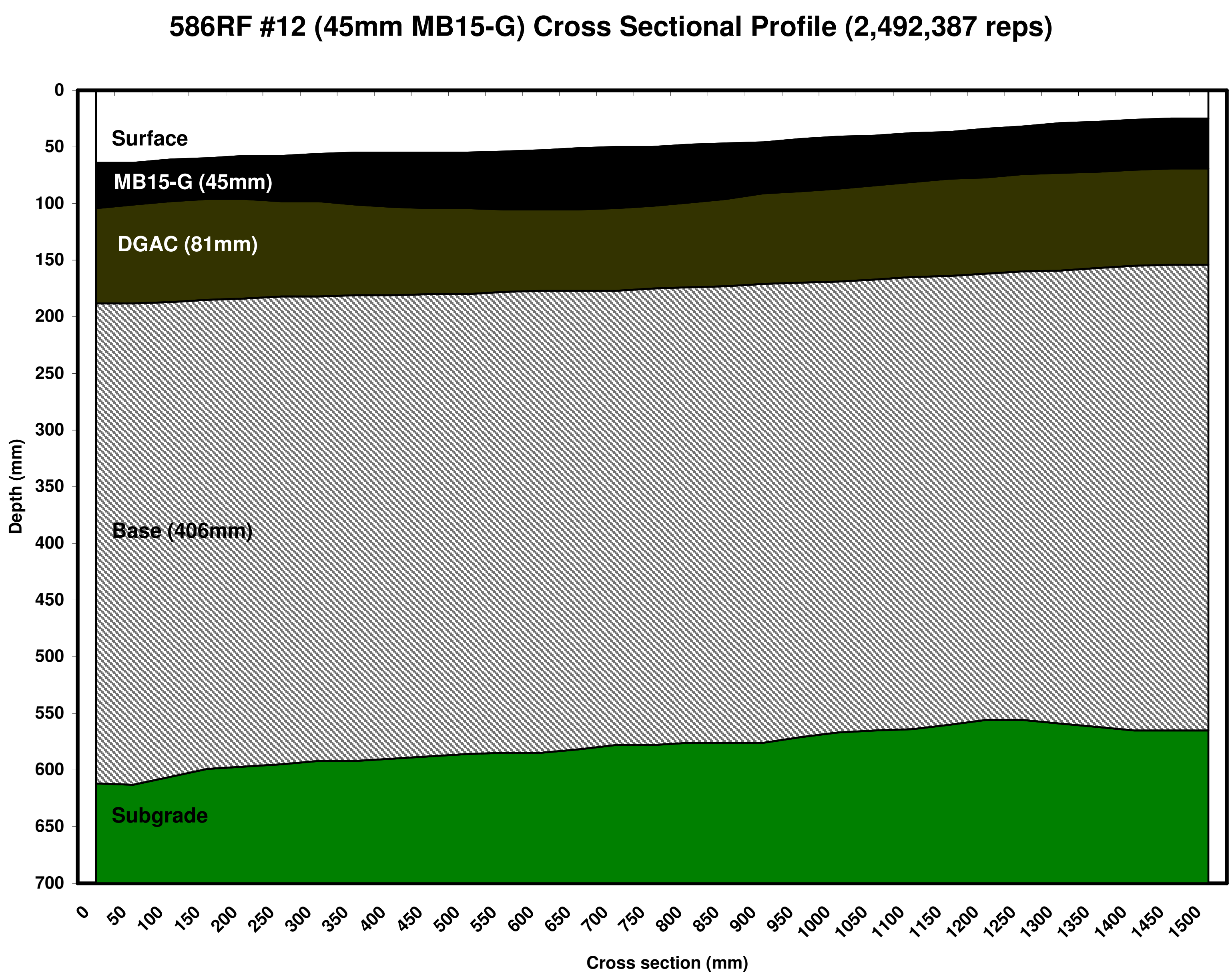

586RF #12 (45mm MB15-G) Cross Sectional Profile (2,492,387 reps)
Surface
MB15-G (45mm)
DGAC (81mm)
Base (406mm)
Subgrade
Depth (mm)
0
50
100
150
200
250
300
350
400
450
500
550
600
650
700
0 50 100 150 200 250 300 350 400 450 500 550 600 650 700 750 800 850 900 950 1000 1050 1100 1150 1200 1250 1300 1350 1400 1450 1500
Cross section (mm)

587RF #4 (45mm RAC-G) Cross Sectional Profile (2,024,793 reps)

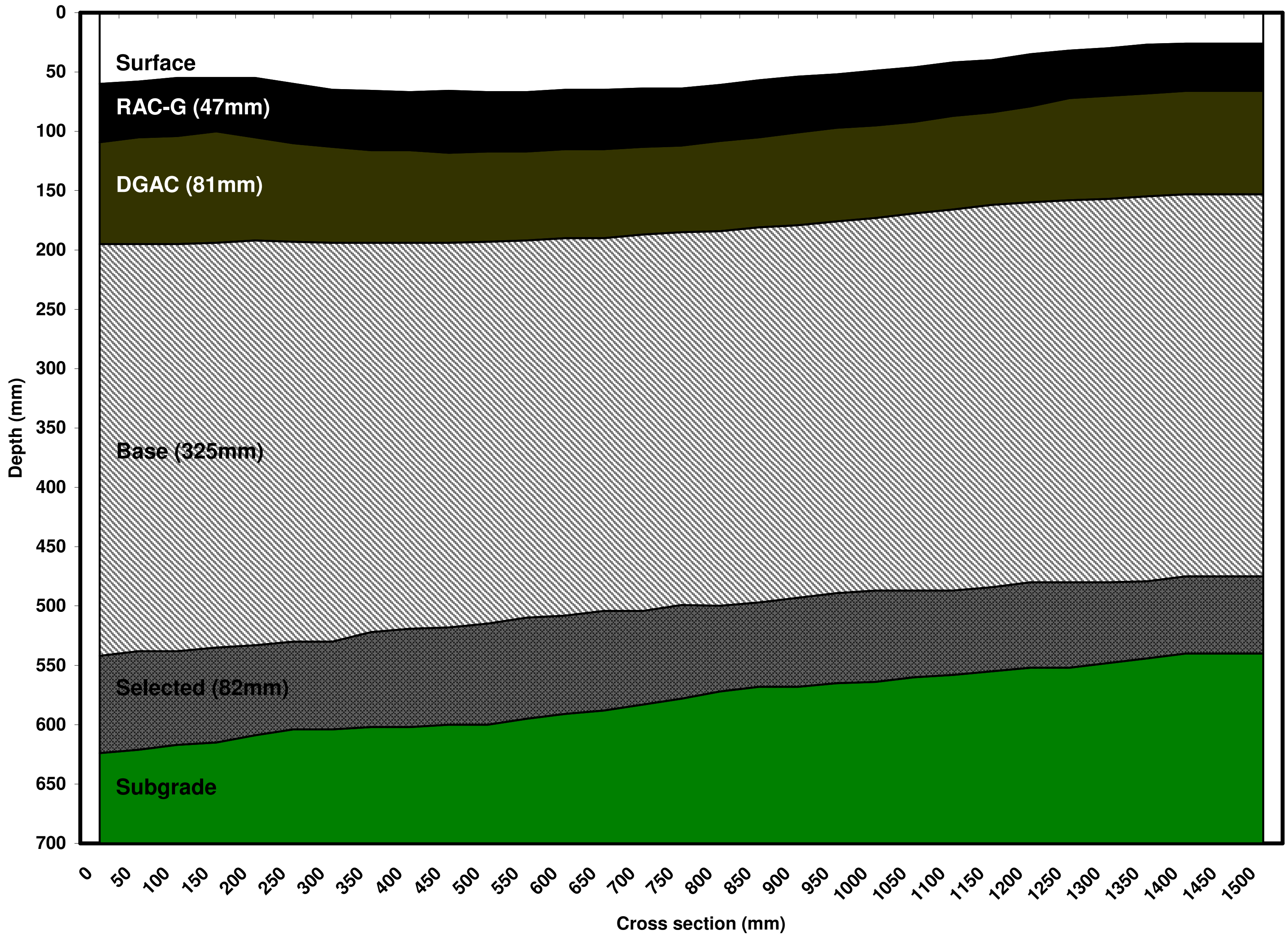

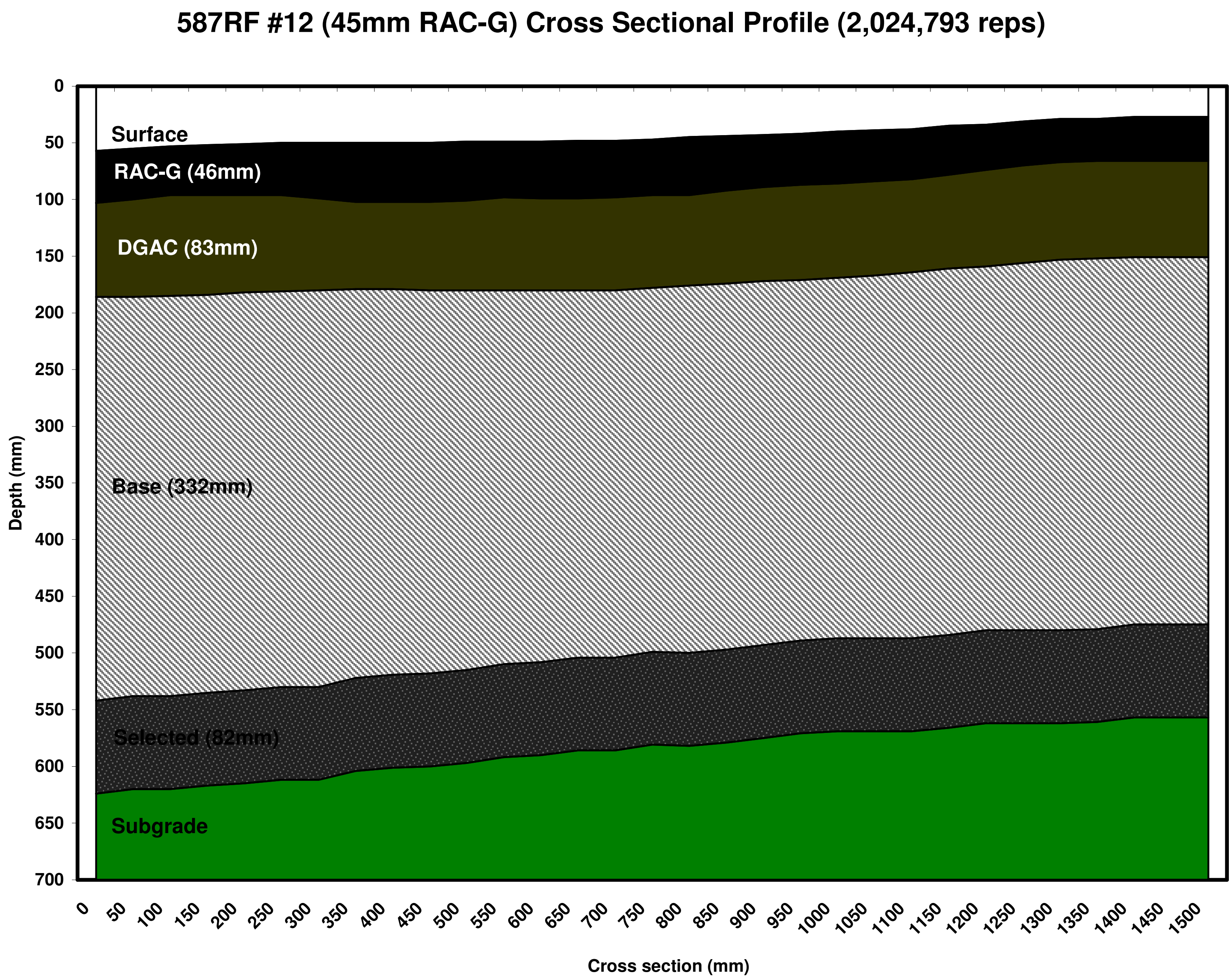
587RF #12 (45mm RAC-G) Cross Sectional Profile (2,024,793 reps)
Surface
RAC-G (46mm)
DGAC (83mm)
Base (332mm)
Selected (82mm)
Subgrade
Depth (mm)
0
50
100
150
200
250
300
350
400
450
500
550
600
650
700
0 50 100 150 200 250 300 350 400 450 500 550 600 650 700 750 800 850 900 950 1000 1050 1100 1150 1200 1250 1300 1350 1400 1450 1500
Cross section (mm)

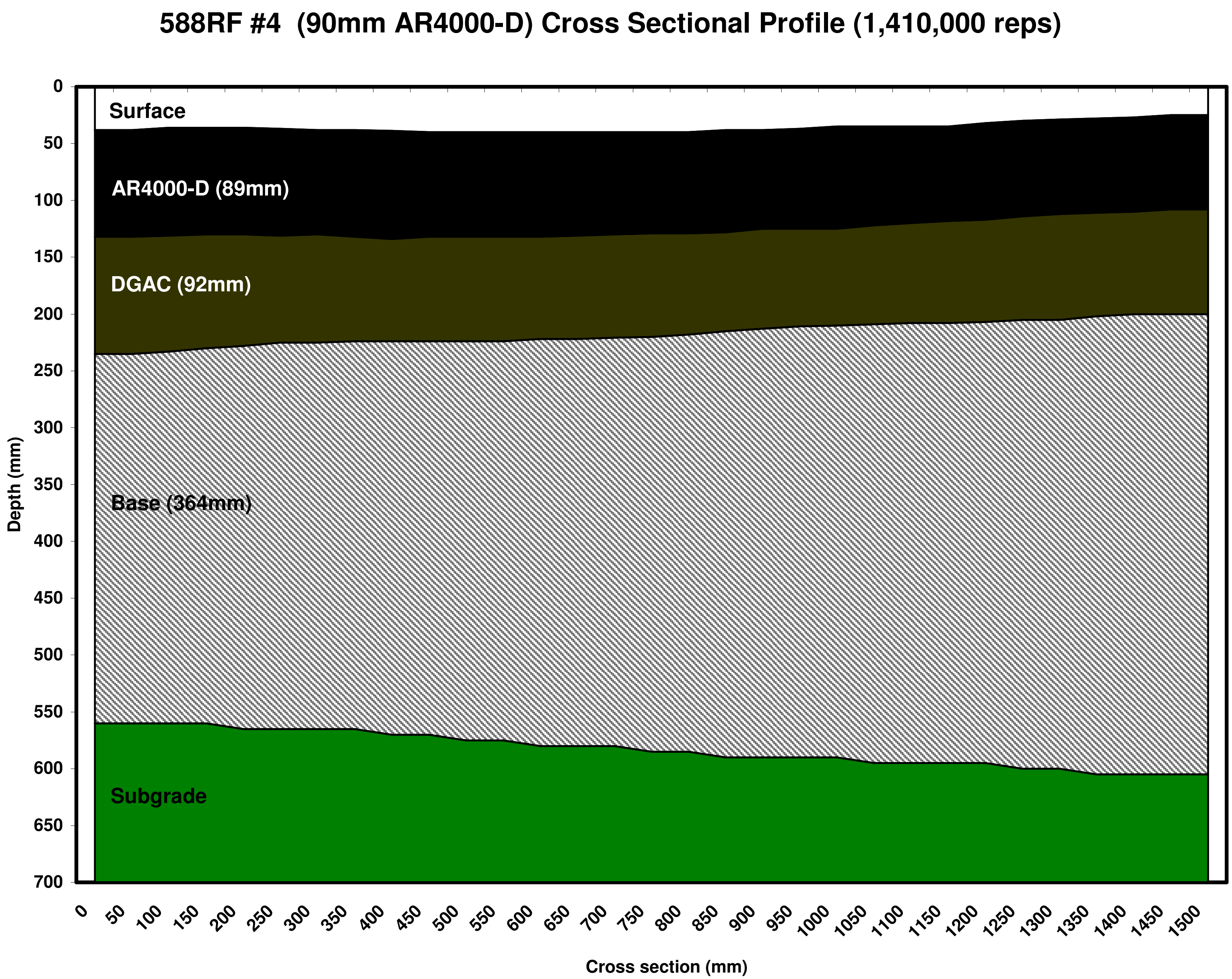
588RF #4 (90mm AR4000-D) Cross Sectional Profile (1,410,000 reps)
Surface
AR4000-D (89mm)
DGAC (92mm)
Base (364mm)
Subgrade
Depth (mm)
0
50
100
150
200
250
300
350
400
450
500
550
600
650
700
Cross section (mm)
0 50 100 150 200 250 300 350 400 450 500 550 600 650 700 750 800 850 900 950 1000 1050 1100 1150 1200 1250 1300 1350 1400 1450 1500

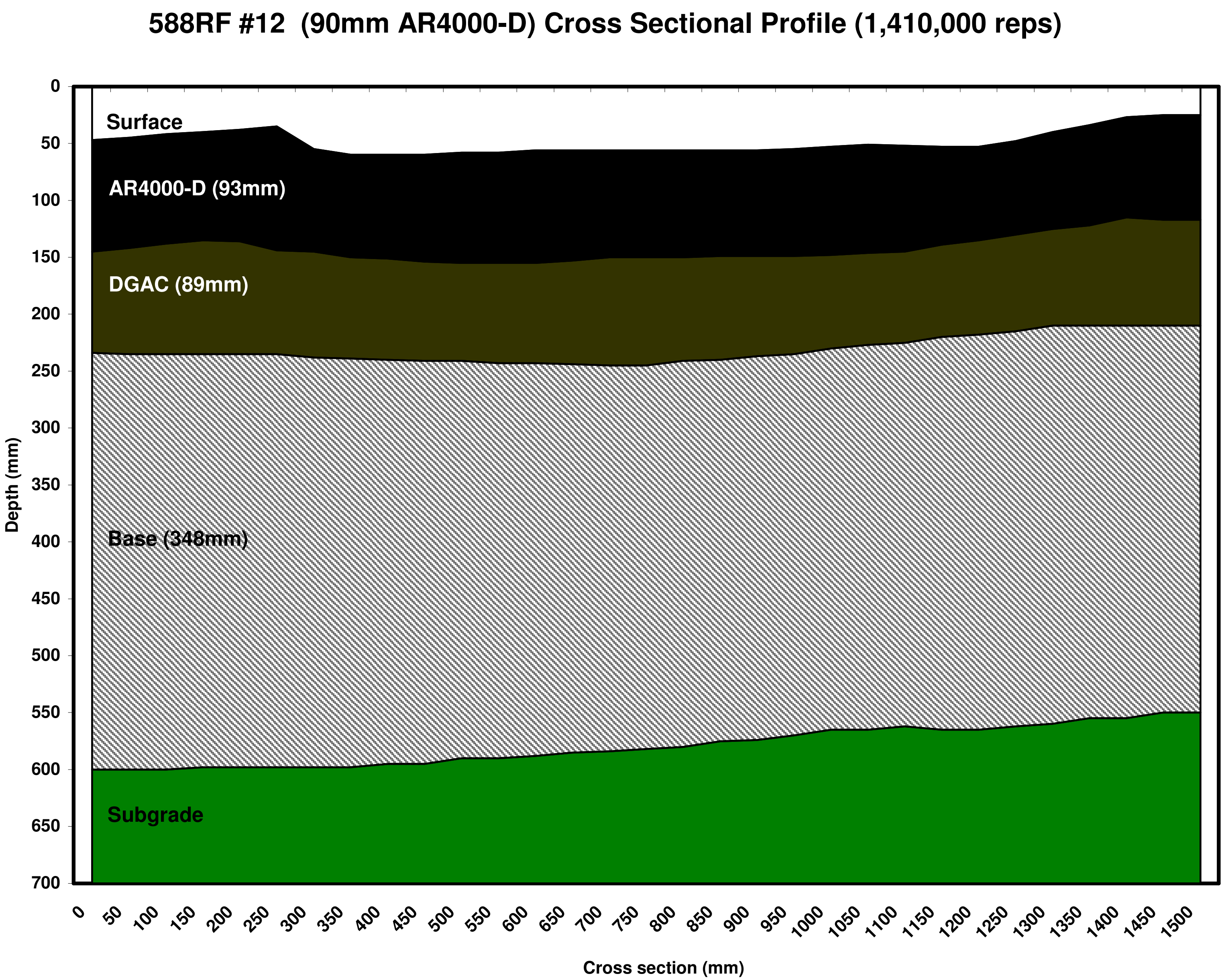
588RF #12 (90mm AR4000-D) Cross Sectional Profile (1,410,000 reps)
Surface
AR4000-D (93mm)
DGAC (89mm)
Base (348mm)
Subgrade
Depth (mm)
0
50
100
150
200
250
300
350
400
450
500
550
600
650
700
0 50 100 150 200 250 300 350 400 450 500 550 600 650 700 750 800 850 900 950 1000 1050 1100 1150 1200 1250 1300 1350 1400 1450 1500
Cross section (mm)

589RF #4 (45mm MB4-G) Cross Sectional Profile (2,086,004 reps)

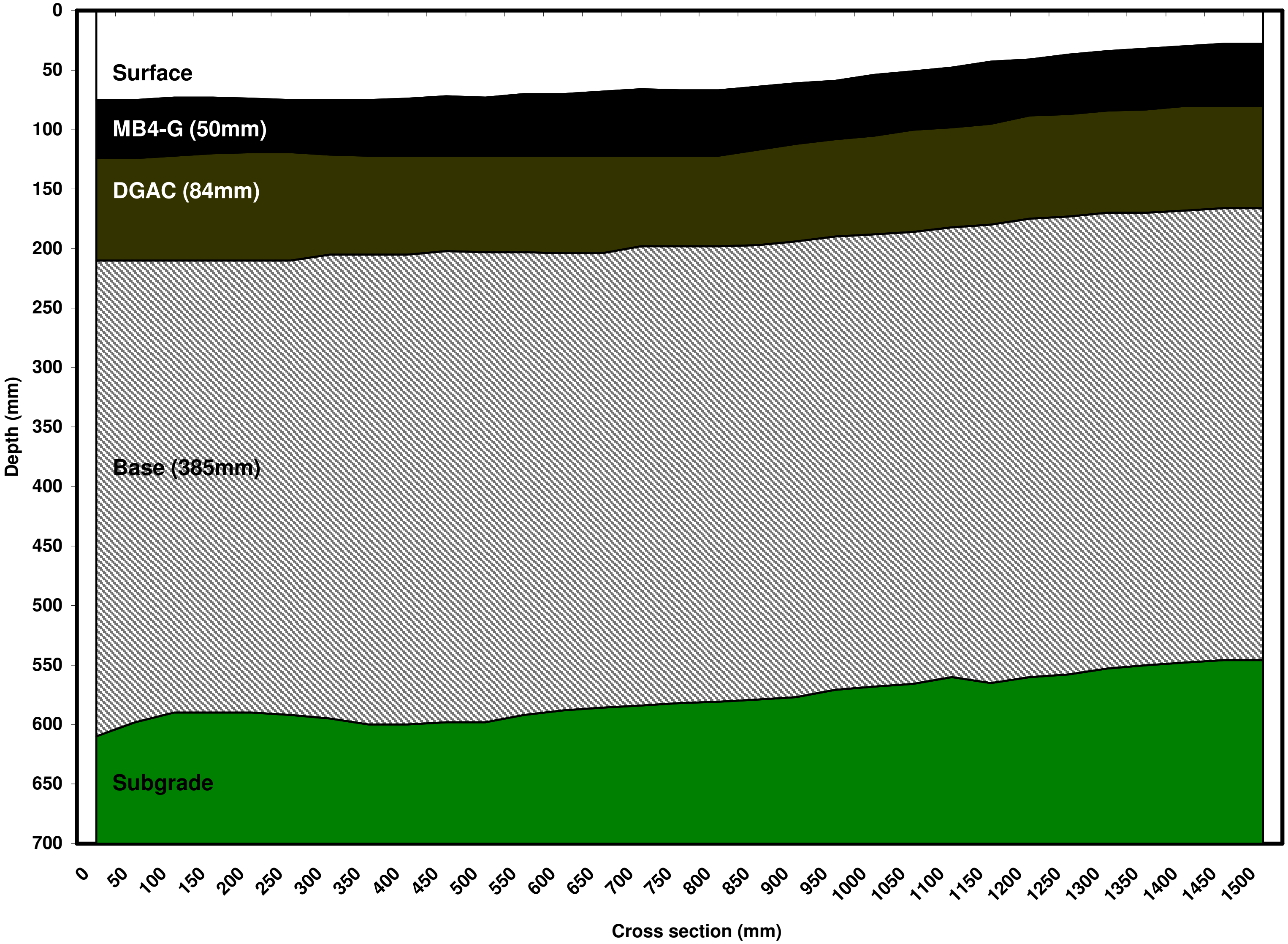

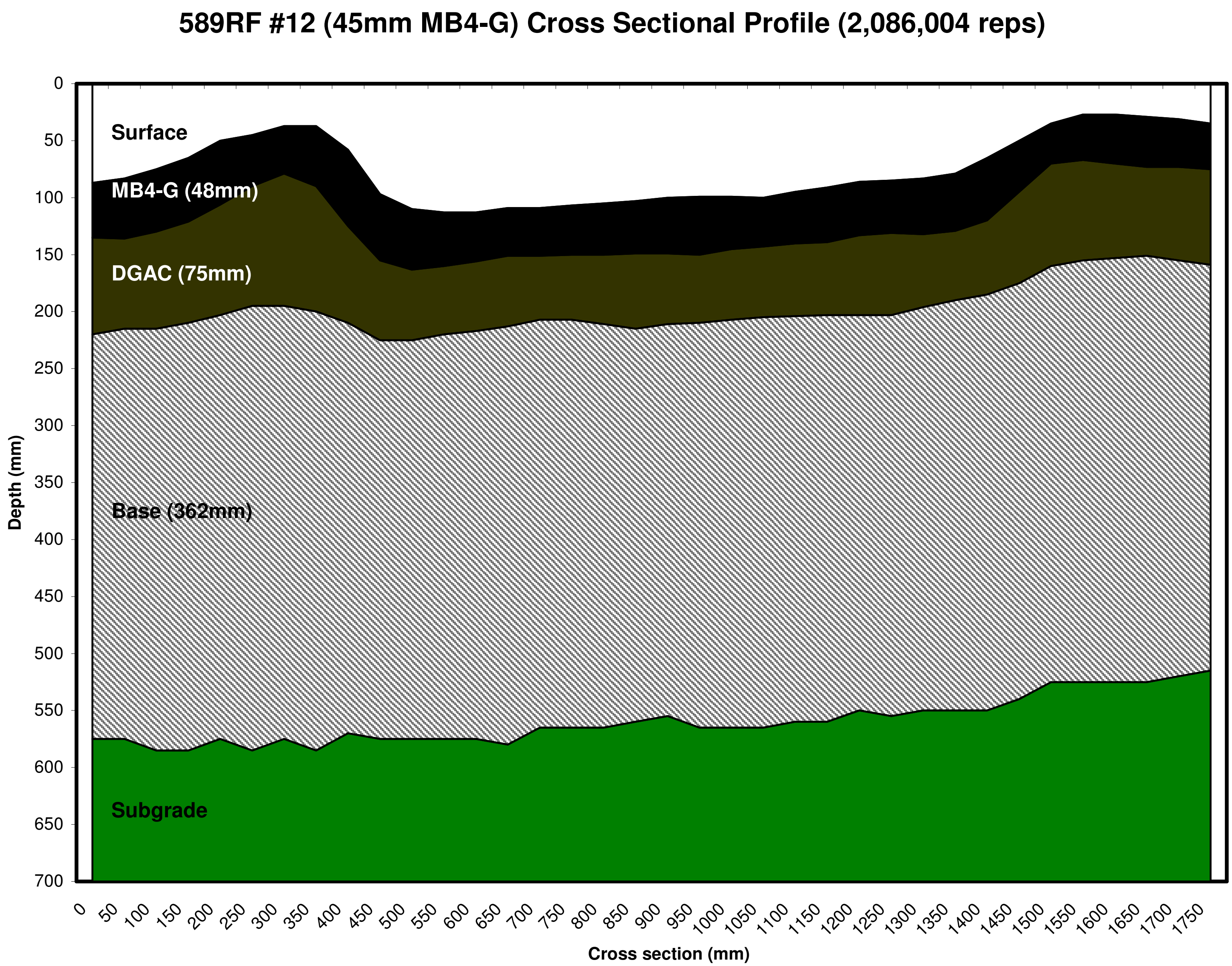

589RF #12 (45mm MB4-G) Cross Sectional Profile (2,086,004 reps)
Surface
MB4-G (48mm)
DGAC (75mm)
Base (362mm)
Subgrade
Depth (mm)
0
50
100
150
200
250
300
350
400
450
500
550
600
650
700
Cross section (mm)
0
50
100
150
200
250
300
350
400
450
500
550
600
650
700
750
800
850
900
950
1000
1050
1100
1150
1200
1250
1300
1350
1400
1450
1500
1550
1600
1650
1700
1750

590RF #4 (90mm MB4-G) Cross Sectional Profile (1,981,365 reps)

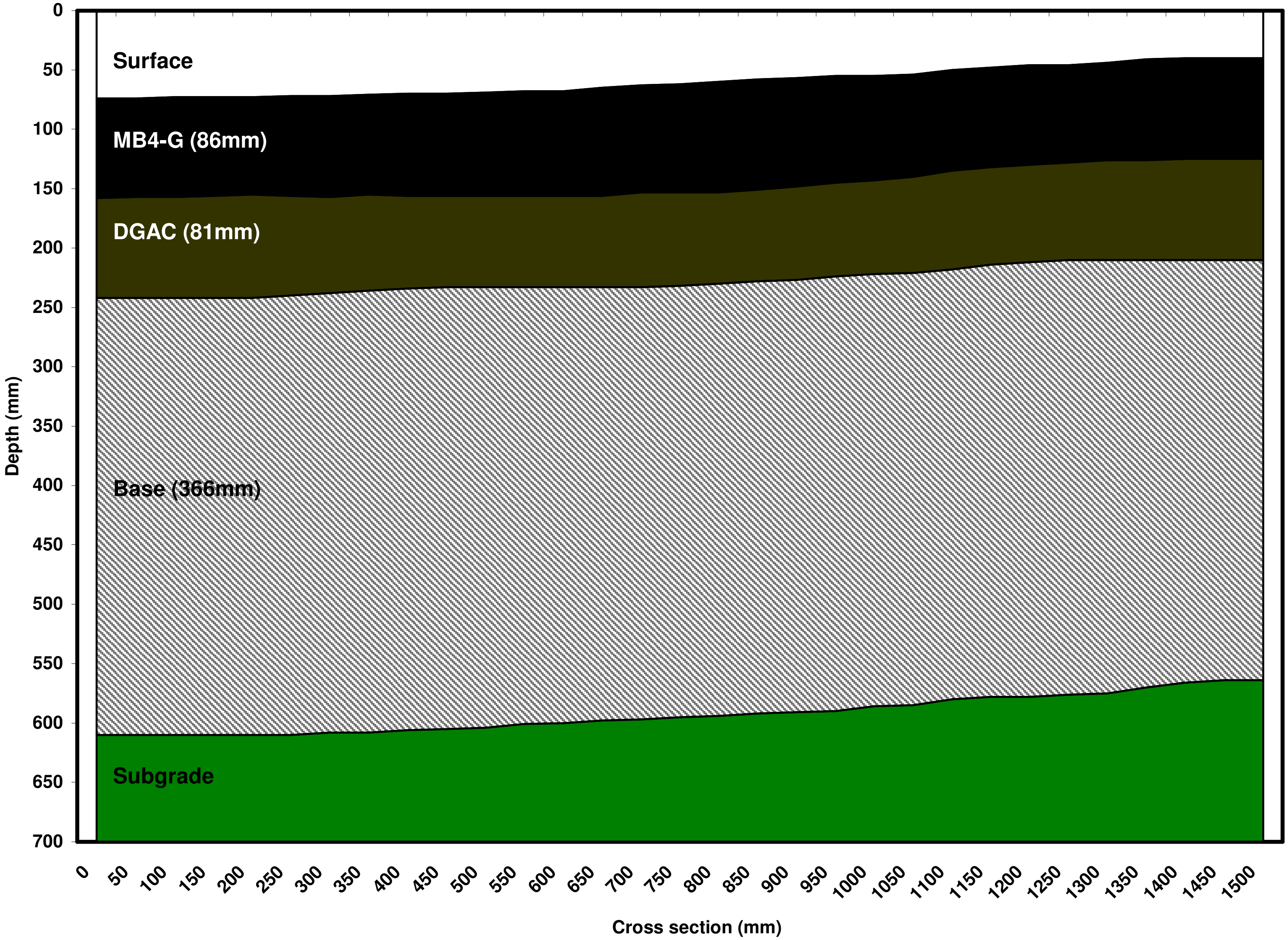

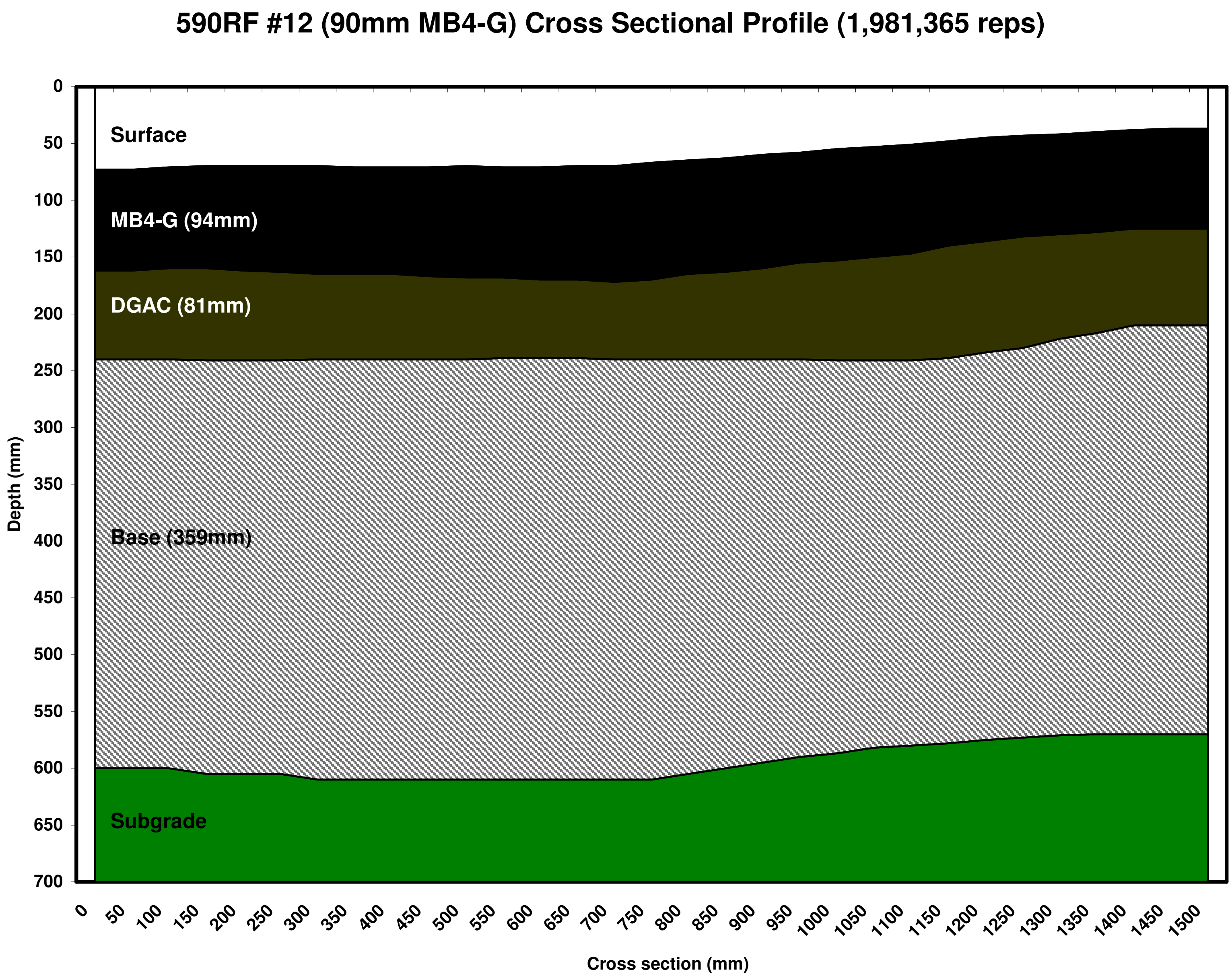
590RF #12 (90mm MB4-G) Cross Sectional Profile (1,981,365 reps)
Surface
MB4-G (94mm)
DGAC (81mm)
Base (359mm)
Subgrade
Depth (mm)
0
50
100
150
200
250
300
350
400
450
500
550
600
650
700
Cross section (mm)
0
50
100
150
200
250
300
350
400
450
500
550
600
650
700
750
800
850
900
950
1000
1050
1100
1150
1200
1250
1300
1350
1400
1450
1500

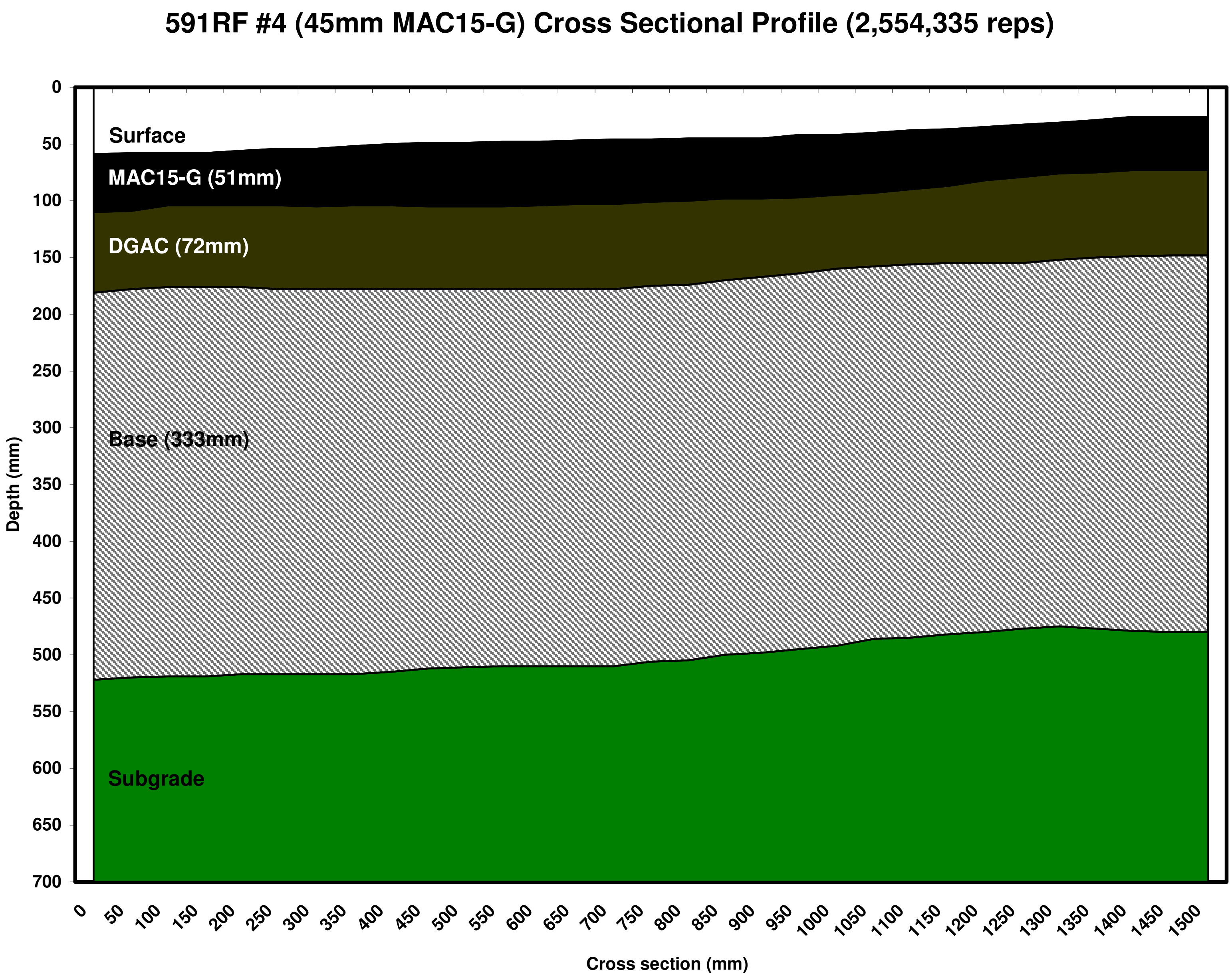

591RF #4 (45mm MAC15-G) Cross Sectional Profile (2,554,335 reps)
Surface
MAC15-G (51mm)
DGAC (72mm)
Base (333mm)
Subgrade
Depth (mm)
0
50
100
150
200
250
300
350
400
450
500
550
600
650
700
Cross section (mm)
0 50 100 150 200 250 300 350 400 450 500 550 600 650 700 750 800 850 900 950 1000 1050 1100 1150 1200 1250 1300 1350 1400 1450 1500

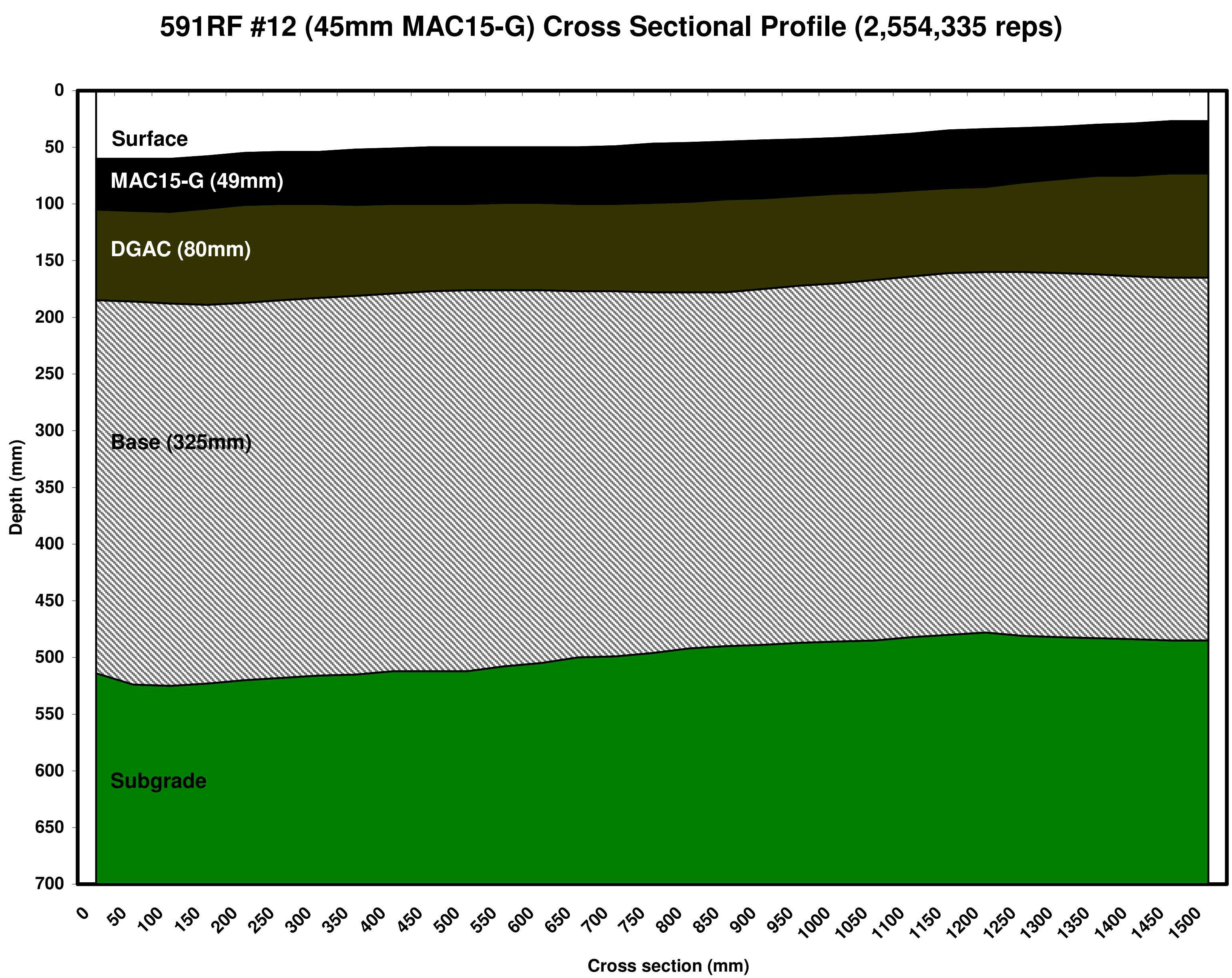
591RF #12 (45mm MAC15-G) Cross Sectional Profile (2,554,335 reps)
Surface
MAC15-G (49mm)
DGAC (80mm)
Base (325mm)
Subgrade
Depth (mm)
0
50
100
150
200
250
300
350
400
450
500
550
600
650
700
Cross section (mm)
0 50 100 150 200 250 300 350 400 450 500 550 600 650 700 750 800 850 900 950 1000 1050 1100 1150 1200 1250 1300 1350 1400 1450 1500

APPENDIX B: DYNAMIC CONE PENETROMETER PLOTS

Summary plots of the Dynamic Cone Penetrometer (DCP) measurements are provided on the following pages. Two plots per test pit are shown: one for the trafficked area and one for the untrafficked area.

580RF#10 (Trafficked)

DCP summary

Area : RFS
Road : MB Road Distance : 10.00 km
Structure Number (DSN_{800}) : 281
B = 42 A = 4601

Moisture : Moist
Position : Section
Base Type : Cemented
Category : 0
Test Date : 2/20/2007
Struct. Cap. (E80s): 5.239×10^6

Category III: Poorly balanced shallow structure (PBS)

User defined layer summary

From-To (mm)	Avg.DN (mm/blow)	Std.Dev. (mm/blow)	CBR (%)	Range 5% - 95%	UCS (kPa)	Range 5% - 95%	E-Mod (MPa)	Range 5% - 95%
0-150	1.31	0.46	246	106- 408	1903	908- 2977	838	360- 2210
150-410	4.56	3.47	60	9- 372	548	107- 2741	223	47- 1702
410-800	16.03	2.26	12	8- 19	135	92- 201	59	41- 86

Redefined layer summary

From-To (mm)	Avg.DN (mm/blow)	Std.Dev. (mm/blow)	CBR (%)	Range 5% - 95%	UCS (kPa)	Range 5% - 95%	E-Mod (MPa)	Range 5% - 95%
0- 70	1.80	0.71	185	63- 379	1487	578- 2787	599	234- 1785
70-193	0.95	0.19	311	214- 399	2340	1686- 2917	1182	708- 2059
193-249	1.43	0.16	228	178- 287	1780	1431- 2182	763	567- 1040
249-295	3.13	0.35	96	68- 138	835	615- 1150	332	248- 450
295-450	10.54	1.14	21	15- 29	215	160- 292	92	69- 123
450-800	16.67	2.02	12	8- 17	129	93- 182	56	41- 78

Balance curve

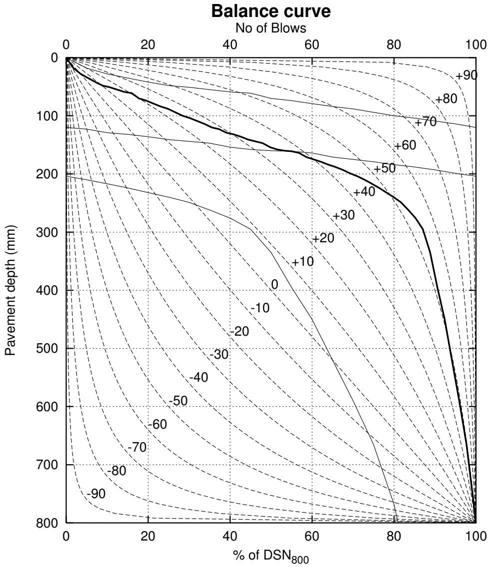

Normalized curve

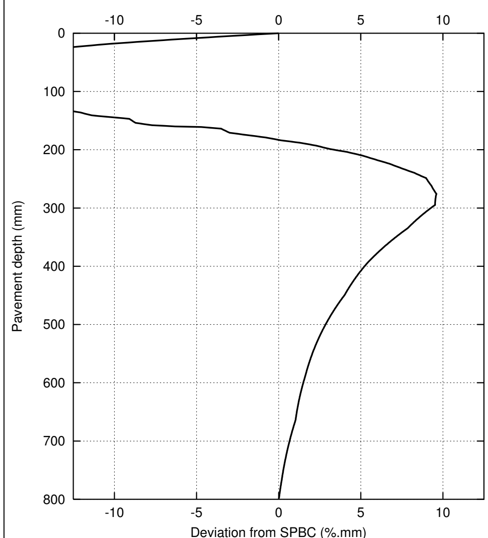

Layer strength diagram

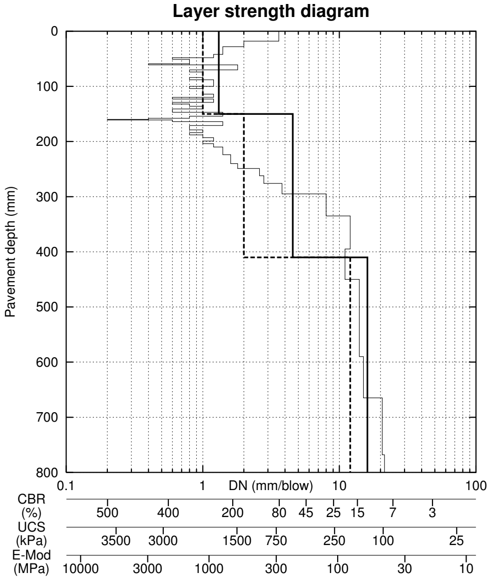

Redefined layer strength diagram

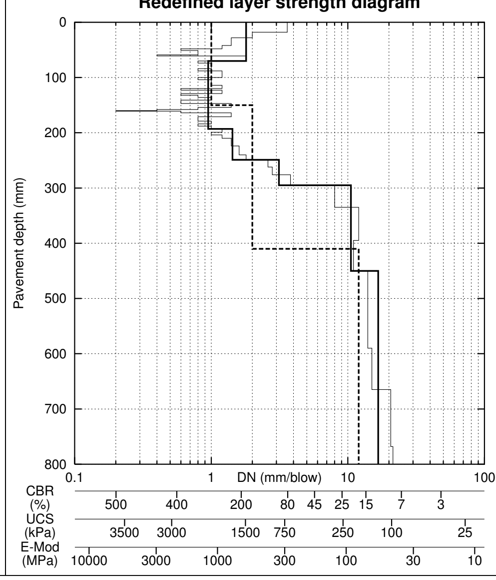

580RF#10 (Untrafficked)

DCP summary

Area : RFS
Road : MB Road Distance : 10.00 km
Structure Number (DSN_{800}) : 271
B = 47 A = 3649

Moisture : Moist Category : 0
Position : Caravan Test Date : 2/20/2007
Base Type : Cemented Struct. Cap. (E80s) : 4.612×10^6
Category III: Poorly balanced shallow structure (PBS)

User defined layer summary

From-To (mm)	Avg.DN (mm/blow)	Std.Dev. (mm/blow)	CBR (%)	Range 5% - 95%	UCS (kPa)	Range 5% - 95%	E-Mod (MPa)	Range 5% - 95%
0-150	1.02	0.34	297	153- 434	2247	1257- 3141	1096	490- 2738
150-410	6.50	4.21	38	7- 256	369	86- 1972	153	38- 884
410-800	18.59	3.41	10	6- 18	114	70- 193	50	31- 83

Redefined layer summary

From-To (mm)	Avg.DN (mm/blow)	Std.Dev. (mm/blow)	CBR (%)	Range 5% - 95%	UCS (kPa)	Range 5% - 95%	E-Mod (MPa)	Range 5% - 95%
0- 90	1.33	0.30	243	147- 354	1882	1209- 2623	825	472- 1518
90-152	0.64	0.14	379	285- 453	2791	2170- 3259	1793	1031- 3280
152-202	1.46	0.15	224	179- 278	1757	1442- 2119	749	573- 990
202-290	3.81	0.84	75	39- 154	669	373- 1266	269	155- 493
290-640	14.14	1.10	14	11- 18	155	125- 193	67	55- 83
640-800	24.97	1.10	7	6- 8	82	73- 93	37	33- 41

Balance curve

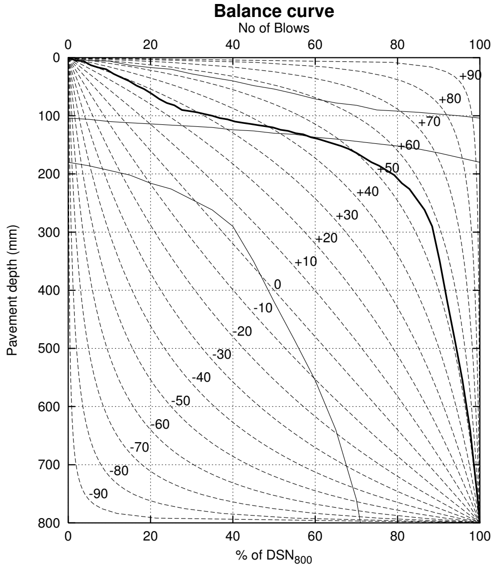

Normalized curve

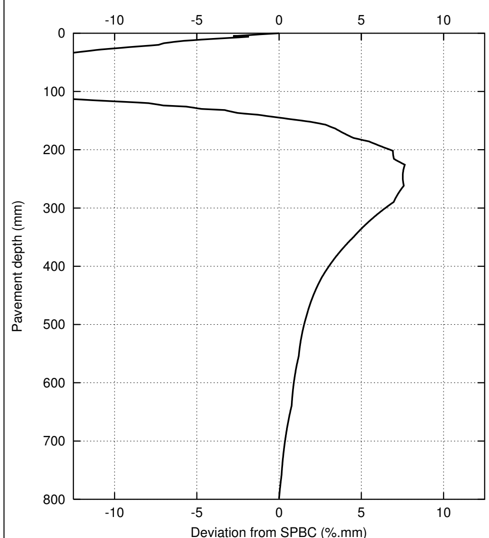

Layer strength diagram

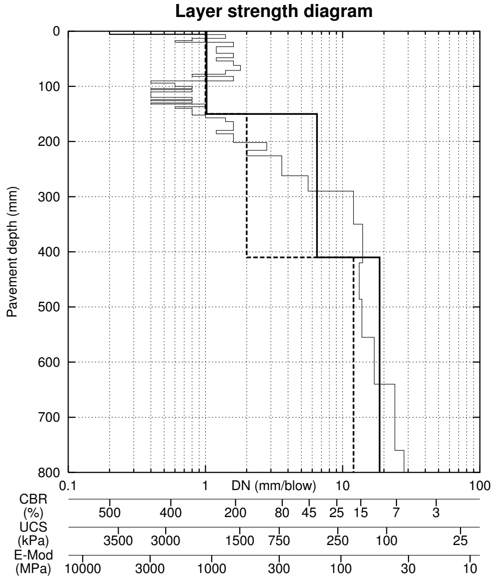

Redefined layer strength diagram

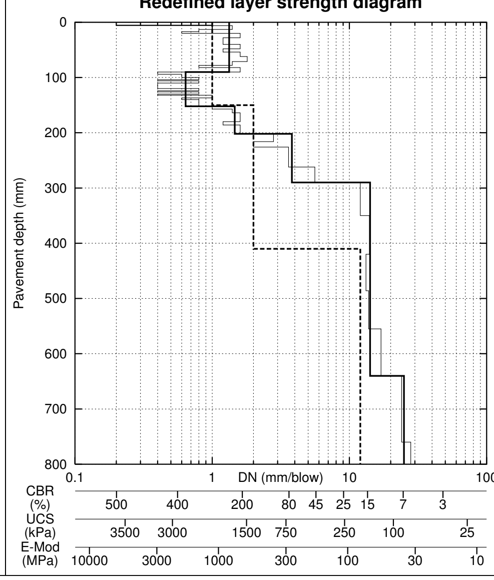

581RF#10 (Trafficked)

DCP summary

Area : RFS
Road : MB Road Distance : 7.00 km
Structure Number (DSN_{800}) : 157
B = 45 A = 4445

Moisture : Moist
Position : Section
Base Type : Cemented

Category : 0
Test Date : 3/22/2007
Struct. Cap. (E80s) : $0.673x10^6$

Category III: Poorly balanced shallow structure (PBS)

User defined layer summary

From-To (mm)	Avg.DN (mm/blow)	Std.Dev. (mm/blow)	CBR (%)	Range 5% - 95%	UCS (kPa)	Range 5% - 95%	E-Mod (MPa)	Range 5% - 95%
0-150	2.00	0.59	170	72- 314	1376	643- 2361	534	259- 1203
150-410	5.82	2.87	44	11- 203	418	128- 1611	172	56- 667
410-800	52.58	13.79	3	1- 6	36	18- 76	17	9- 34

Redefined layer summary

From-To (mm)	Avg.DN (mm/blow)	Std.Dev. (mm/blow)	CBR (%)	Range 5% - 95%	UCS (kPa)	Range 5% - 95%	E-Mod (MPa)	Range 5% - 95%
0- 44	3.19	0.74	94	47- 189	816	444- 1512	325	183- 612
44-136	1.49	0.25	220	147- 307	1724	1213- 2317	730	474- 1160
136-288	2.89	0.48	107	64- 178	913	583- 1437	362	236- 571
288-438	11.28	2.97	19	9- 45	199	100- 426	85	44- 175
438-800	56.39	7.55	2	2- 4	33	23- 48	15	11- 22

Balance curve

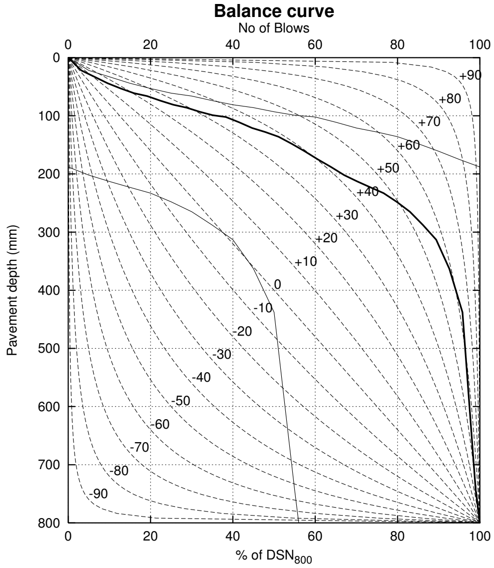

Normalized curve

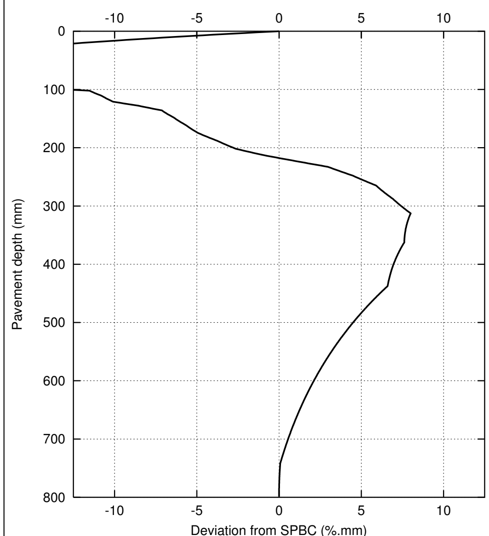

Layer strength diagram

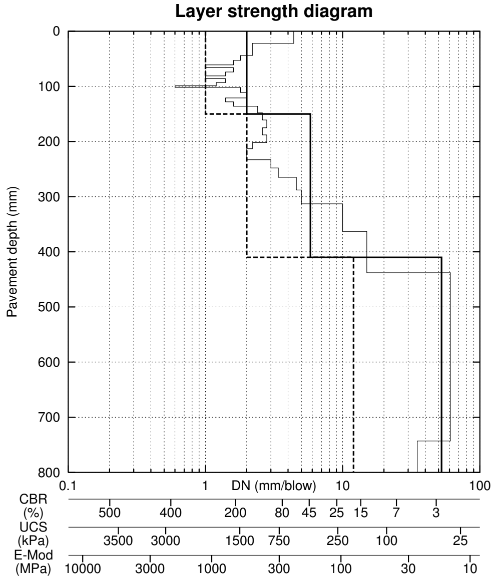

Redefined layer strength diagram

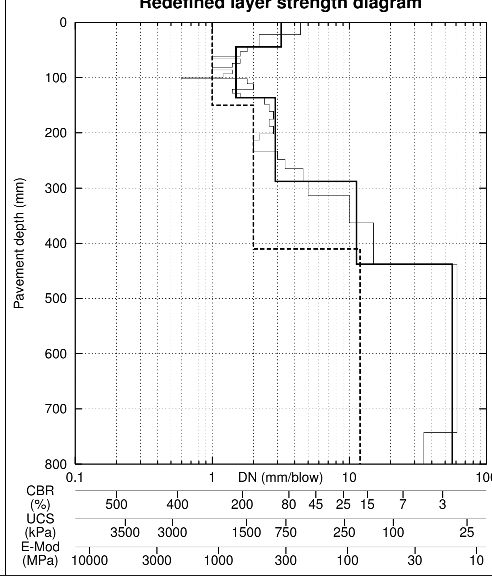

581RF#10 (Untrafficked)

DCP summary

Area : RFS
Road : MB Road Distance : 7.00 km
Structure Number (DSN_{800}) : 188
B = 40 A = 5431

Moisture : Moist
Position : Traffic
Base Type : Cemented
Category VI: Poorly balanced deep structure (PBD)

Category : 0
Test Date : 3/22/2007
Struct. Cap. (E80s): 1.264×10^6

User defined layer summary

From-To (mm)	Avg.DN (mm/blow)	Std.Dev. (mm/blow)	CBR (%)	Range 5% - 95%	UCS (kPa)	Range 5% - 95%	E-Mod (MPa)	Range 5% - 95%
0-150	2.05	0.41	164	91- 257	1337	791- 1984	520	316- 892
150-410	4.97	3.44	53	9- 329	497	108- 2459	203	48- 1308
410-800	30.35	9.27	5	2- 15	66	30- 159	30	14- 69

Redefined layer summary

From-To (mm)	Avg.DN (mm/blow)	Std.Dev. (mm/blow)	CBR (%)	Range 5% - 95%	UCS (kPa)	Range 5% - 95%	E-Mod (MPa)	Range 5% - 95%
0- 44	2.95	0.17	104	87- 124	892	765- 1045	354	306- 411
44-110	1.90	0.14	177	144- 208	1425	1191- 1646	564	466- 686
110-245	1.46	0.19	223	170- 290	1750	1375- 2205	745	534- 1060
245-316	3.81	0.80	75	40- 148	669	385- 1221	269	159- 477
316-800	26.20	9.35	6	2- 21	78	32- 218	35	15- 93

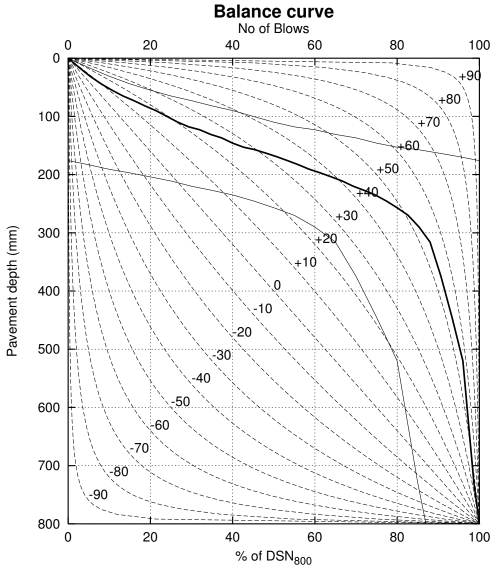

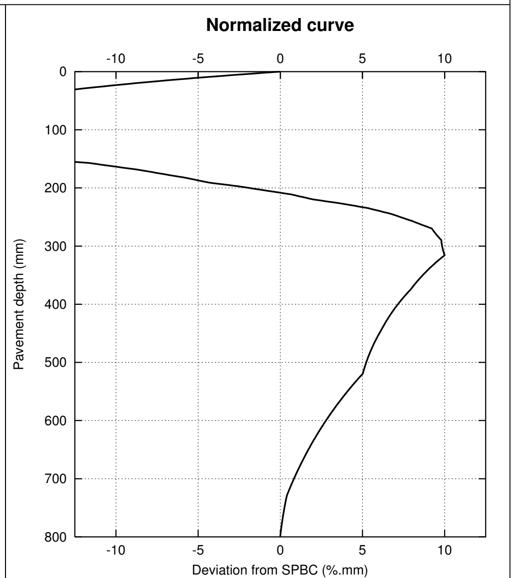

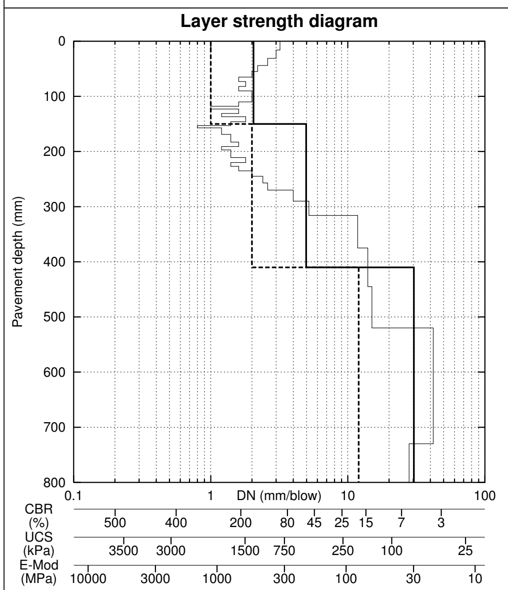

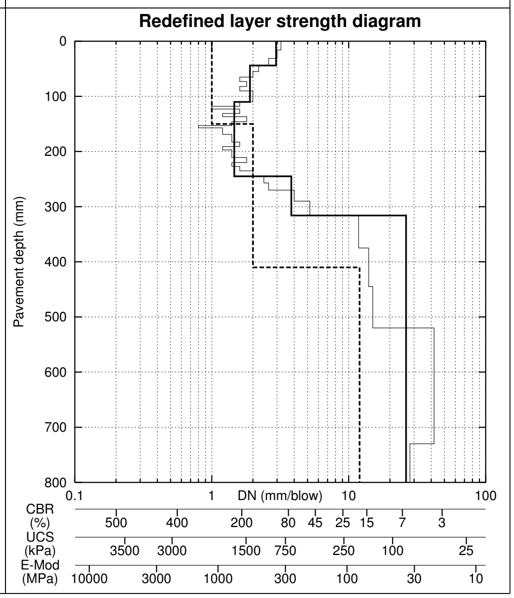

582RF#10 (Trafficked)

DCP summary

Area : RFS
Road : MB Road   Distance : 6.00 km
Structure Number (DSN_{800}) : 175
B = 33   A = 4082

Moisture : Moist
Position : Section
Base Type : Cemented
Category : 0
Test Date : 3/22/2007
Struct. Cap. (E80s) : $0.985x10^6$
Category VI: Poorly balanced deep structure (PBD)

User defined layer summary

From-To (mm)	Avg.DN (mm/blow)	Std.Dev. (mm/blow)	CBR (%)	Range 5% - 95%	UCS (kPa)	Range 5% - 95%	E-Mod (MPa)	Range 5% - 95%
0-150	2.66	1.03	118	39- 305	1000	381- 2302	394	158- 1146
150-410	6.05	4.37	42	7- 306	400	83- 2307	165	37- 1150
410-800	15.66	1.33	12	10- 16	138	109- 175	60	48- 75

Redefined layer summary

From-To (mm)	Avg.DN (mm/blow)	Std.Dev. (mm/blow)	CBR (%)	Range 5% - 95%	UCS (kPa)	Range 5% - 95%	E-Mod (MPa)	Range 5% - 95%
0- 95	3.61	1.06	80	34- 196	711	335- 1557	285	139- 637
95-211	1.50	0.21	219	161- 290	1720	1314- 2202	728	511- 1057
211-328	3.60	0.80	80	42- 165	713	398- 1345	286	165- 523
328-800	16.12	1.41	12	9- 16	134	105- 171	58	46- 74

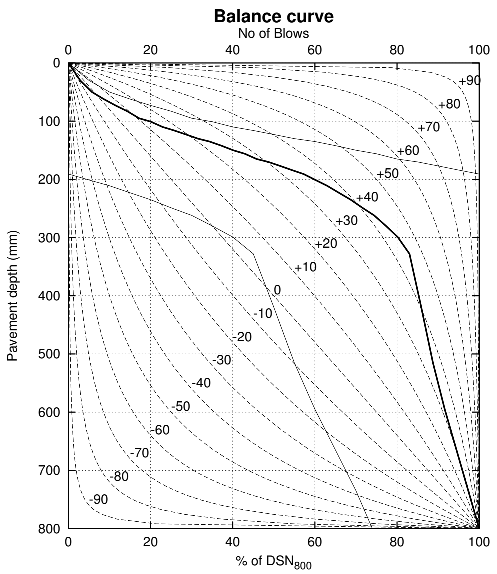

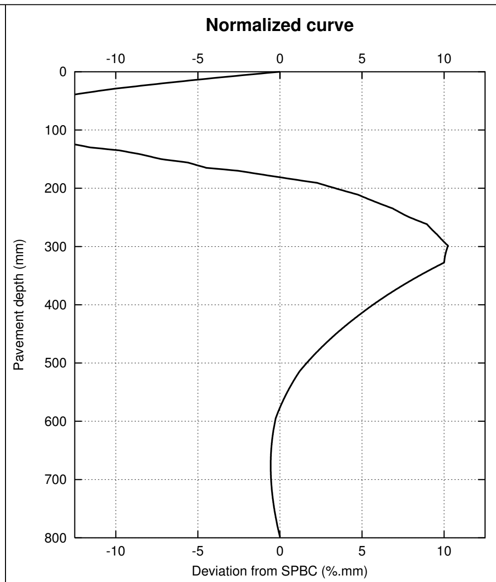

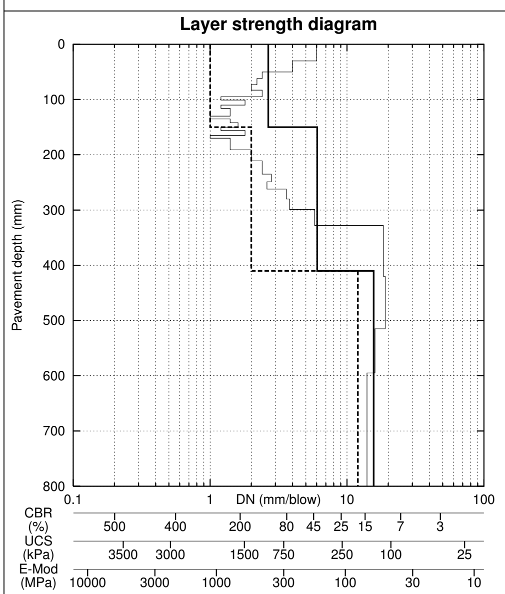

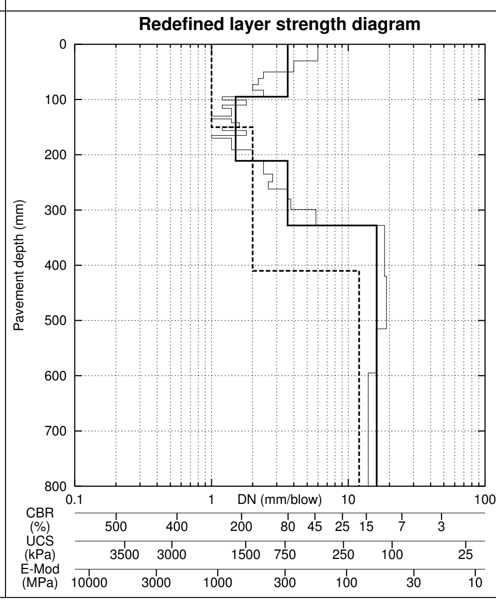

582RF#10 (Untrafficked)

DCP summary

Area : RFS
Road : MB Road Distance : 6.00 km
Structure Number (DSN_{800}) : 213
B = 34 A = 6319

Moisture : Moist Category : 0
Position : Caravan Test Date : 3/22/2007
Base Type : Cemented Struct. Cap. (E80s): $1.979x10^6$
Category VI: Poorly balanced deep structure (PBD)

User defined layer summary

From-To (mm)	Avg.DN (mm/blow)	Std.Dev. (mm/blow)	CBR (%)	Range 5% - 95%	UCS (kPa)	Range 5% - 95%	E-Mod (MPa)	Range 5% - 95%
0-150	2.53	0.74	126	53- 267	1061	497- 2049	417	203- 937
150-410	2.90	1.53	106	26- 354	910	263- 2626	361	111- 1522
410-800	24.21	5.34	7	4- 15	85	47- 160	38	22- 69

Redefined layer summary

From-To (mm)	Avg.DN (mm/blow)	Std.Dev. (mm/blow)	CBR (%)	Range 5% - 95%	UCS (kPa)	Range 5% - 95%	E-Mod (MPa)	Range 5% - 95%
0- 95	3.22	0.32	93	68- 128	809	616- 1075	323	249- 422
95-124	1.98	0.23	172	121- 222	1388	1020- 1741	542	402- 740
124-181	1.17	0.14	269	213- 327	2063	1677- 2449	948	703- 1297
181-297	1.62	0.28	203	132- 291	1612	1102- 2207	667	433- 1061
297-398	4.49	1.15	61	28- 141	558	286- 1171	227	120- 458
398-800	24.09	5.25	7	4- 15	85	48- 160	38	22- 69

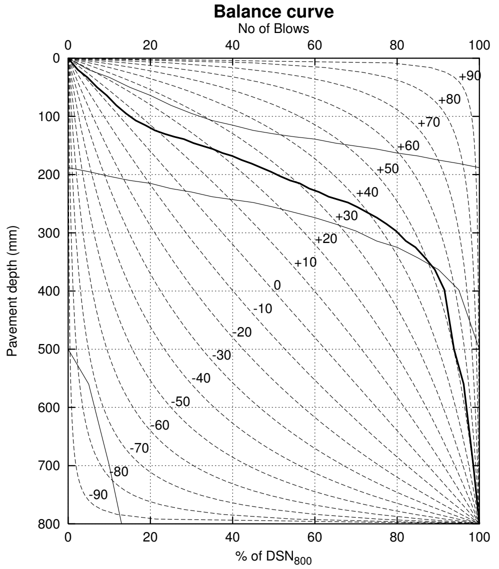

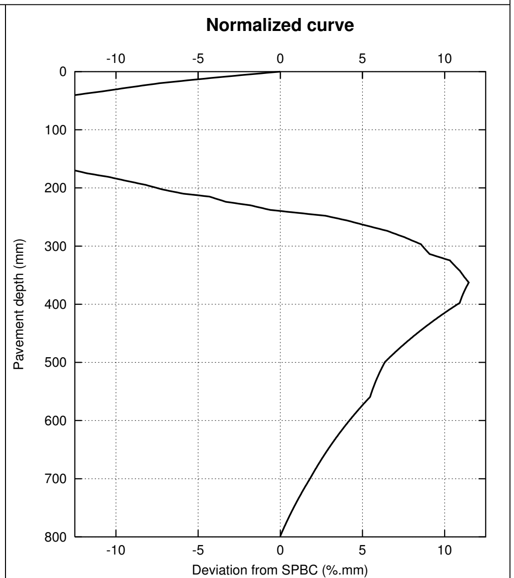

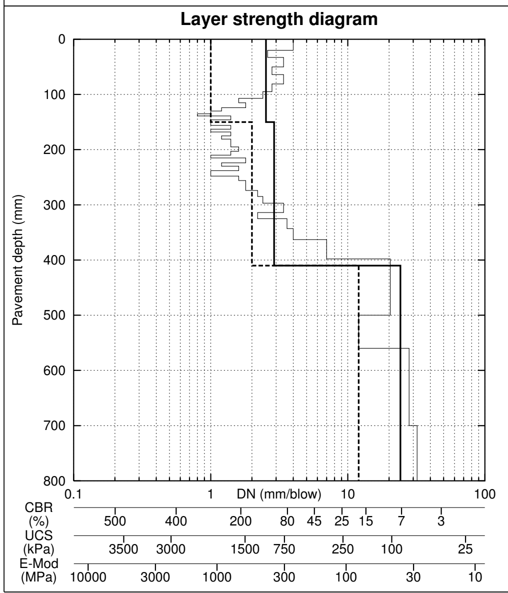

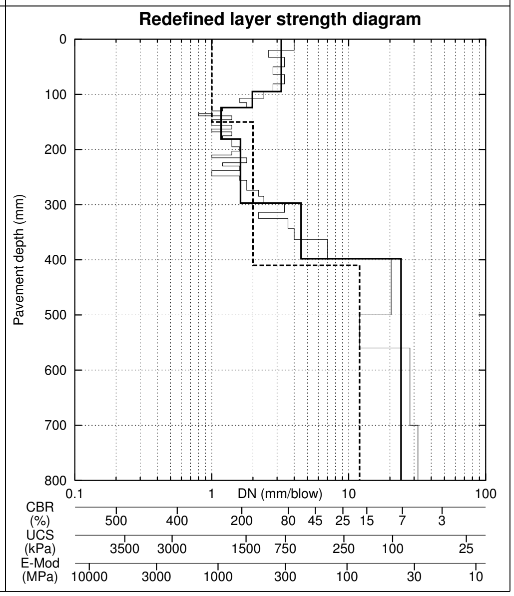

583RF#10 (Trafficked)

DCP summary

Area : RFS
Road : MB Road Distance : 7.00 km
Structure Number (DSN_{800}) : 190
B = 43 A = 4626

Moisture : Moist
Position : Section
Base Type : Cemented

Category : 0
Test Date : 2/20/2007
Struct. Cap. (E80s) : 1.316×10^{6}

Category III: Poorly balanced shallow structure (PBS)

User defined layer summary

From-To (mm)	Avg.DN (mm/blow)	Std.Dev. (mm/blow)	CBR (%)	Range 5% - 95%	UCS (kPa)	Range 5% - 95%	E-Mod (MPa)	Range 5% - 95%
0-150	1.67	0.42	198	102- 324	1575	879- 2432	647	349- 1277
150-410	6.96	5.60	35	5- 314	342	63- 2362	142	29- 1204
410-800	29.75	1.69	6	5- 7	67	58- 79	30	26- 35

Redefined layer summary

From-To (mm)	Avg.DN (mm/blow)	Std.Dev. (mm/blow)	CBR (%)	Range 5% - 95%	UCS (kPa)	Range 5% - 95%	E-Mod (MPa)	Range 5% - 95%
0- 65	2.24	0.33	147	94- 212	1210	818- 1674	473	326- 702
65-226	1.47	0.24	223	153- 307	1745	1252- 2318	742	488- 1161
226-300	3.27	0.84	91	43- 196	794	408- 1561	317	168- 639
300-800	26.86	4.70	6	4- 11	76	47- 125	34	22- 55

Balance curve

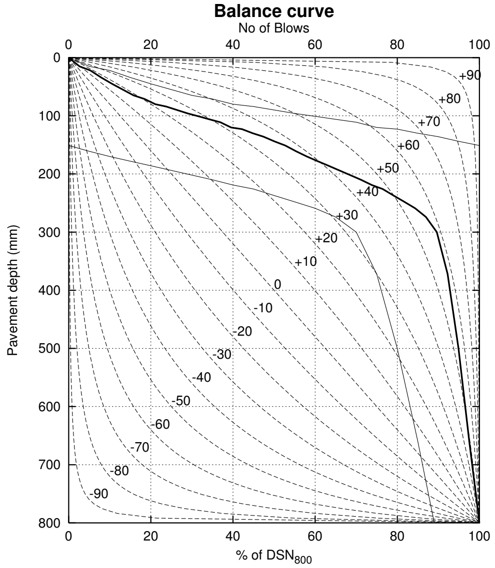

Normalized curve

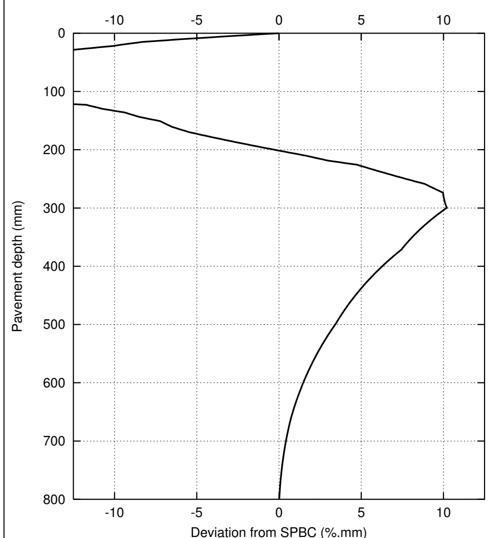

Layer strength diagram

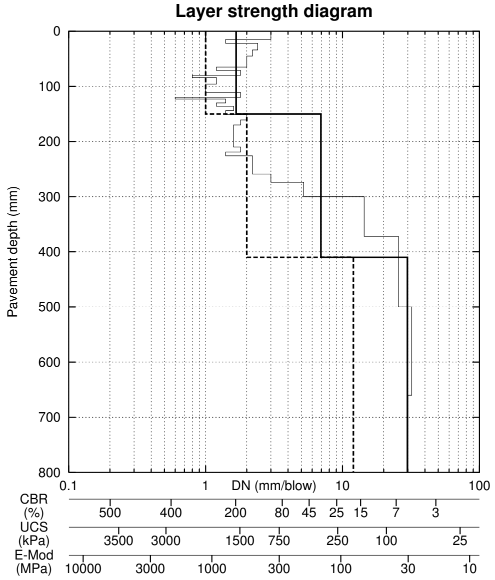

Redefined layer strength diagram

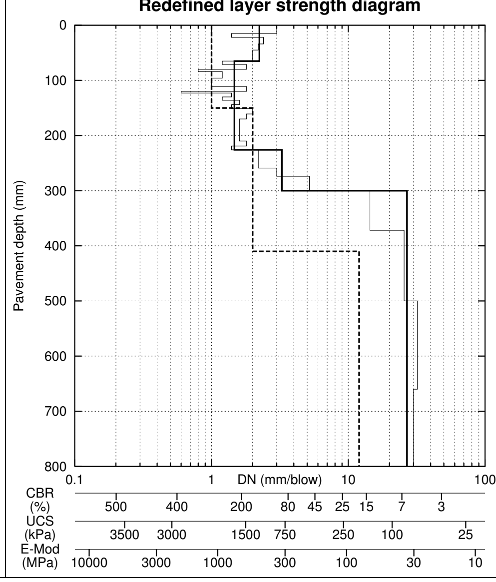

583RF#10 (Untrafficked)

DCP summary

Area : RFS
Road : MB Road Distance : 7.00 km
Structure Number (DSN_{800}) : 229
B = 44 A = 3416

Moisture : Moist
Position : Caravan
Base Type : Cemented

Category : 0
Test Date : 2/20/2007
Struct. Cap. (E80s) : 2.540×10^6

Category III: Poorly balanced shallow structure (PBS)

User defined layer summary

From-To (mm)	Avg.DN (mm/blow)	Std.Dev. (mm/blow)	CBR (%)	Range 5% - 95%	UCS (kPa)	Range 5% - 95%	E-Mod (MPa)	Range 5% - 95%
0-150	1.24	0.29	257	155- 371	1981	1269- 2737	890	495- 1696
150-410	7.75	6.01	30	5- 280	303	58- 2135	127	26- 1002
410-800	18.02	0.64	10	9- 12	118	107- 130	52	47- 57

Redefined layer summary

From-To (mm)	Avg.DN (mm/blow)	Std.Dev. (mm/blow)	CBR (%)	Range 5% - 95%	UCS (kPa)	Range 5% - 95%	E-Mod (MPa)	Range 5% - 95%
0- 90	1.42	0.33	229	130- 347	1789	1091- 2579	768	428- 1457
90-145	0.94	0.12	312	252- 368	2348	1947- 2716	1190	867- 1661
145-221	1.51	0.33	217	126- 329	1709	1059- 2464	722	417- 1314
221-290	4.75	0.67	57	37- 90	524	357- 785	213	148- 313
290-800	17.69	0.70	11	9- 12	120	108- 135	53	48- 59

Balance curve

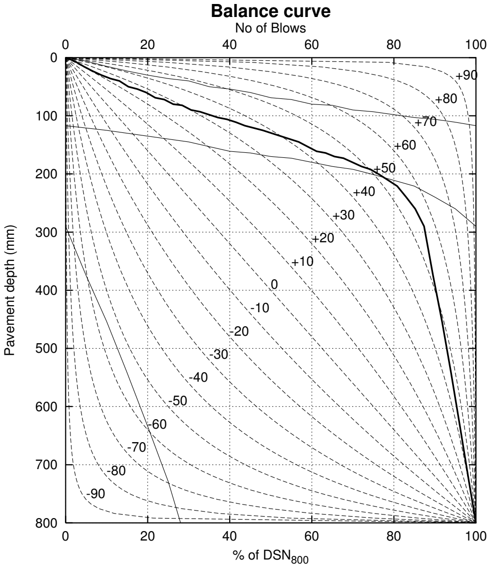

Normalized curve

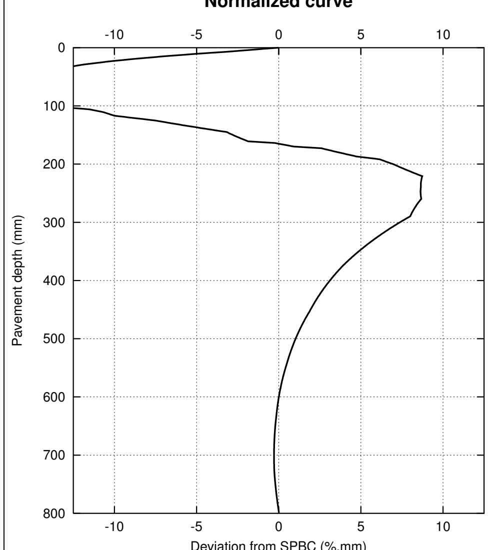

Layer strength diagram

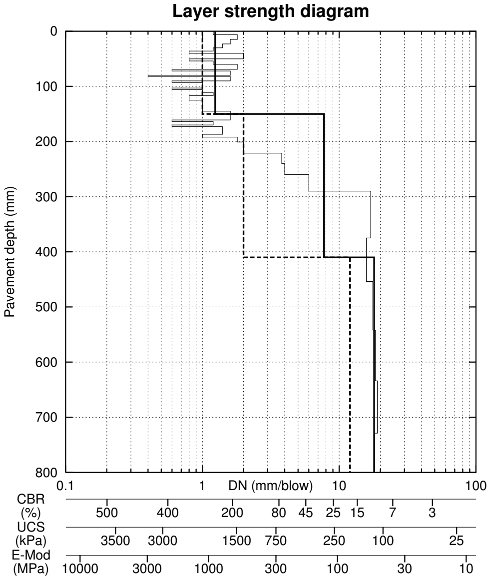

Redefined layer strength diagram

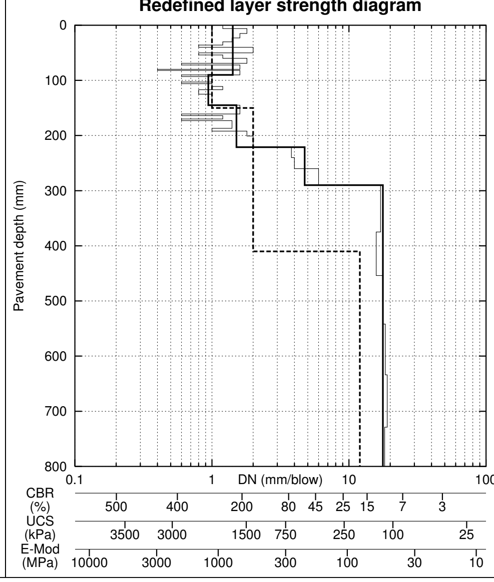

584RF#10 (Trafficked)

DCP summary

Area : RFS
Road : MB Road   Distance : 7.00 km
Structure Number (DSN_{800}) : 156
B = 37   A = 2475

Moisture : Moist
Position : Section
Base Type : Cemented

Category : 0
Test Date : 3/14/2007
Struct. Cap. (E80s) : 0.660×10^6

Category V: Averagely balanced deep structure (ABD)

User defined layer summary

From-To (mm)	Avg.DN (mm/blow)	Std.Dev. (mm/blow)	CBR (%)	Range 5% - 95%	UCS (kPa)	Range 5% - 95%	E-Mod (MPa)	Range 5% - 95%
0-150	1.89	0.40	178	97- 282	1432	838- 2148	568	334- 1013
150-410	10.19	5.82	22	5- 139	223	59- 1152	95	27- 451
410-800	14.04	1.26	14	11- 19	156	122- 201	68	53- 86

Redefined layer summary

From-To (mm)	Avg.DN (mm/blow)	Std.Dev. (mm/blow)	CBR (%)	Range 5% - 95%	UCS (kPa)	Range 5% - 95%	E-Mod (MPa)	Range 5% - 95%
0- 99	1.65	0.34	200	116- 306	1590	985- 2311	655	389- 1154
99-238	2.94	0.58	104	57- 188	894	530- 1501	355	216- 607
238-800	14.41	2.28	14	9- 23	151	99- 238	66	44- 101

Balance curve

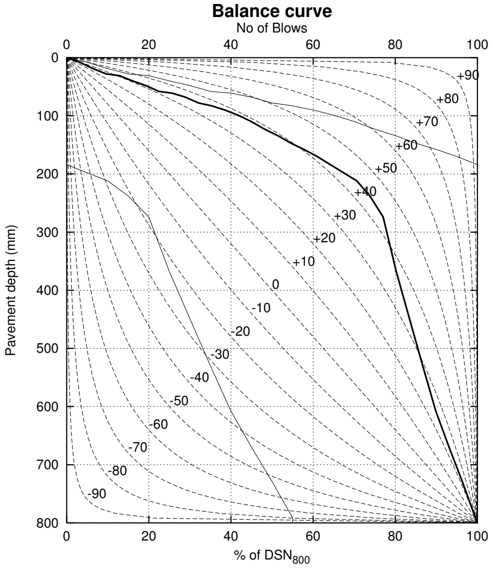

Normalized curve

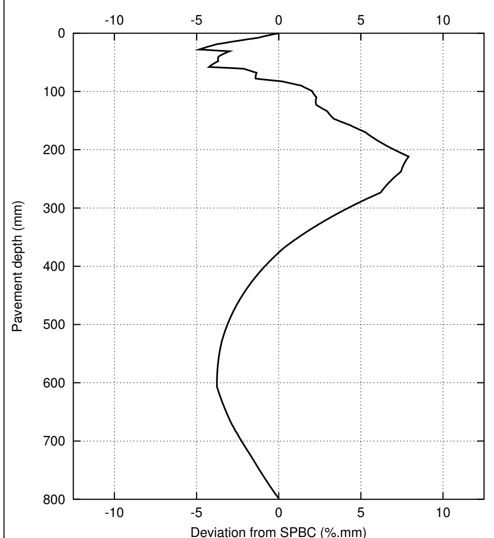

Layer strength diagram

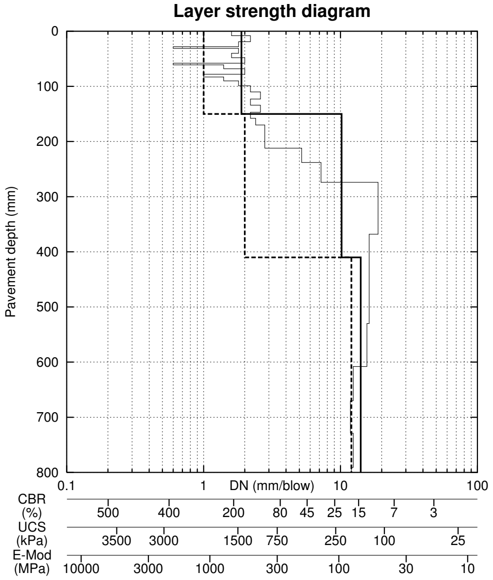

Redefined layer strength diagram

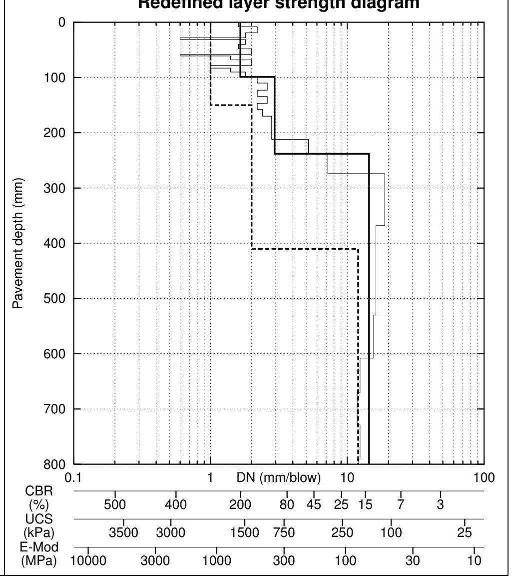

584RF#10 (Untrafficked)

DCP summary

Area : RFS
Road : MB Road Distance : 7.00 km
Structure Number (DSN_{800}) : 149
B = 45 A = 2627
Moisture : Moist
Position : Caravan
Base Type : Cemented
Category : 0
Test Date : 3/14/2007
Struct. Cap. (E80s) : 0.560×10^6
Category II: Averagely balanced shallow structure (ABS)

User defined layer summary

From-To (mm)	Avg.DN (mm/blow)	Std.Dev. (mm/blow)	CBR (%)	Range 5% - 95%	UCS (kPa)	Range 5% - 95%	E-Mod (MPa)	Range 5% - 95%
0-150	1.75	0.35	190	111- 291	1521	944- 2210	617	373- 1064
150-410	13.93	10.20	14	2- 151	157	32- 1244	68	15- 485
410-800	24.31	2.40	7	5- 10	84	65- 112	38	29- 49

Redefined layer summary

From-To (mm)	Avg.DN (mm/blow)	Std.Dev. (mm/blow)	CBR (%)	Range 5% - 95%	UCS (kPa)	Range 5% - 95%	E-Mod (MPa)	Range 5% - 95%
0-184	1.79	0.34	186	110- 281	1489	939- 2140	600	371- 1006
184-246	4.50	1.04	61	30- 130	556	303- 1084	226	127- 426
246-800	23.98	2.84	7	5- 11	86	62- 120	38	28- 53

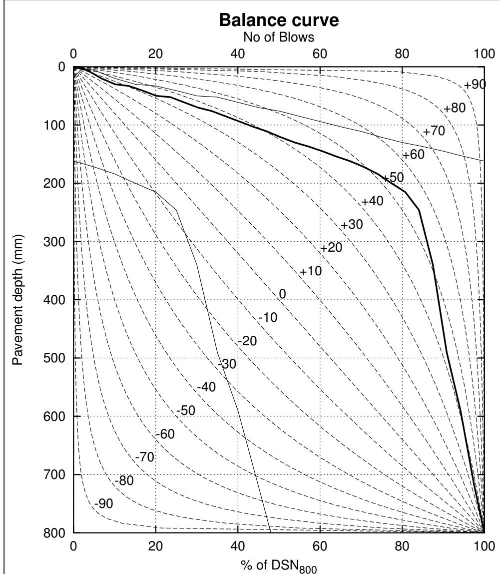

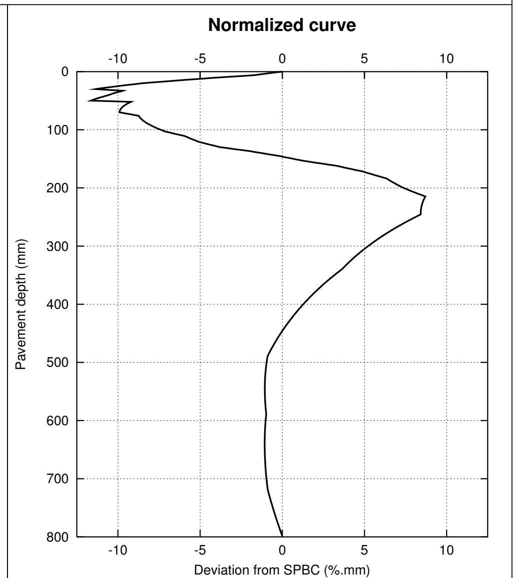

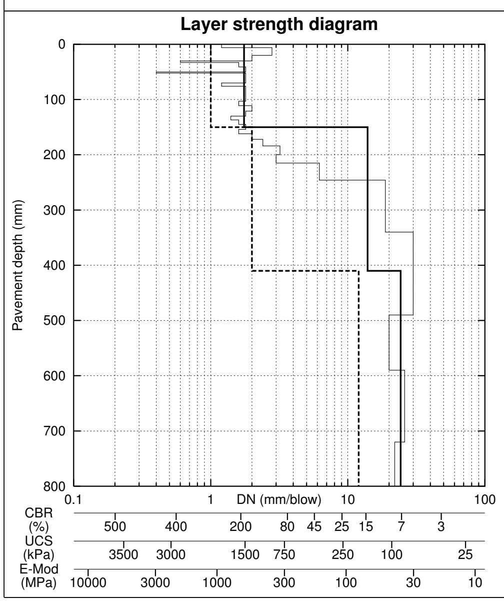

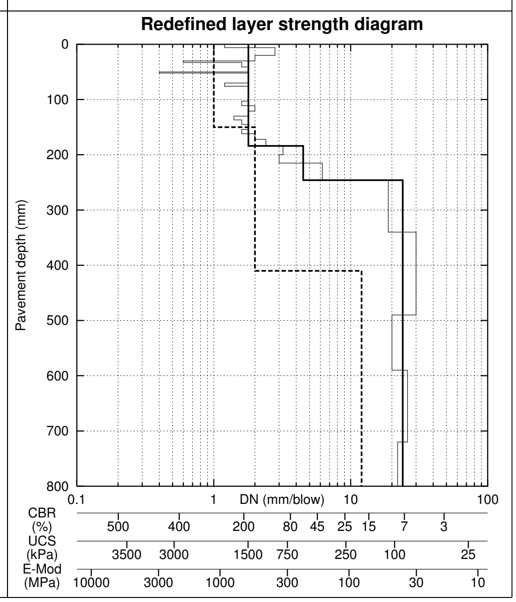

585RF#10 (Trafficked)

DCP summary

Area : RFS
Road : MB Road   Distance : 7.00 km
Structure Number (DSN_{800}) : 208
B = 41   A = 3092
Moisture : Moist
Position : Section
Base Type : Cemented
Category : 0
Test Date : 12/19/2006
Struct. Cap. (E80s) : $1.803x10^6$
Category III: Poorly balanced shallow structure (PBS)

User defined layer summary

From-To (mm)	Avg.DN (mm/blow)	Std.Dev. (mm/blow)	CBR (%)	Range 5% - 95%	UCS (kPa)	Range 5% - 95%	E-Mod (MPa)	Range 5% - 95%
0-150	1.42	0.33	229	131- 346	1788	1095- 2573	767	430- 1448
150-410	8.39	6.15	28	5- 245	277	57- 1896	117	26- 834
410-800	14.73	0.81	13	11- 16	148	127- 172	64	56- 74

Redefined layer summary

From-To (mm)	Avg.DN (mm/blow)	Std.Dev. (mm/blow)	CBR (%)	Range 5% - 95%	UCS (kPa)	Range 5% - 95%	E-Mod (MPa)	Range 5% - 95%
0- 32	2.14	0.06	156	143- 171	1279	1180- 1383	498	462- 539
32-187	1.26	0.23	253	173- 344	1952	1400- 2557	870	549- 1427
187-252	2.78	0.57	112	61- 201	954	556- 1594	377	226- 658
252-800	14.68	0.86	14	11- 16	148	126- 175	64	55- 75

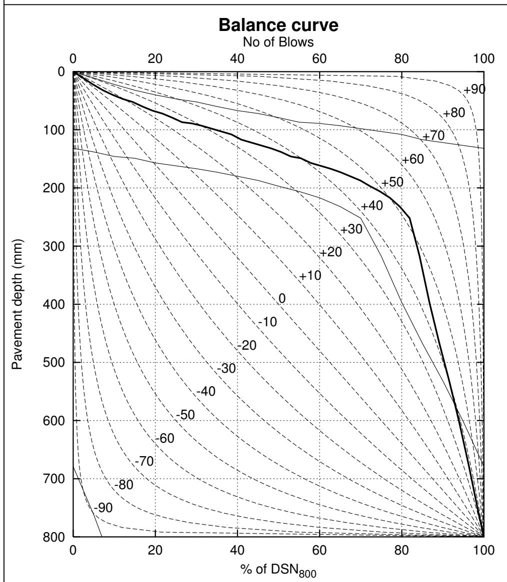

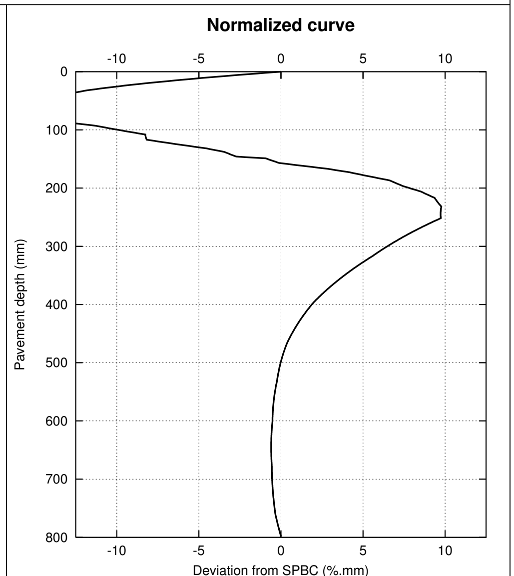

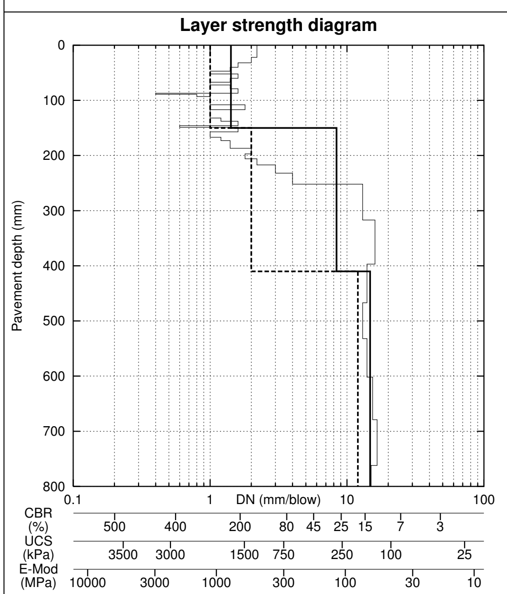

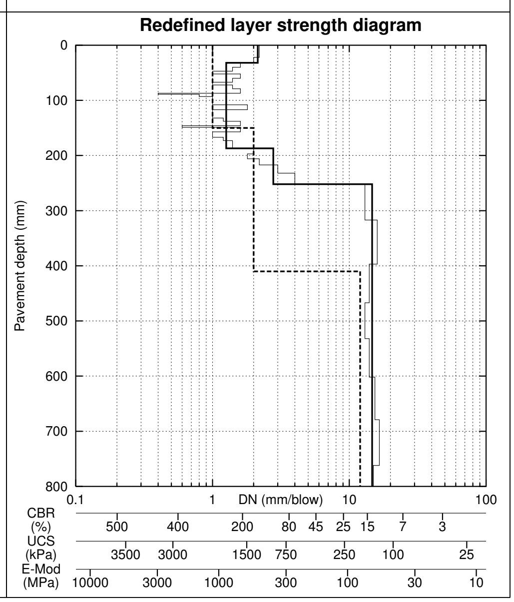

585RF#10 (Untrafficked)

DCP summary

Area : RFS		Moisture : Moist	Category : 0
Road : MB Road	Distance : 7.00 km	Position : Caravan	Test Date : 12/19/2006
Structure Number (DSN_{800}) : 181		Base Type : Cemented	Struct. Cap. (E80s) : 1.126×10^6
B = 39	A = 4345	Category VI: Poorly balanced deep structure (PBD)	

User defined layer summary

From-To (mm)	Avg.DN (mm/blow)	Std.Dev. (mm/blow)	CBR (%)	Range 5% - 95%	UCS (kPa)	Range 5% - 95%	E-Mod (MPa)	Range 5% - 95%
0-150	2.01	0.46	168	86- 276	1366	753- 2112	531	301- 985
150-410	6.11	4.70	41	6- 324	396	76- 2431	163	34- 1277
410-800	22.27	2.20	8	6- 11	93	71- 123	41	32- 54

Redefined layer summary

From-To (mm)	Avg.DN (mm/blow)	Std.Dev. (mm/blow)	CBR (%)	Range 5% - 95%	UCS (kPa)	Range 5% - 95%	E-Mod (MPa)	Range 5% - 95%
0-266	1.97	0.42	172	91- 274	1389	793- 2098	542	316- 974
266-335	4.92	0.97	54	30- 103	503	298- 888	206	125- 353
335-800	22.03	2.02	8	6- 11	94	73- 122	42	33- 54

Balance curve

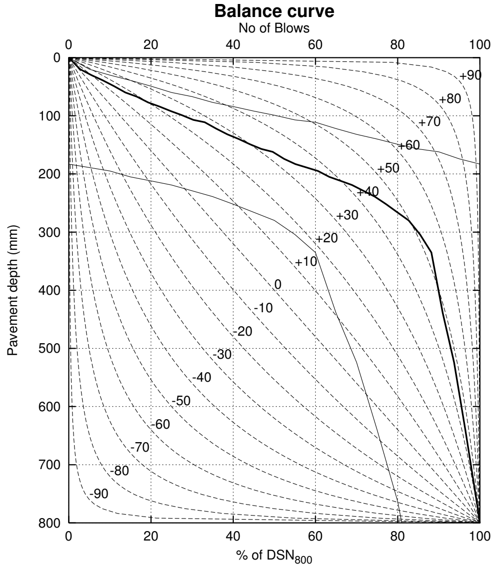

Normalized curve

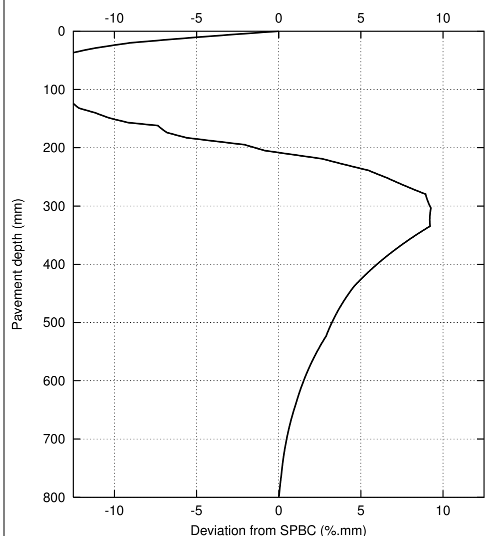

Layer strength diagram

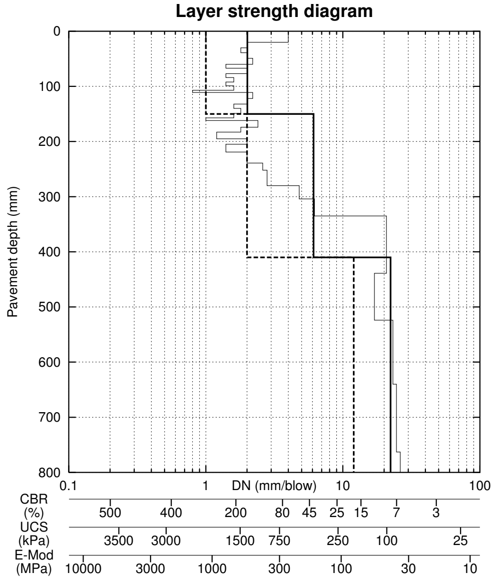

Redefined layer strength diagram

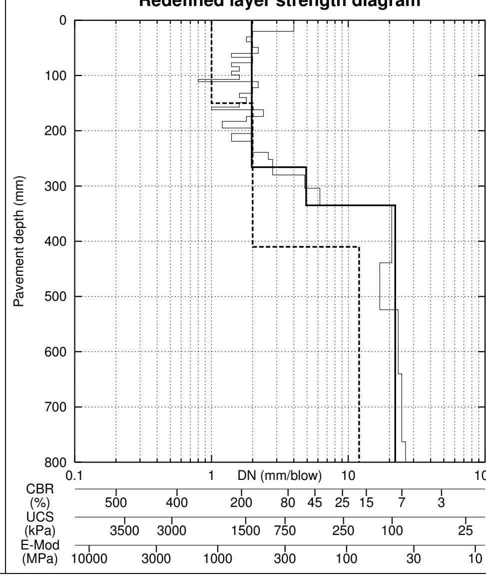

586RF#4 (Trafficked)

DCP summary

Area : RFS
Road : MB Road Distance : 4.00 km
Structure Number (DSN_{800}) : 337
B = 36 A = 6718

Moisture : Moist
Position : Section
Base Type : Cemented
Category VI: Poorly balanced deep structure (PBD)

Category : 0
Test Date : 3/24/2007
Struct. Cap. (E80s) : 9.824×10^6

User defined layer summary

From-To (mm)	Avg.DN (mm/blow)	Std.Dev. (mm/blow)	CBR (%)	Range 5% - 95%	UCS (kPa)	Range 5% - 95%	E-Mod (MPa)	Range 5% - 95%
0-150	1.79	0.79	187	58- 397	1495	532- 2904	603	217- 2028
150-410	2.89	2.62	107	13- 468	914	147- 3356	362	64- 3890
410-800	15.61	0.83	13	11- 15	139	120- 161	60	53- 70

Redefined layer summary

From-To (mm)	Avg.DN (mm/blow)	Std.Dev. (mm/blow)	CBR (%)	Range 5% - 95%	UCS (kPa)	Range 5% - 95%	E-Mod (MPa)	Range 5% - 95%
0-181	1.65	0.68	201	68- 399	1594	615- 2917	658	249- 2059
181-291	0.81	0.15	340	251- 416	2533	1940- 3026	1396	862- 2347
291-336	2.40	0.49	135	73- 228	1122	655- 1786	440	264- 766
336-800	15.01	1.97	13	9- 20	145	101- 210	63	45- 90

Balance curve

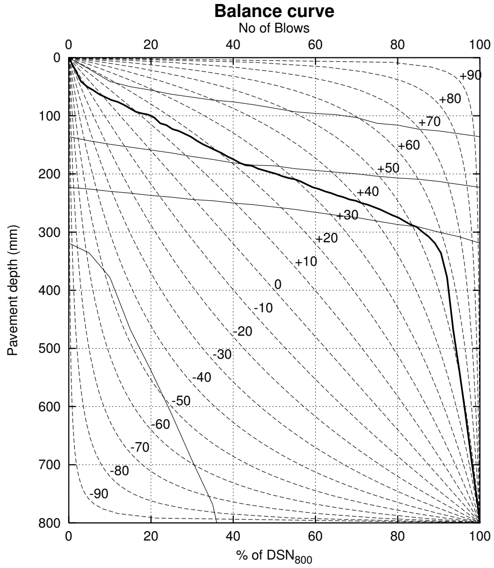

Normalized curve

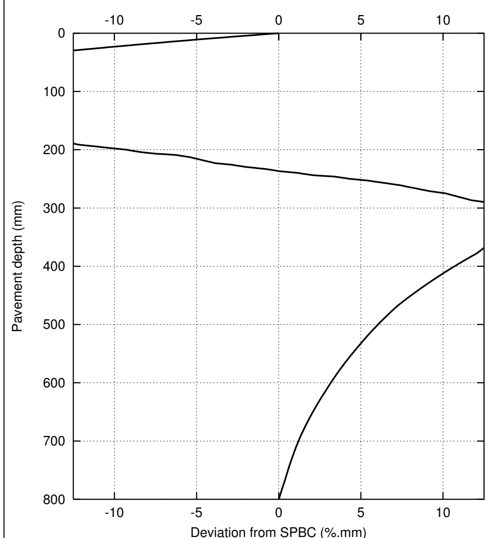

Layer strength diagram

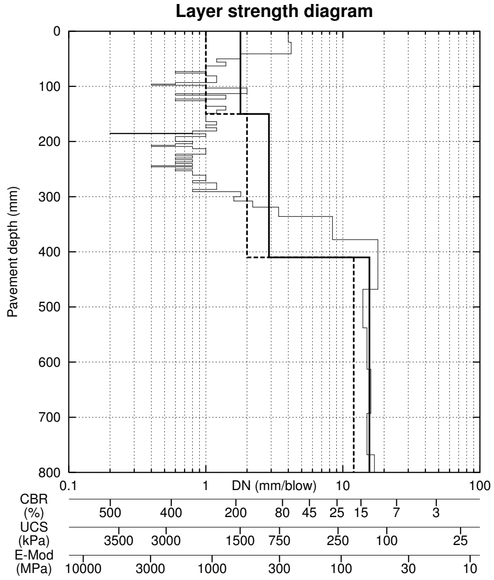

Redefined layer strength diagram

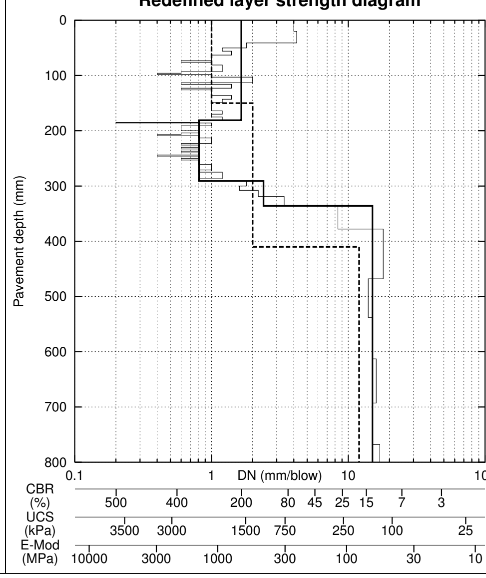

586RF#4 (Untrafficked)

DCP summary

Area : RFS		Moisture : Moist	Category : 0
Road : MB Road	Distance : 4.00 km	Position : Caravan	Test Date : 3/24/2007
Structure Number (DSN_{800}) : 295		Base Type : Cemented	Struct. Cap. (E80s) : $6.154x10^6$
B = 32	A = 6212	Category VI: Poorly balanced deep structure (PBD)	

User defined layer summary

From-To (mm)	Avg.DN (mm/blow)	Std.Dev. (mm/blow)	CBR (%)	Range 5% - 95%	UCS (kPa)	Range 5% - 95%	E-Mod (MPa)	Range 5% - 95%
0-150	2.17	0.81	153	53- 336	1255	494- 2505	490	202- 1362
150-410	2.18	1.30	153	32- 422	1253	319- 3068	489	133- 2477
410-800	13.67	0.72	15	13- 18	161	139- 187	69	60- 80

Redefined layer summary

From-To (mm)	Avg.DN (mm/blow)	Std.Dev. (mm/blow)	CBR (%)	Range 5% - 95%	UCS (kPa)	Range 5% - 95%	E-Mod (MPa)	Range 5% - 95%
0- 91	3.09	0.32	98	71- 137	847	637- 1140	337	257- 447
91-304	1.07	0.15	286	218- 353	2175	1712- 2619	1035	723- 1511
304-363	2.57	0.59	124	62- 230	1041	568- 1793	410	230- 770
363-800	13.08	1.89	16	10- 25	169	114- 255	73	50- 108

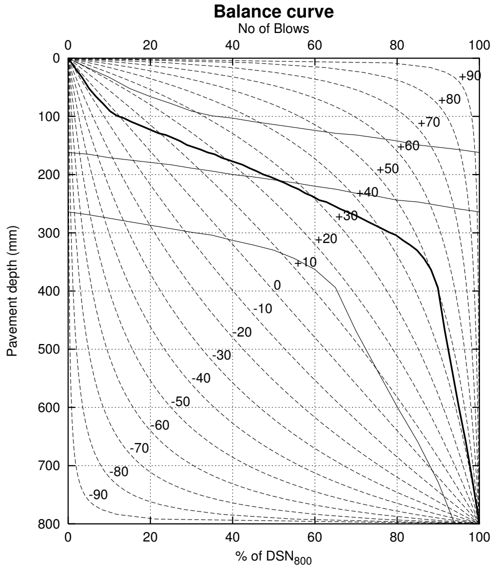

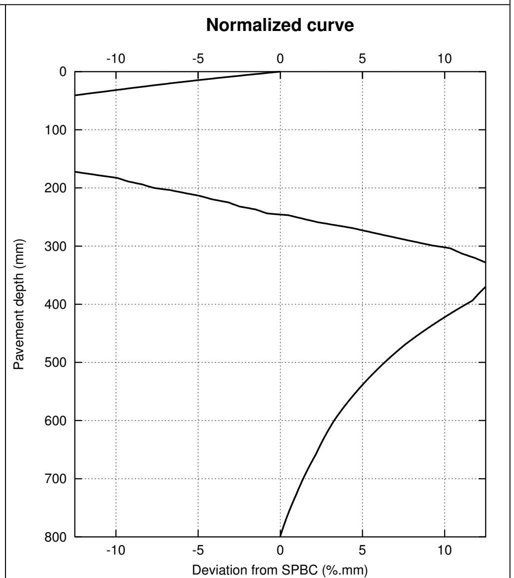

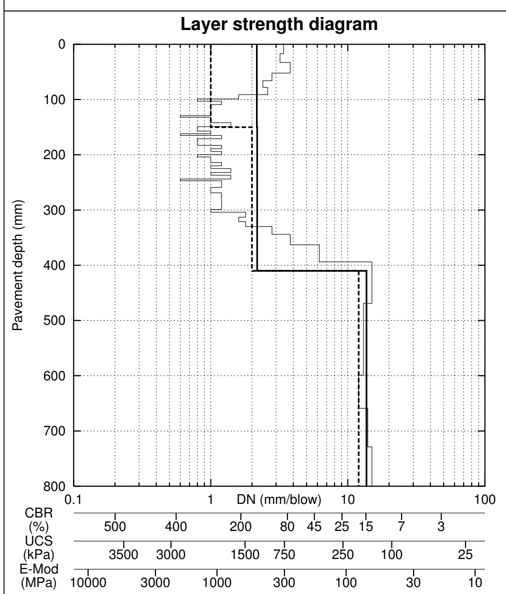

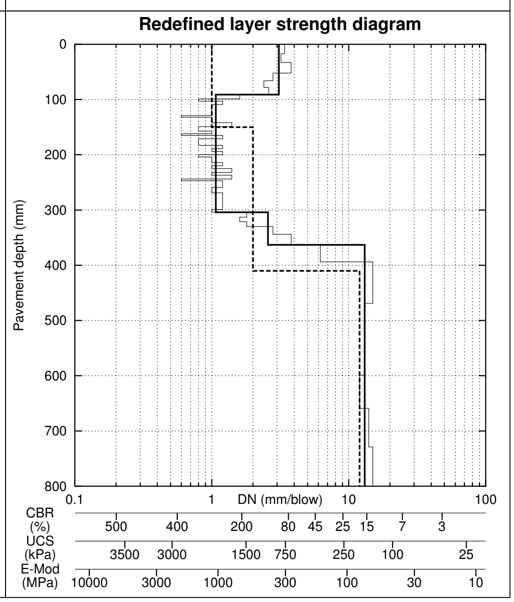

586RF#12 (Trafficked)
Did not penetrate.

586RF#12 (Untrafficked)

DCP summary

Area : RFS
Road : MB Road   Distance : 12.00 km
Structure Number (DSN_{800}) : 239
B = 42   A = 3519
Moisture : Moist
Position : Traffic
Base Type : Cemented
Category : 0
Test Date : 03/24/07
Struct. Cap. (E80s) : 2.937×10^6
Category III: Poorly balanced shallow structure (PBS)

User defined layer summary

From-To (mm)	Avg.DN (mm/blow)	Std.Dev. (mm/blow)	CBR (%)	Range 5% - 95%	UCS (kPa)	Range 5% - 95%	E-Mod (MPa)	Range 5% - 95%
0-150	1.31	0.34	245	135- 371	1899	1126- 2735	835	441- 1693
150-410	5.60	3.86	46	8- 306	436	95- 2309	179	42- 1152
410-800	19.65	5.18	9	4- 22	107	54- 229	47	25- 97

Redefined layer summary

From-To (mm)	Avg.DN (mm/blow)	Std.Dev. (mm/blow)	CBR (%)	Range 5% - 95%	UCS (kPa)	Range 5% - 95%	E-Mod (MPa)	Range 5% - 95%
0- 31	2.08	0.12	162	134- 187	1318	1117- 1494	513	438- 603
31-180	1.14	0.24	273	179- 372	2088	1443- 2741	967	574- 1702
180-230	1.72	0.24	193	133- 263	1536	1110- 2021	626	436- 918
230-290	3.50	0.93	83	38- 189	736	368- 1511	295	153- 612
290-800	17.54	4.86	11	5- 27	122	59- 270	53	27- 114

Balance curve

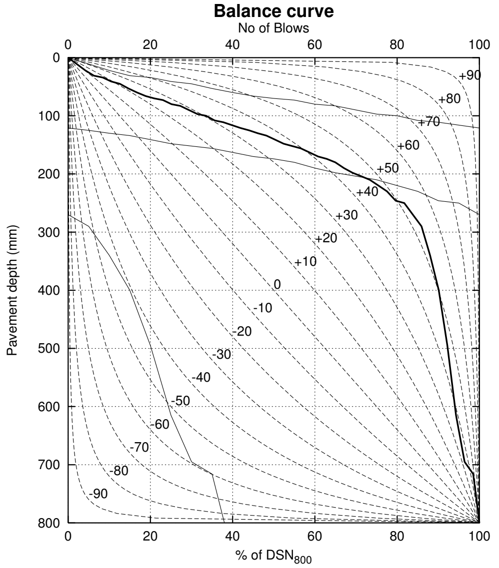

Normalized curve

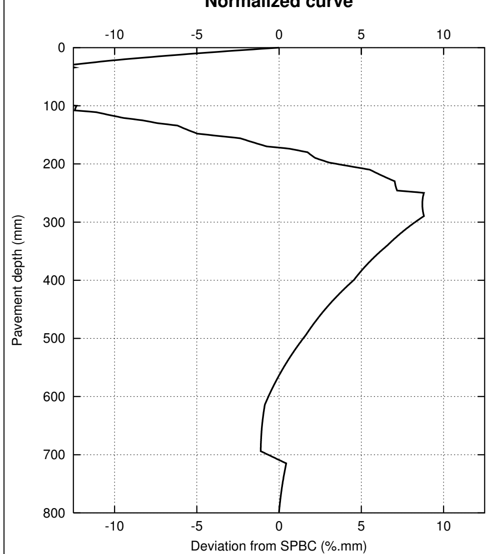

Layer strength diagram

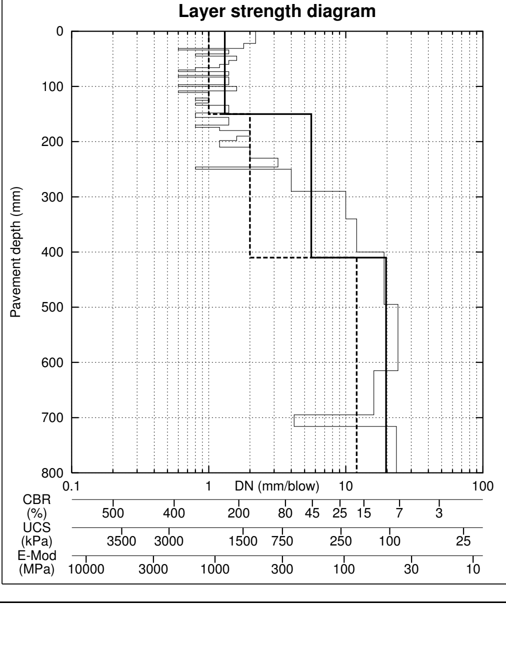

Redefined layer strength diagram

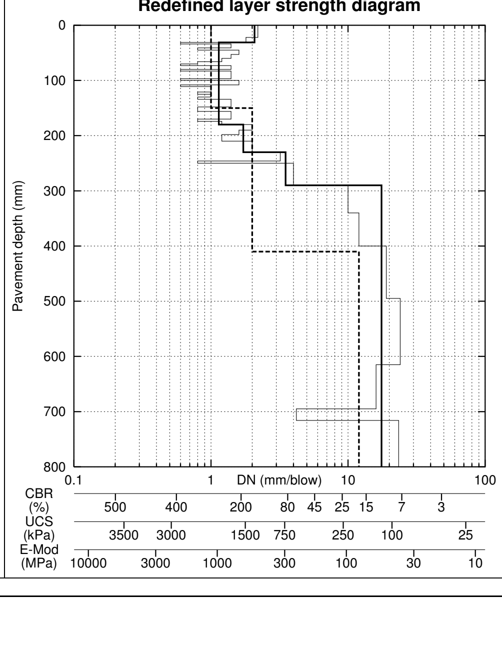

587RF#4 (Trafficked)

DCP summary

Area : RFS
Road : MB Road   Distance : 4.00 km
Structure Number (DSN_{800}) : 193
B = 38   A = 4767

Moisture : Moist   Category : 0
Position : Section   Test Date : 03/24/07
Base Type : Cemented   Struct. Cap. (E80s) : 1.392×10^6
Category VI: Poorly balanced deep structure (PBD)

User defined layer summary

From-To (mm)	Avg.DN (mm/blow)	Std.Dev. (mm/blow)	CBR (%)	Range 5% - 95%	UCS (kPa)	Range 5% - 95%	E-Mod (MPa)	Range 5% - 95%
0-150	2.17	0.85	153	50- 346	1257	473- 2573	490	194- 1447
150-410	4.86	3.11	55	11- 310	511	121- 2338	208	53- 1180
410-800	22.69	2.93	8	5- 12	91	64- 132	41	29- 58

Redefined layer summary

From-To (mm)	Avg.DN (mm/blow)	Std.Dev. (mm/blow)	CBR (%)	Range 5% - 95%	UCS (kPa)	Range 5% - 95%	E-Mod (MPa)	Range 5% - 95%
0-284	2.03	0.62	166	68- 316	1351	616- 2375	525	249- 1217
284-408	9.66	2.87	23	10- 61	237	110- 559	100	49- 227
408-800	22.72	2.93	8	5- 12	91	64- 132	41	29- 57

Balance curve

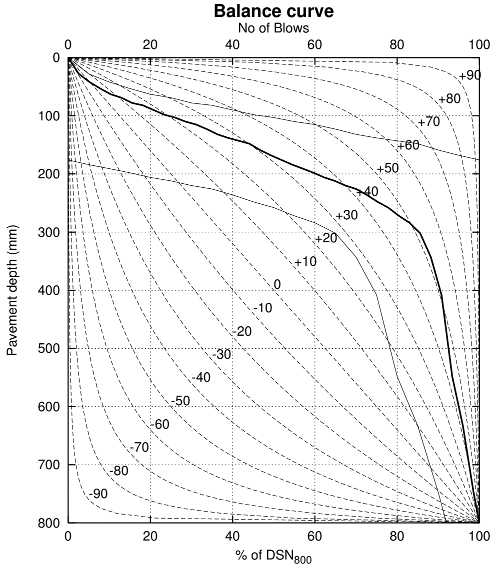

Normalized curve

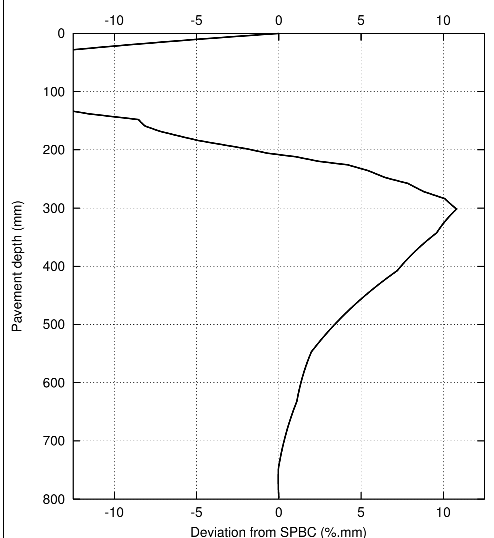

Layer strength diagram

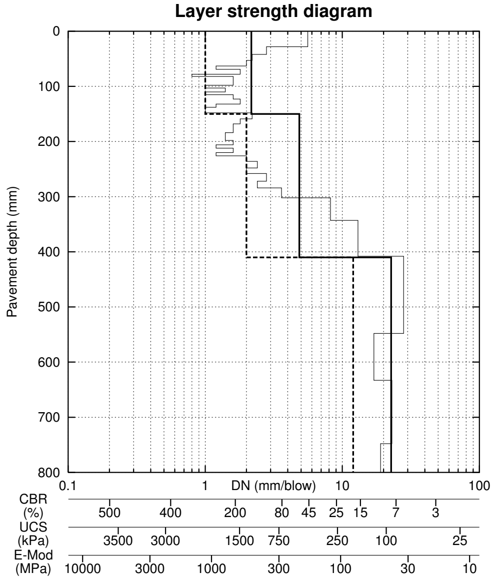

Redefined layer strength diagram

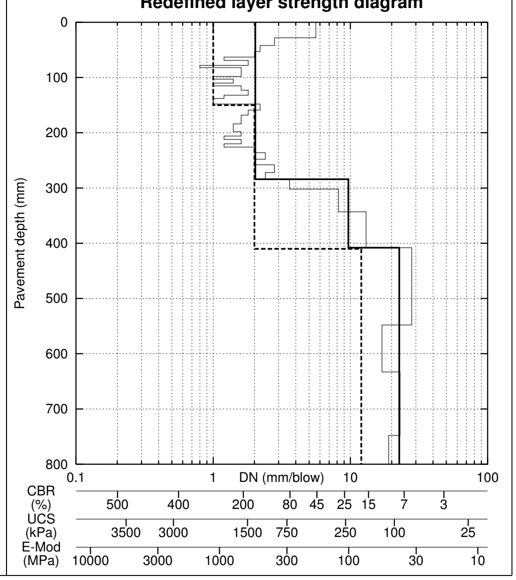

587RF#4 (Untrafficked)

DCP summary

Area : RFS
Road : MB Road   Distance : 4.00 km
Structure Number (DSN_{800}) : 217
B = 44   A = 4543

Moisture : Moist
Position : Traffic
Base Type : Cemented
Category III: Poorly balanced shallow structure (PBS)

Category : 0
Test Date : 03/24/07
Struct. Cap. (E80s) : 2.112×10^6

User defined layer summary

From-To (mm)	Avg.DN (mm/blow)	Std.Dev. (mm/blow)	CBR (%)	Range 5% - 95%	UCS (kPa)	Range 5% - 95%	E-Mod (MPa)	Range 5% - 95%
0-150	1.52	0.43	216	104- 359	1701	896- 2660	717	356- 1571
150-410	7.14	6.41	34	4- 346	332	54- 2576	138	25- 1452
410-800	24.79	2.00	7	5- 9	83	66- 104	37	30- 46

Redefined layer summary

From-To (mm)	Avg.DN (mm/blow)	Std.Dev. (mm/blow)	CBR (%)	Range 5% - 95%	UCS (kPa)	Range 5% - 95%	E-Mod (MPa)	Range 5% - 95%
0-241	1.49	0.39	220	114- 351	1725	971- 2606	731	383- 1493
241-298	3.86	0.38	74	54- 101	660	506- 872	266	206- 346
298-800	23.32	2.99	8	5- 11	88	63- 127	39	28- 56

Balance curve

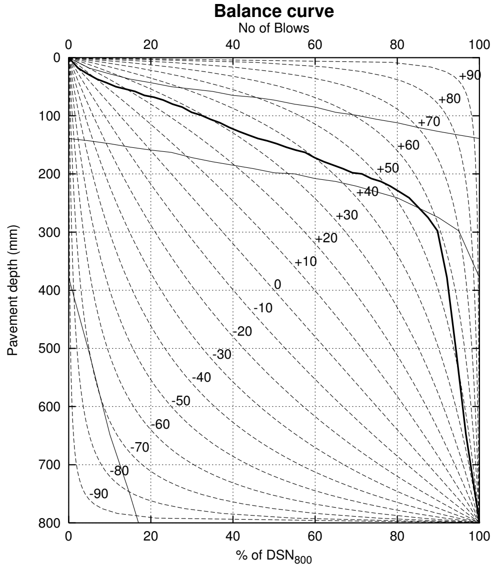

Normalized curve

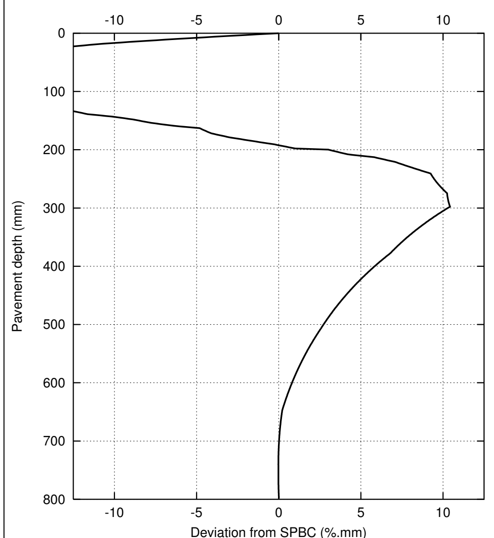

Layer strength diagram

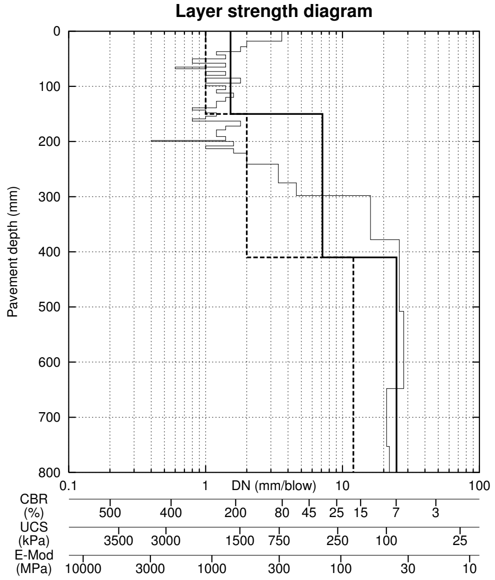

Redefined layer strength diagram

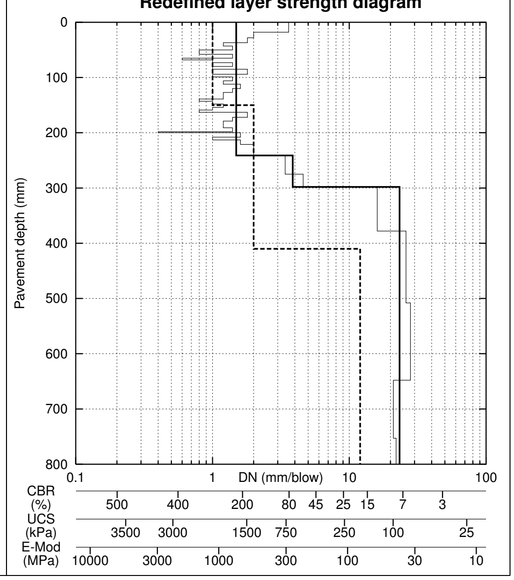

587RF#12 (Trafficked)

DCP summary

Area : RFS
Road : MB Road Distance : 12.00 km
Structure Number (DSN_{800}) : 234
B = 37 A = 4345

Moisture : Moist
Position : Section
Base Type : Cemented
Category : 0
Test Date : 03/24/07
Struct. Cap. (E80s) : $2.725x10^6$
Category VI: Poorly balanced deep structure (PBD)

User defined layer summary

From-To (mm)	Avg.DN (mm/blow)	Std.Dev. (mm/blow)	CBR (%)	Range 5% - 95%	UCS (kPa)	Range 5% - 95%	E-Mod (MPa)	Range 5% - 95%
0-150	1.70	0.48	195	91- 338	1554	794- 2522	635	317- 1382
150-410	4.91	3.78	54	8- 363	504	98- 2682	206	43- 1605
410-800	16.42	2.93	12	7- 21	131	81- 218	57	36- 93

Redefined layer summary

From-To (mm)	Avg.DN (mm/blow)	Std.Dev. (mm/blow)	CBR (%)	Range 5% - 95%	UCS (kPa)	Range 5% - 95%	E-Mod (MPa)	Range 5% - 95%
0- 47	2.46	0.42	131	78- 207	1094	695- 1636	430	279- 681
47-237	1.33	0.29	242	148- 351	1880	1219- 2609	824	476- 1497
237-307	3.10	0.78	97	46- 203	843	437- 1612	335	180- 668
307-800	15.53	2.88	13	7- 23	139	85- 237	61	38- 101

Balance curve

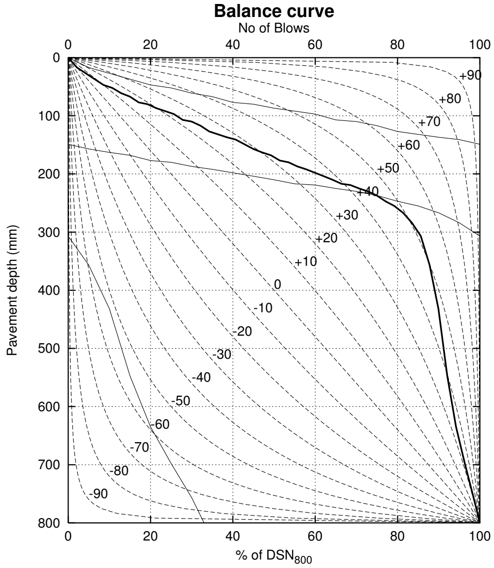

Normalized curve

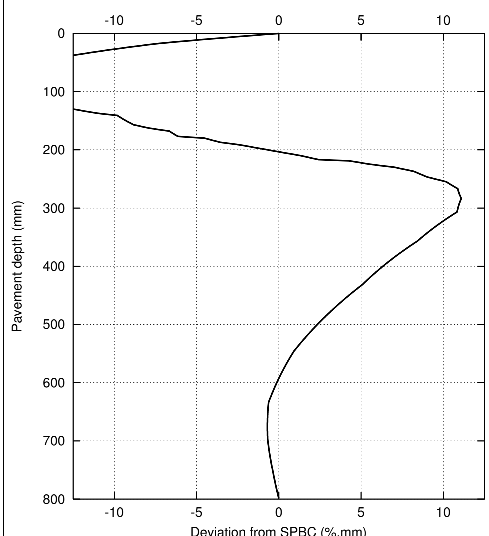

Layer strength diagram

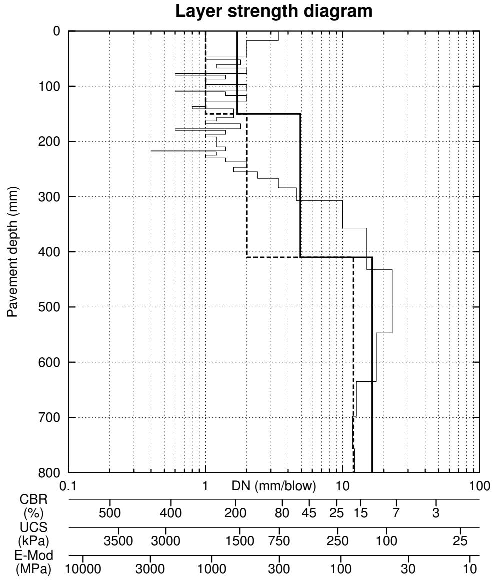

Redefined layer strength diagram

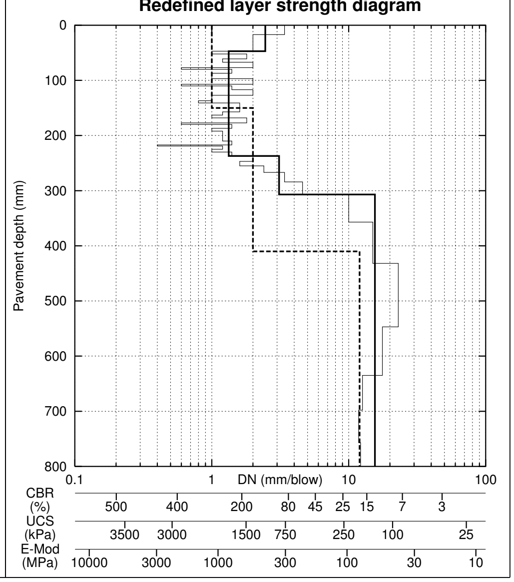

587RF#12 (Untrafficked)

DCP summary

Area : RFS
Road : MB Road Distance : 12.00 km
Structure Number (DSN_{800}) : 239
B = 42 A = 3519
Moisture : Moist
Position : Traffic
Base Type : Cemented
Category : 0
Test Date : 03/24/07
Struct. Cap. (E80s) : 2.937×10^6
Category III: Poorly balanced shallow structure (PBS)

User defined layer summary

From-To (mm)	Avg.DN (mm/blow)	Std.Dev. (mm/blow)	CBR (%)	Range 5% - 95%	UCS (kPa)	Range 5% - 95%	E-Mod (MPa)	Range 5% - 95%
0-150	1.31	0.34	245	135- 371	1899	1126- 2735	835	441- 1693
150-410	5.60	3.86	46	8- 306	436	95- 2309	179	42- 1152
410-800	19.65	5.18	9	4- 22	107	54- 229	47	25- 97

Redefined layer summary

From-To (mm)	Avg.DN (mm/blow)	Std.Dev. (mm/blow)	CBR (%)	Range 5% - 95%	UCS (kPa)	Range 5% - 95%	E-Mod (MPa)	Range 5% - 95%
0- 31	2.08	0.12	162	134- 187	1318	1117- 1494	513	438- 603
31-180	1.14	0.24	273	179- 372	2088	1443- 2741	967	574- 1702
180-230	1.72	0.24	193	133- 263	1536	1110- 2021	626	436- 918
230-290	3.50	0.93	83	38- 189	736	368- 1511	295	153- 612
290-800	17.54	4.86	11	5- 27	122	59- 270	53	27- 114

Balance curve

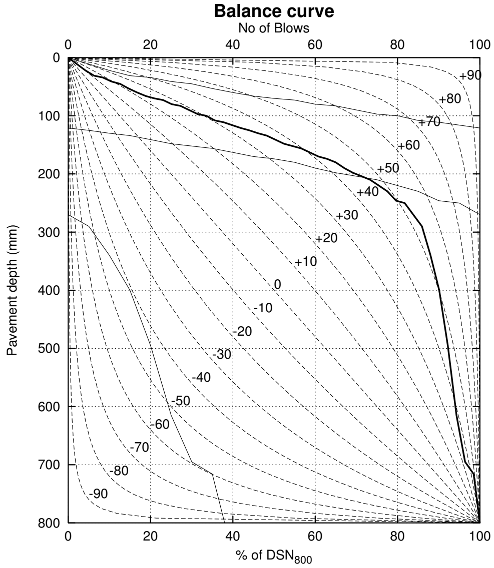

Normalized curve

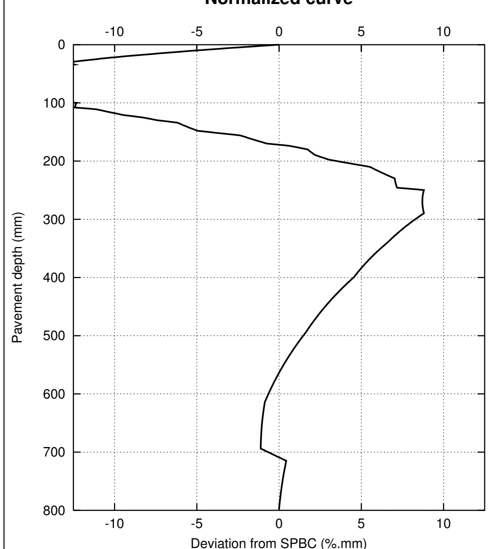

Layer strength diagram

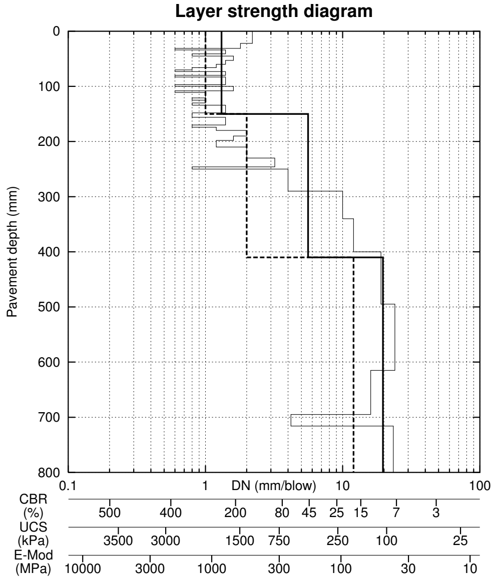

Redefined layer strength diagram

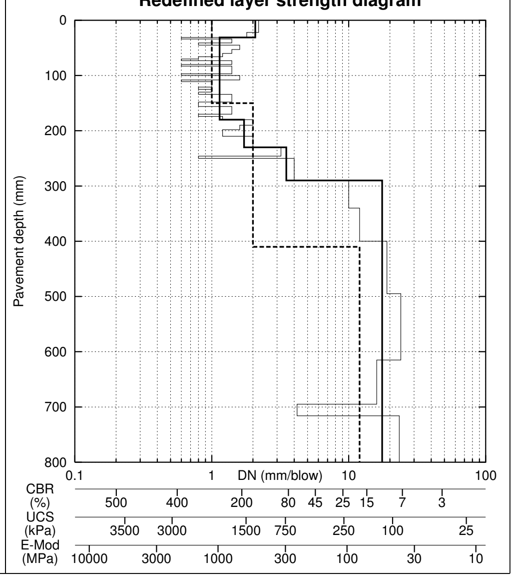

588RF#4 (Trafficked)

DCP summary

Area : RFS
Road : MB Road Distance : 4.00 km
Structure Number (DSN_{800}) : 163
B = 38 A = 4369

Moisture : Moist Category : 0
Position : Section Test Date : 3/22/2007
Base Type : Cemented Struct. Cap. (E80s): $0.782x10^6$
Category VI: Poorly balanced deep structure (PBD)

User defined layer summary

From-To (mm)	Avg.DN (mm/blow)	Std.Dev. (mm/blow)	CBR (%)	Range 5% - 95%	UCS (kPa)	Range 5% - 95%	E-Mod (MPa)	Range 5% - 95%
0-150	2.24	0.62	147	65- 282	1213	592- 2150	474	240- 1014
150-410	10.48	9.82	21	3- 290	216	34- 2200	92	16- 1055
410-800	21.70	4.85	8	4- 17	96	53- 183	43	24- 78

Redefined layer summary

From-To (mm)	Avg.DN (mm/blow)	Std.Dev. (mm/blow)	CBR (%)	Range 5% - 95%	UCS (kPa)	Range 5% - 95%	E-Mod (MPa)	Range 5% - 95%
0-105	2.60	0.70	122	55- 246	1026	512- 1909	404	209- 842
105-210	1.49	0.28	219	141- 314	1722	1165- 2365	729	456- 1207
210-264	3.80	0.68	75	44- 134	673	418- 1120	271	172- 439
264-800	21.50	5.66	8	4- 20	97	49- 207	43	22- 88

Balance curve

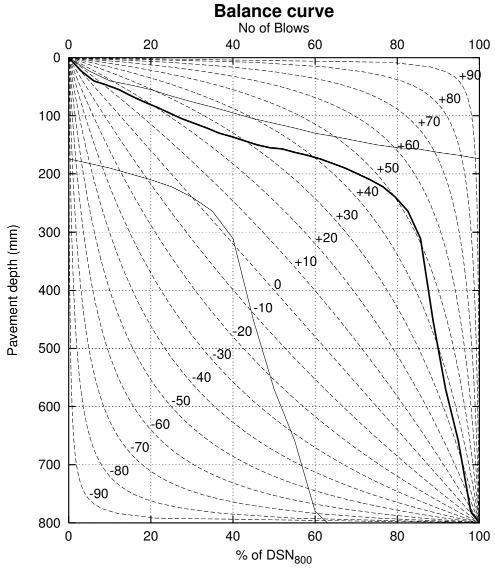

Normalized curve

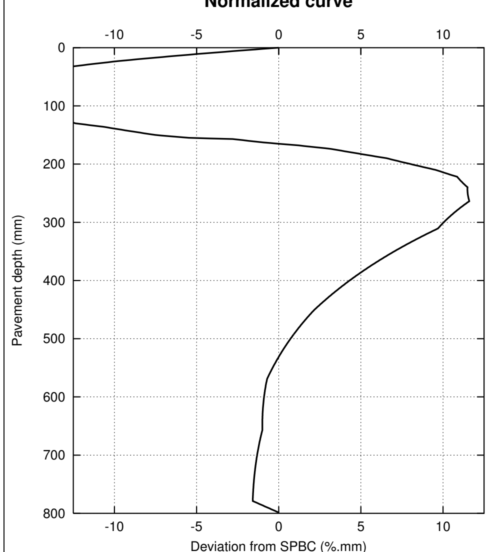

Layer strength diagram

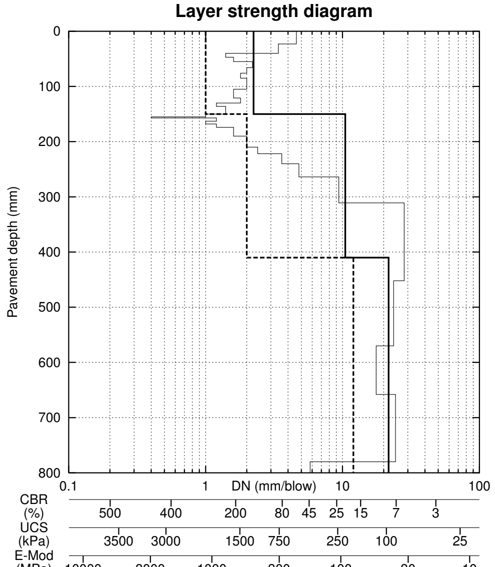

Redefined layer strength diagram

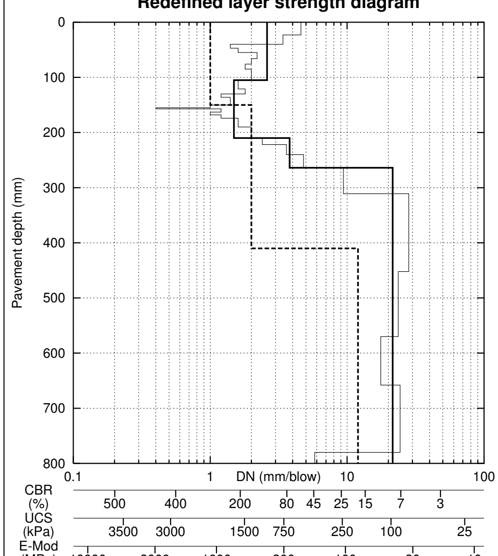

588RF#4 (Untrafficked)

DCP summary

Area : RFS
Road : MB Road   Distance : 4.00 km
Structure Number (DSN_{800}) : 186
B = 36   A = 5959

Moisture : Moist   Category : 0
Position : Caravan   Test Date : 3/22/2007
Base Type : Cemented   Struct. Cap. (E80s): 1.239×10^6
Category VI: Poorly balanced deep structure (PBD)

User defined layer summary

From-To (mm)	Avg.DN (mm/blow)	Std.Dev. (mm/blow)	CBR (%)	Range 5% - 95%	UCS (kPa)	Range 5% - 95%	E-Mod (MPa)	Range 5% - 95%
0-150	2.74	0.98	114	41- 284	969	393- 2164	383	162- 1026
150-410	4.21	2.73	66	13- 341	599	140- 2538	242	61- 1402
410-800	25.98	4.51	7	4- 12	78	49- 129	35	23- 56

Redefined layer summary

From-To (mm)	Avg.DN (mm/blow)	Std.Dev. (mm/blow)	CBR (%)	Range 5% - 95%	UCS (kPa)	Range 5% - 95%	E-Mod (MPa)	Range 5% - 95%
0- 79	3.98	0.27	71	57- 88	638	529- 774	257	215- 309
79-271	1.68	0.35	197	113- 305	1570	958- 2305	645	379- 1149
271-393	5.96	2.17	42	15- 141	406	163- 1168	168	70- 457
393-800	26.04	4.43	7	4- 11	78	50- 127	35	23- 56

Balance curve

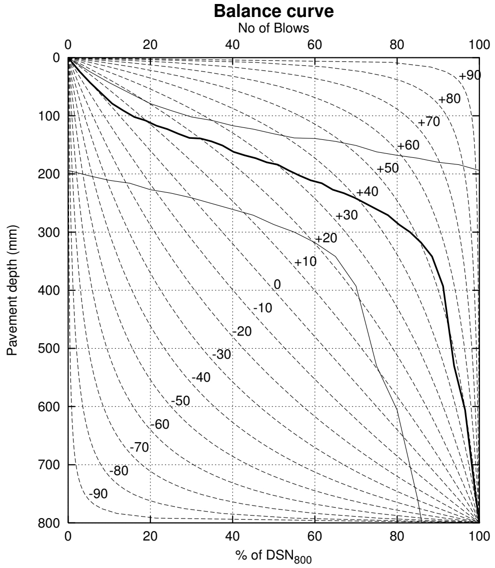

Normalized curve

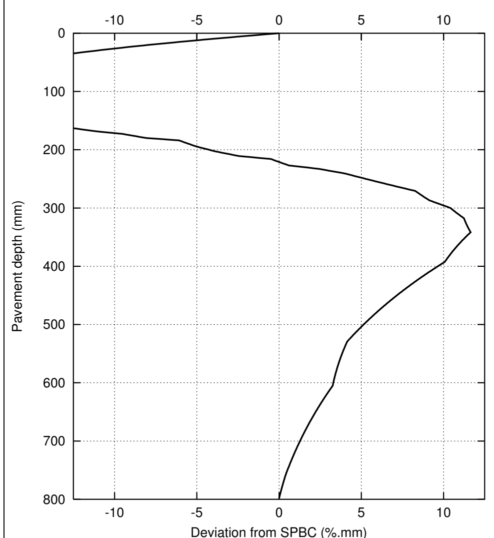

Layer strength diagram

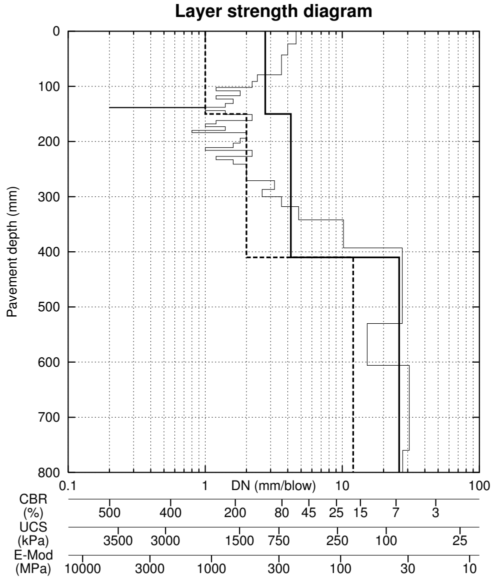

Redefined layer strength diagram

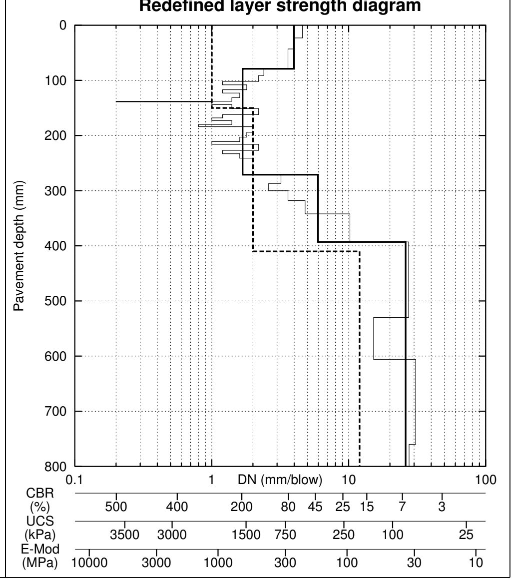

588RF#12 (Trafficked)

DCP summary

Area : RFS
Road : MB Road Distance : 12.00 km
Structure Number (DSN_{800}) : 138
B = 37 A = 4643

Moisture : Moist
Position : Section
Base Type : Cemented
Category : 0
Test Date : 3/22/2007
Struct. Cap. (E80s) : $0.435x10^6$
Category VI: Poorly balanced deep structure (PBD)

User defined layer summary

From-To (mm)	Avg.DN (mm/blow)	Std.Dev. (mm/blow)	CBR (%)	Range 5% - 95%	UCS (kPa)	Range 5% - 95%	E-Mod (MPa)	Range 5% - 95%
0-150	2.96	0.69	103	51- 204	889	481- 1616	353	197- 669
150-410	5.85	3.63	44	9- 265	415	101- 2032	171	45- 925
410-800	31.25	0.87	5	5- 6	64	59- 69	29	27- 31

Redefined layer summary

From-To (mm)	Avg.DN (mm/blow)	Std.Dev. (mm/blow)	CBR (%)	Range 5% - 95%	UCS (kPa)	Range 5% - 95%	E-Mod (MPa)	Range 5% - 95%
0-276	2.69	0.59	117	61- 214	988	556- 1683	390	226- 707
276-385	7.81	1.60	30	16- 59	300	174- 542	126	75- 220
385-800	31.30	0.85	5	5- 6	64	59- 69	29	27- 31

Balance curve

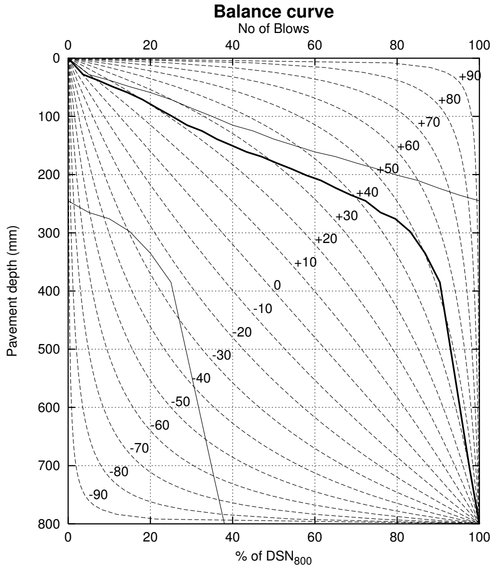

Normalized curve

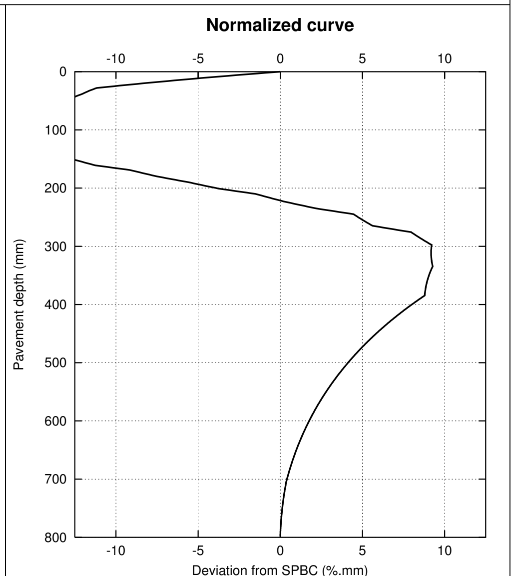

Layer strength diagram

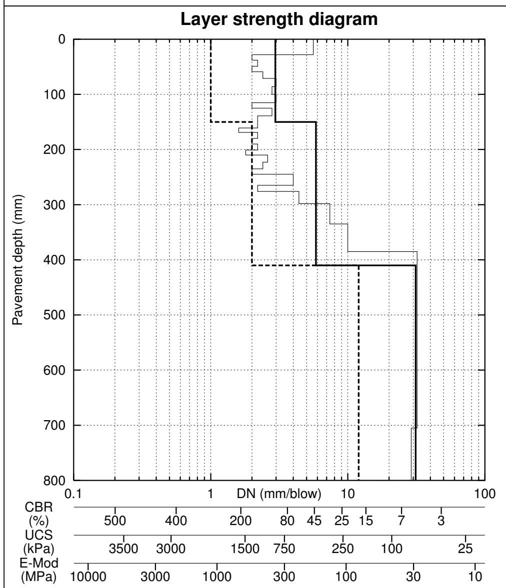

Redefined layer strength diagram

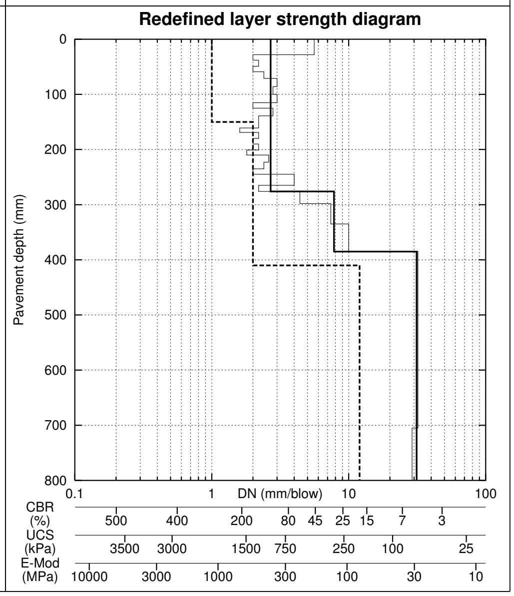

588RF#12 (Untrafficked)

DCP summary

Area : RFS
Road : MB Road Distance : 12.00 km
Structure Number (DSN_{800}) : 223
B = 38 A = 5686

Moisture : Moist Category : 0
Position : Traffic Test Date : 3/22/2007
Base Type : Cemented Struct. Cap. (E80s) : 2.305×10^6
Category VI: Poorly balanced deep structure (PBD)

User defined layer summary

From-To (mm)	Avg.DN (mm/blow)	Std.Dev. (mm/blow)	CBR (%)	Range 5% - 95%	UCS (kPa)	Range 5% - 95%	E-Mod (MPa)	Range 5% - 95%
0-150	2.60	1.43	122	28- 381	1028	285- 2802	405	120- 1812
150-410	6.87	6.95	35	4- 391	347	49- 2864	144	23- 1939
410-800	20.11	3.14	9	6- 15	104	69- 163	46	31- 70

Redefined layer summary

From-To (mm)	Avg.DN (mm/blow)	Std.Dev. (mm/blow)	CBR (%)	Range 5% - 95%	UCS (kPa)	Range 5% - 95%	E-Mod (MPa)	Range 5% - 95%
0- 68	4.56	0.27	60	50- 72	548	465- 649	223	191- 261
68-259	1.41	0.52	231	93- 405	1804	807- 2954	777	322- 2148
259-348	7.80	3.18	30	10- 115	301	110- 979	126	48- 387
348-800	20.82	3.25	9	5- 14	100	66- 157	44	30- 68

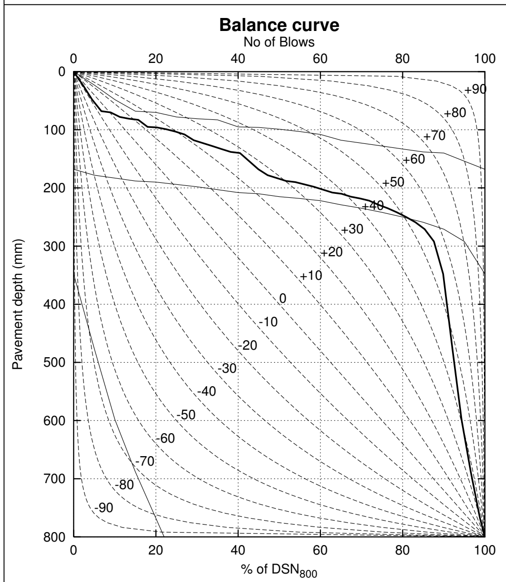

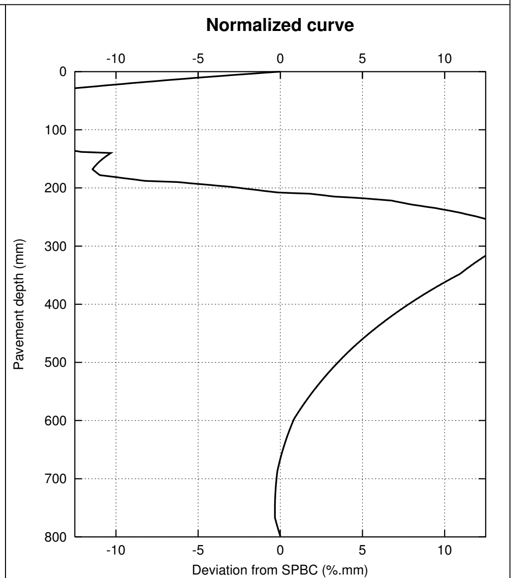

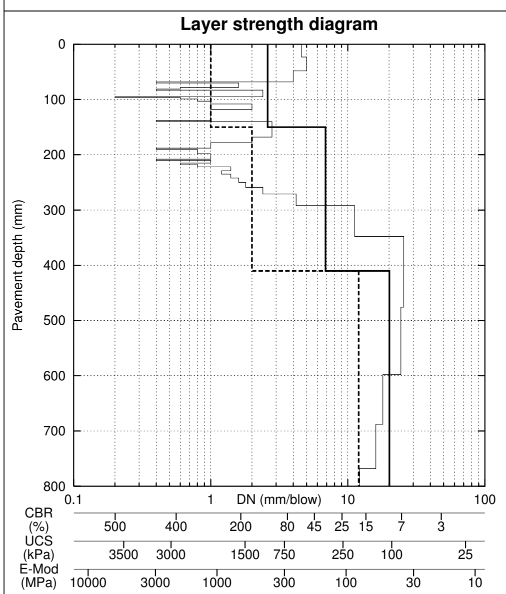

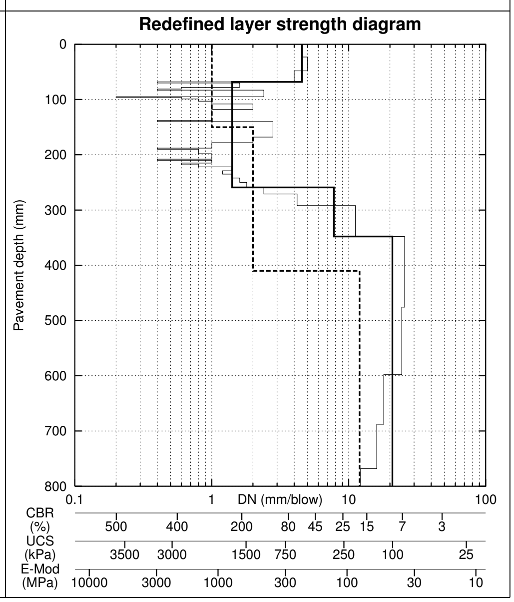

589RF#4 (Trafficked)

DCP summary

Area : RFS
Road : MB Road Distance : 4.00 km
Structure Number (DSN_{800}) : 232
B = 40 A = 2373

Moisture : Moist
Position : Section
Base Type : Cemented

Category : 0
Test Date : 3/21/2007
Struct. Cap. (E80s) : $2.670x10^6$

Category II: Averagely balanced shallow structure (ABS)

User defined layer summary

From-To (mm)	Avg.DN (mm/blow)	Std.Dev. (mm/blow)	CBR (%)	Range 5% - 95%	UCS (kPa)	Range 5% - 95%	E-Mod (MPa)	Range 5% - 95%
0-150	1.34	0.27	240	155- 340	1867	1270- 2536	816	495- 1400
150-410	6.61	5.27	37	6- 321	362	67- 2408	150	30- 1252
410-800	13.25	0.96	15	12- 19	166	137- 204	72	59- 87

Redefined layer summary

From-To (mm)	Avg.DN (mm/blow)	Std.Dev. (mm/blow)	CBR (%)	Range 5% - 95%	UCS (kPa)	Range 5% - 95%	E-Mod (MPa)	Range 5% - 95%
0-244	1.45	0.28	225	142- 326	1765	1174- 2442	754	459- 1288
244-292	3.39	0.63	87	50- 160	764	465- 1303	306	191- 507
292-800	13.80	1.10	15	11- 19	159	128- 199	69	56- 85

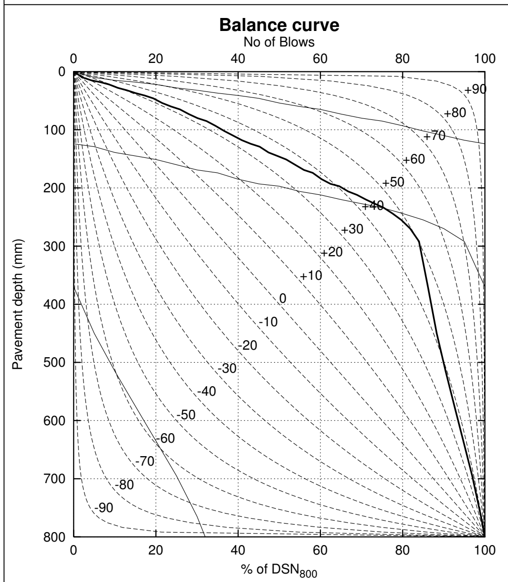

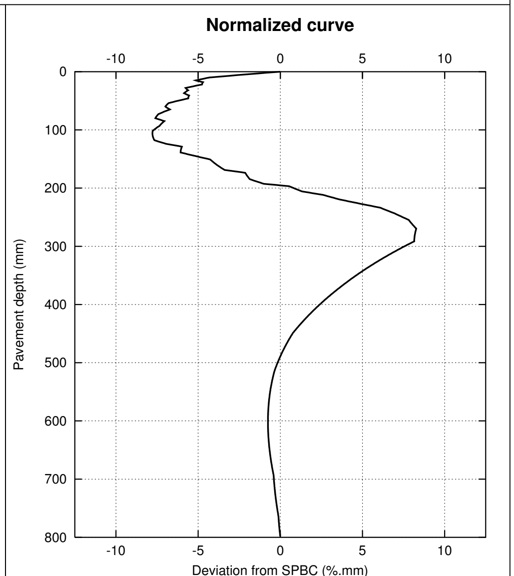

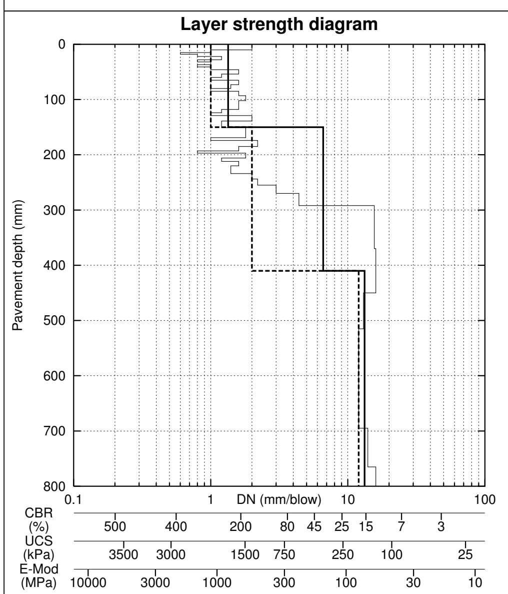

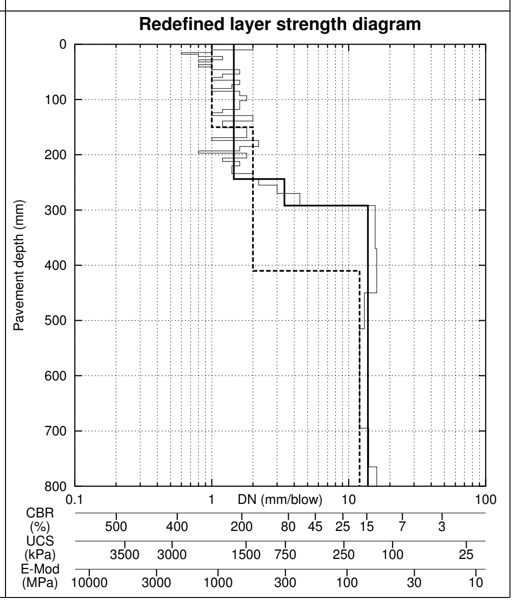

589RF#4 (Untrafficked)

DCP summary

Area : RFS
Road : MB Road Distance : 4.00 km
Structure Number (DSN_{800}) : 217
B = 43 A = 2798
Moisture : Moist
Position : Traffic
Base Type : Cemented
Category : 0
Test Date : 3/21/2007
Struct. Cap. (E80s) : 2.115×10^6
Category II: Averagely balanced shallow structure (ABS)

User defined layer summary

From-To (mm)	Avg.DN (mm/blow)	Std.Dev. (mm/blow)	CBR (%)	Range 5% - 95%	UCS (kPa)	Range 5% - 95%	E-Mod (MPa)	Range 5% - 95%
0-150	1.30	0.16	246	191- 307	1909	1524- 2319	842	619- 1162
150-410	7.44	5.86	32	5- 294	317	60- 2231	133	27- 1081
410-800	16.82	1.45	11	9- 15	127	101- 163	56	45- 70

Redefined layer summary

From-To (mm)	Avg.DN (mm/blow)	Std.Dev. (mm/blow)	CBR (%)	Range 5% - 95%	UCS (kPa)	Range 5% - 95%	E-Mod (MPa)	Range 5% - 95%
0-228	1.40	0.23	232	164- 315	1809	1331- 2366	780	517- 1208
228-280	3.84	0.95	74	36- 167	664	348- 1357	267	145- 527
280-800	16.51	1.94	12	8- 17	130	95- 182	57	42- 78

Balance curve

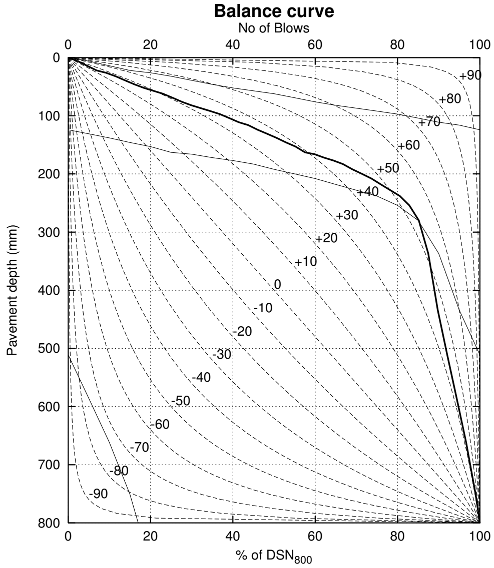

Normalized curve

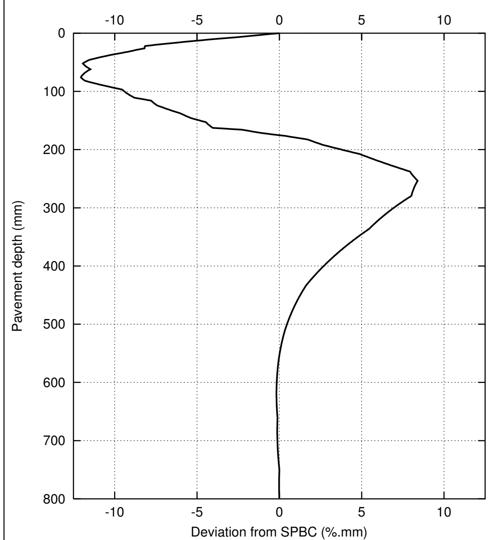

Layer strength diagram

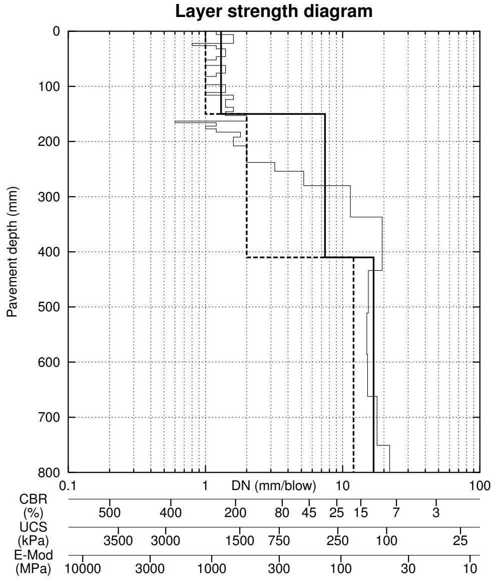

Redefined layer strength diagram

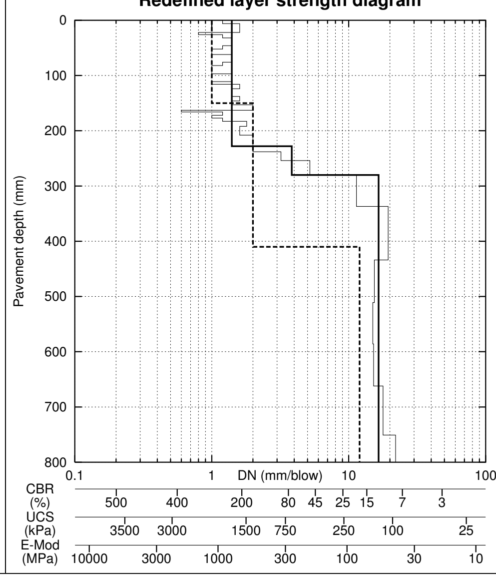

589RF#12 (Trafficked)

DCP summary

Area : RFS
Road : MB Road Distance : 12.00 km
Structure Number (DSN_{800}) : 175
B = 39 A = 3530

Moisture : Moist
Position : Section
Base Type : Cemented
Category VI: Poorly balanced deep structure (PBD)

Category : 0
Test Date : 3/21/2007
Struct. Cap. (E80s) : 0.991×10^6

User defined layer summary

From-To (mm)	Avg.DN (mm/blow)	Std.Dev. (mm/blow)	CBR (%)	Range 5% - 95%	UCS (kPa)	Range 5% - 95%	E-Mod (MPa)	Range 5% - 95%
0-150	1.86	0.24	180	126- 240	1449	1059- 1865	578	417- 814
150-410	7.81	6.18	30	4- 285	300	56- 2173	126	26- 1033
410-800	19.13	0.98	10	8- 11	110	96- 127	49	43- 56

Redefined layer summary

From-To (mm)	Avg.DN (mm/blow)	Std.Dev. (mm/blow)	CBR (%)	Range 5% - 95%	UCS (kPa)	Range 5% - 95%	E-Mod (MPa)	Range 5% - 95%
0-268	1.95	0.37	173	99- 264	1399	852- 2026	548	339- 921
268-800	18.16	2.02	10	7- 15	117	86- 161	51	39- 69

Balance curve

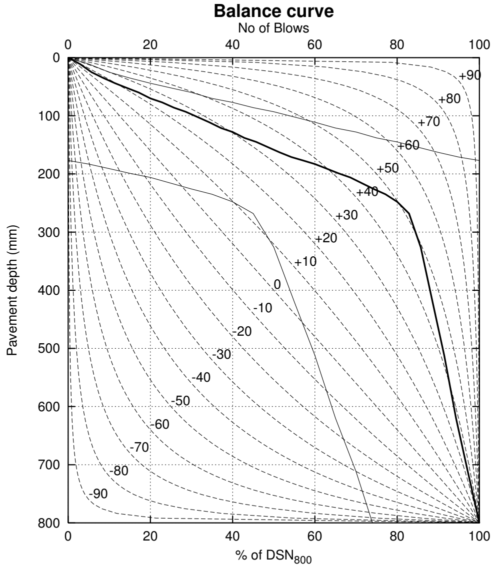

Normalized curve

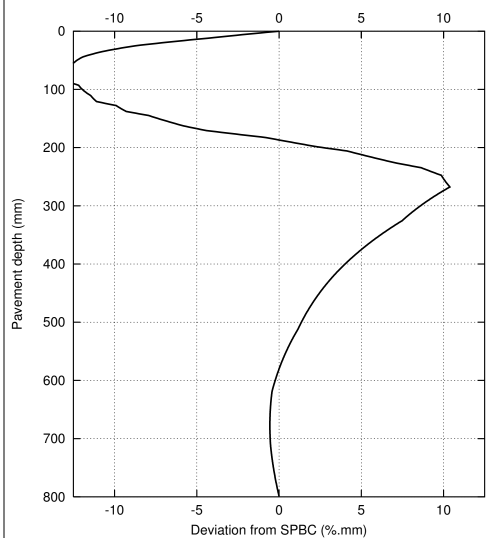

Layer strength diagram

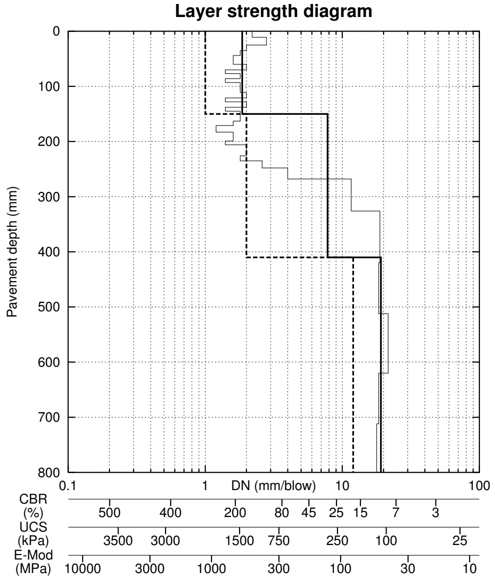

Redefined layer strength diagram

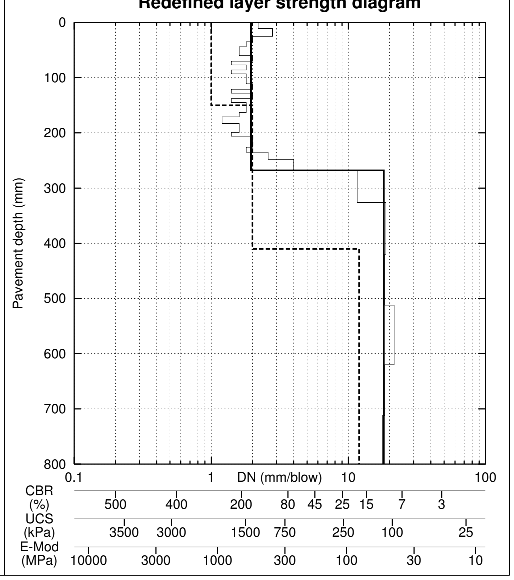

589RF#12 (Untrafficked)

DCP summary

Area : RFS
Road : MB Road Distance : 12.00 km
Structure Number (DSN_{800}) : 185
B = 47 A = 3140

Moisture : Moist
Position : Traffic
Base Type : Cemented
Category III: Poorly balanced shallow structure (PBS)

Category : 0
Test Date : 3/21/2007
Struct. Cap. (E80s) : 1.198×10^6

User defined layer summary

From-To (mm)	Avg.DN (mm/blow)	Std.Dev. (mm/blow)	CBR (%)	Range 5% - 95%	UCS (kPa)	Range 5% - 95%	E-Mod (MPa)	Range 5% - 95%
0-150	1.35	0.31	239	142- 353	1859	1173- 2618	810	459- 1509
150-410	11.18	8.21	19	3- 190	201	41- 1520	86	19- 617
410-800	24.27	0.91	7	6- 8	85	76- 94	38	34- 42

Redefined layer summary

From-To (mm)	Avg.DN (mm/blow)	Std.Dev. (mm/blow)	CBR (%)	Range 5% - 95%	UCS (kPa)	Range 5% - 95%	E-Mod (MPa)	Range 5% - 95%
0- 69	1.61	0.29	204	129- 297	1620	1083- 2249	672	425- 1097
69-112	0.88	0.10	325	268- 377	2432	2052- 2775	1278	940- 1764
112-194	1.67	0.17	198	157- 248	1577	1284- 1920	648	500- 849
194-254	4.13	0.59	68	44- 107	612	417- 918	247	172- 364
254-800	22.89	3.13	8	5- 12	90	62- 133	40	28- 58

Balance curve

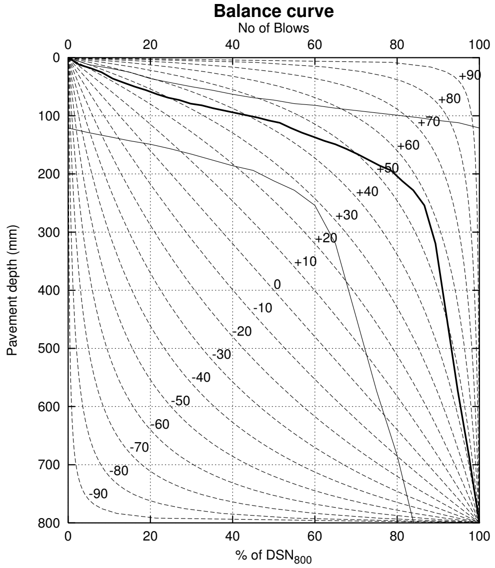

Normalized curve

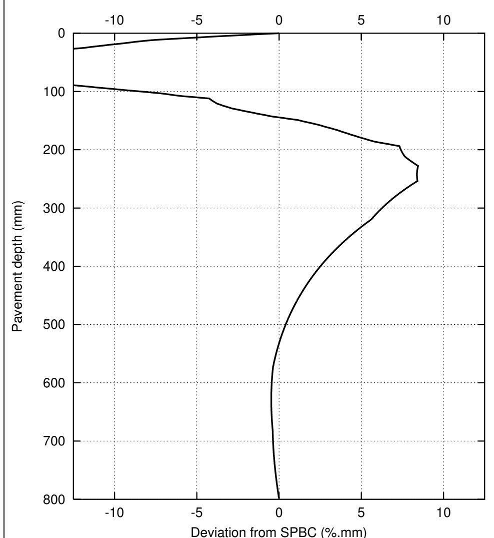

Layer strength diagram

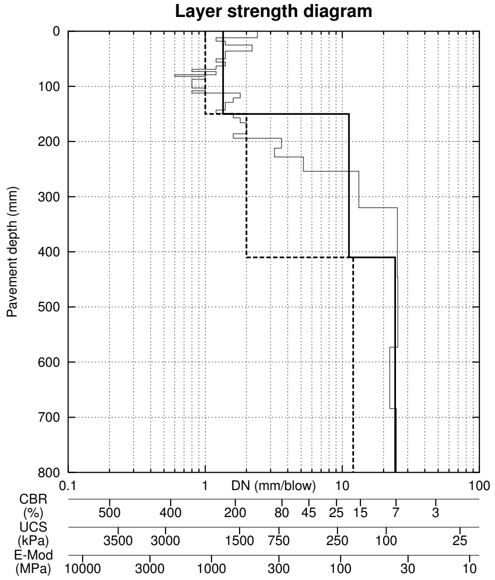

Redefined layer strength diagram

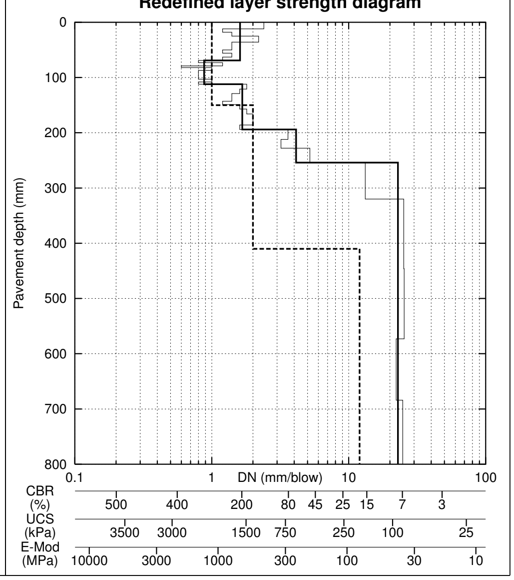

590RF#4 (Trafficked)

DCP summary

Area : RFS
Road : MB Road Distance : 4.00 km
Structure Number (DSN_{800}) : 153
B = 31 A = 3786

Moisture : Moist
Position : Section
Base Type : Cemented

Category : 0
Test Date : 3/21/2007
Struct. Cap. (E80s) : 0.625×10^6
Category VI: Poorly balanced deep structure (PBD)

User defined layer summary

From–To (mm)	Avg.DN (mm/blow)	Std.Dev. (mm/blow)	CBR (%)	Range 5% – 95%	UCS (kPa)	Range 5% – 95%	E-Mod (MPa)	Range 5% – 95%
0–150	1.91	0.48	177	86– 300	1423	757– 2267	563	303– 1114
150–410	10.96	4.61	20	6– 78	206	73– 695	88	33– 279
410–800	12.23	1.82	17	11– 28	182	122– 278	78	53– 117

Redefined layer summary

From–To (mm)	Avg.DN (mm/blow)	Std.Dev. (mm/blow)	CBR (%)	Range 5% – 95%	UCS (kPa)	Range 5% – 95%	E-Mod (MPa)	Range 5% – 95%
0– 64	2.59	0.21	123	95– 160	1032	824– 1303	407	328– 507
64–102	1.92	0.15	176	141– 209	1416	1166– 1649	559	456– 688
102–155	1.22	0.17	260	193– 332	2004	1540– 2482	906	628– 1335
155–204	3.57	0.83	81	41– 172	721	393– 1392	289	162– 544
204–560	14.42	1.25	14	11– 18	151	119– 193	66	52– 83
560–800	10.38	0.77	21	17– 27	219	178– 270	93	77– 114

Balance curve

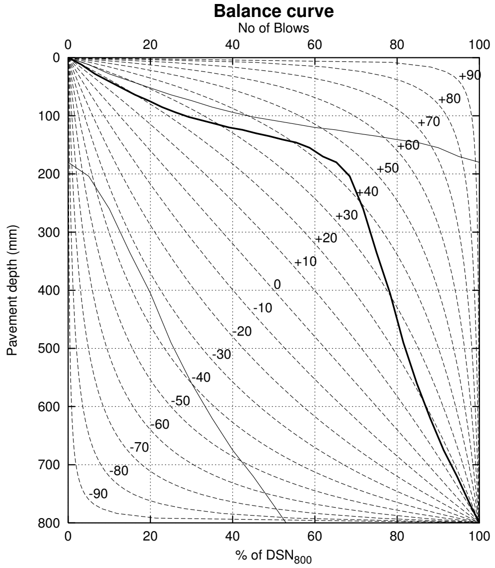

Normalized curve

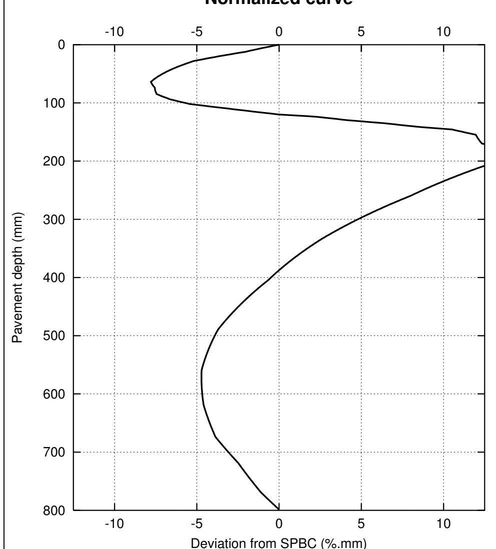

Layer strength diagram

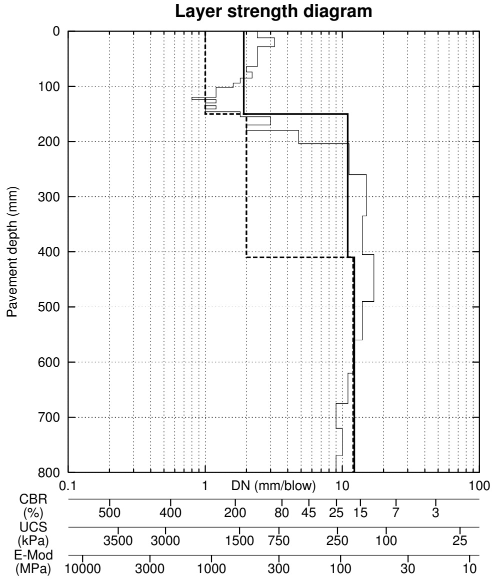

Redefined layer strength diagram

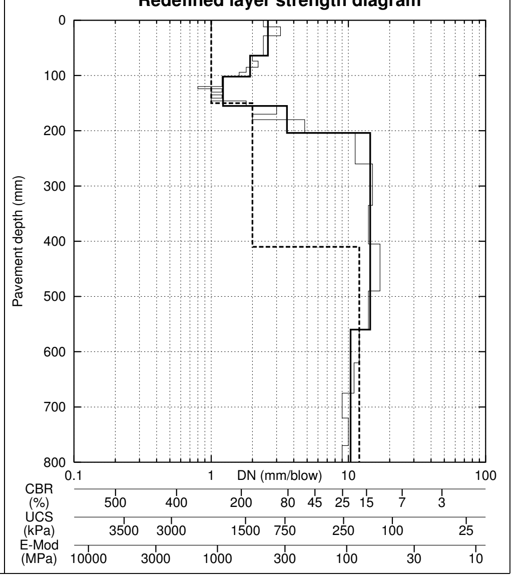

590RF#4 (Untrafficked)

DCP summary

Area : RFS
Road : MB Road Distance : 4.00 km
Structure Number (DSN_{800}) : 174
B = 39 A = 3327

Moisture : Moist
Position : Traffic
Base Type : Cemented

Category : 0
Test Date : 3/21/2007
Struct. Cap. (E80s) : 0.970×10^6

Category VI: Poorly balanced deep structure (PBD)

User defined layer summary

From-To (mm)	Avg.DN (mm/blow)	Std.Dev. (mm/blow)	CBR (%)	Range 5% - 95%	UCS (kPa)	Range 5% - 95%	E-Mod (MPa)	Range 5% - 95%
0-150	1.61	0.33	205	120- 311	1625	1017- 2345	674	401- 1187
150-410	10.51	6.86	21	4- 171	216	50- 1382	92	23- 538
410-800	15.18	1.58	13	9- 18	143	108- 192	62	47- 82

Redefined layer summary

From-To (mm)	Avg.DN (mm/blow)	Std.Dev. (mm/blow)	CBR (%)	Range 5% - 95%	UCS (kPa)	Range 5% - 95%	E-Mod (MPa)	Range 5% - 95%
0- 92	1.92	0.30	175	111- 250	1416	943- 1932	558	373- 857
92-161	1.17	0.12	268	216- 321	2056	1702- 2410	943	718- 1254
161-228	2.93	0.70	105	51- 209	900	480- 1649	357	196- 688
228-800	15.26	2.27	13	8- 21	142	95- 217	62	42- 92

Balance curve

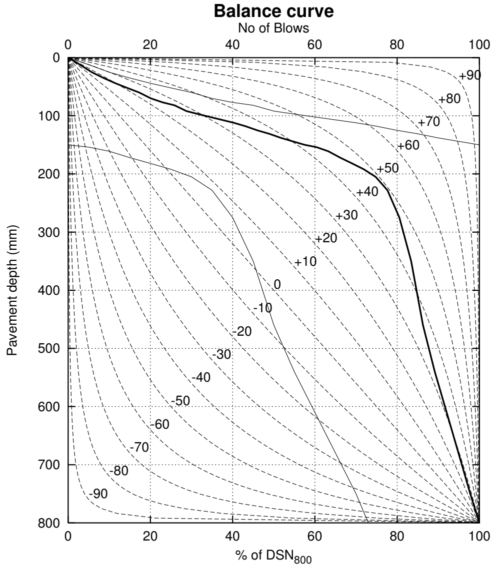

Normalized curve

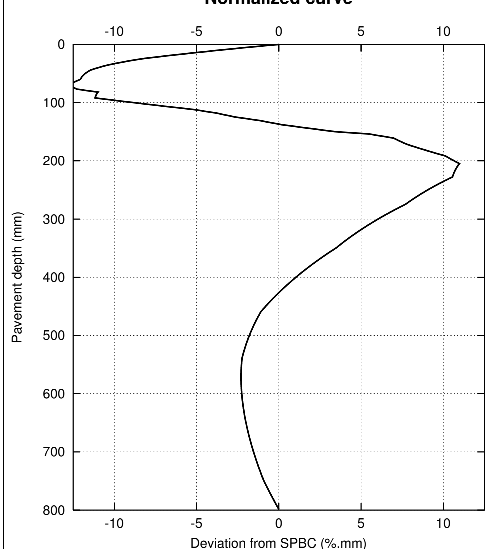

Layer strength diagram

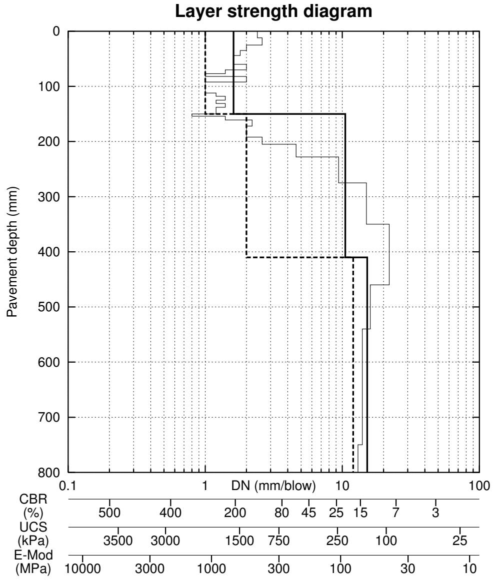

Redefined layer strength diagram

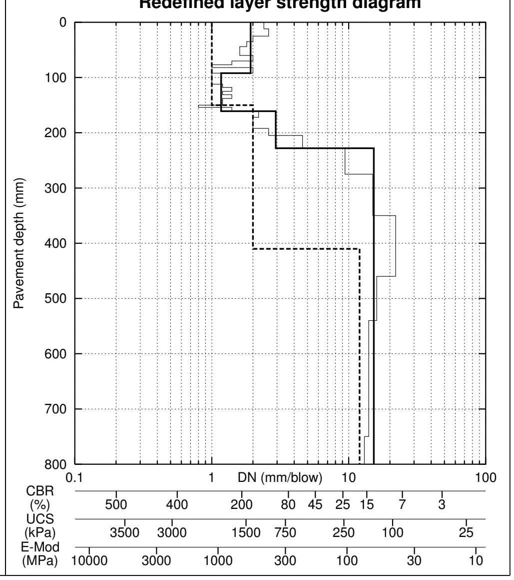

590RF#12 (Trafficked)

DCP summary

Area : RFS
Road : MB Road Distance : 12.00 km
Structure Number (DSN_{800}) : 153
B = 30 A = 3471

Moisture : Moist Category : 0
Position : Section Test Date : 3/21/2007
Base Type : Cemented Struct. Cap. (E80s) : $0.618x10^6$
Category VI: Poorly balanced deep structure (PBD)

User defined layer summary

From-To (mm)	Avg.DN (mm/blow)	Std.Dev. (mm/blow)	CBR (%)	Range 5% - 95%	UCS (kPa)	Range 5% - 95%	E-Mod (MPa)	Range 5% - 95%
0-150	2.00	0.34	170	102- 247	1378	880- 1914	535	349- 846
150-410	10.84	5.87	20	5- 117	208	58- 988	89	27- 390
410-800	12.23	2.50	17	9- 33	182	106- 327	78	47- 137

Redefined layer summary

From-To (mm)	Avg.DN (mm/blow)	Std.Dev. (mm/blow)	CBR (%)	Range 5% - 95%	UCS (kPa)	Range 5% - 95%	E-Mod (MPa)	Range 5% - 95%
0-190	2.01	0.38	169	96- 256	1368	830- 1975	531	331- 886
190-800	12.53	2.84	17	8- 35	177	97- 340	76	43- 142

Balance curve

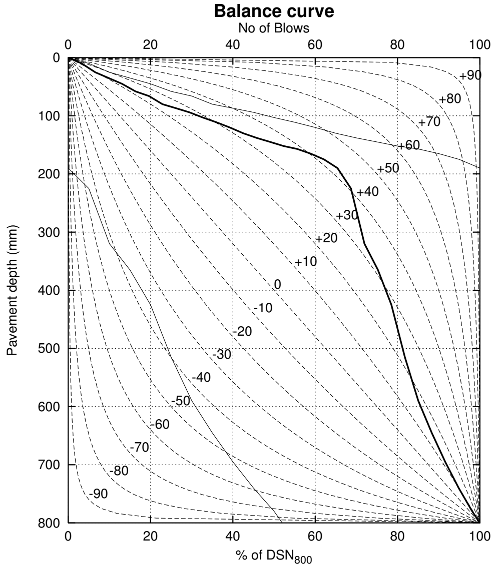

Normalized curve

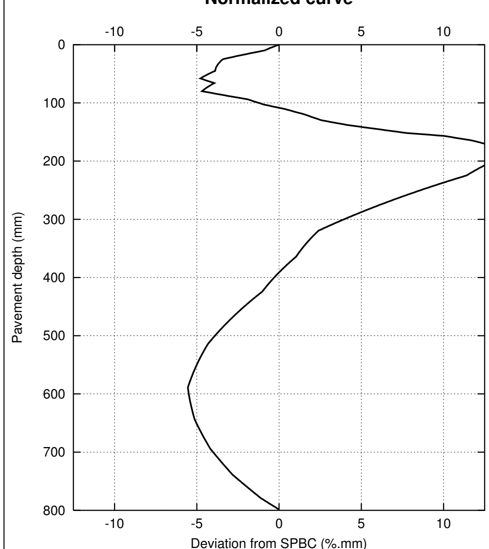

Layer strength diagram

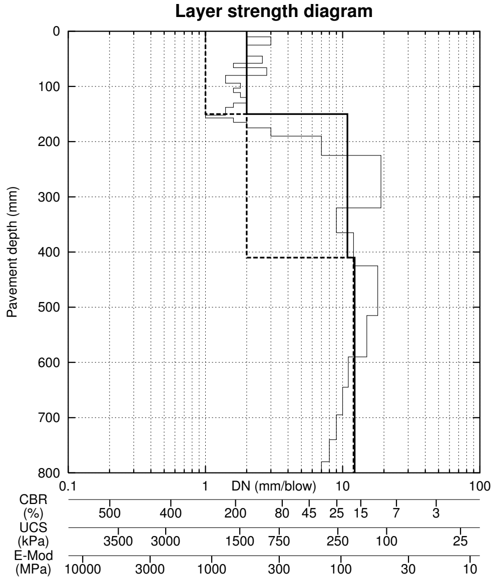

Redefined layer strength diagram

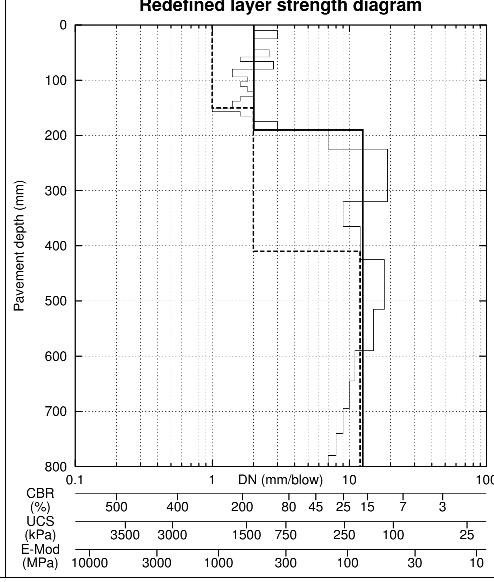

590RF#12 (Untrafficked)

DCP summary

Area : RFS
Road : MB Road **Distance** : 12.00 km
Structure Number (DSN_{800}) : 220
B = 47 **A** = 3362

Moisture : Moist
Position : Traffic
Base Type : Cemented

Category : 0
Test Date : 3/21/2007
Struct. Cap. (E80s) : 2.196×10^6

Category III: Poorly balanced shallow structure (PBS)

User defined layer summary

From-To (mm)	Avg.DN (mm/blow)	Std.Dev. (mm/blow)	CBR (%)	Range 5% - 95%	UCS (kPa)	Range 5% - 95%	E-Mod (MPa)	Range 5% - 95%
0-150	1.10	0.34	281	146- 417	2140	1206- 3034	1007	471- 2372
150-410	12.81	7.61	16	3- 111	173	44- 947	74	20- 375
410-800	17.95	3.12	10	6- 18	119	75- 195	52	33- 83

Redefined layer summary

From-To (mm)	Avg.DN (mm/blow)	Std.Dev. (mm/blow)	CBR (%)	Range 5% - 95%	UCS (kPa)	Range 5% - 95%	E-Mod (MPa)	Range 5% - 95%
0- 35	1.84	0.33	181	110- 269	1458	936- 2062	582	370- 947
35-150	0.92	0.23	317	201- 420	2380	1596- 3049	1222	659- 2418
150-210	2.56	0.51	124	68- 214	1046	618- 1683	412	250- 707
210-800	17.72	2.71	11	7- 18	120	80- 186	53	36- 80

Balance curve

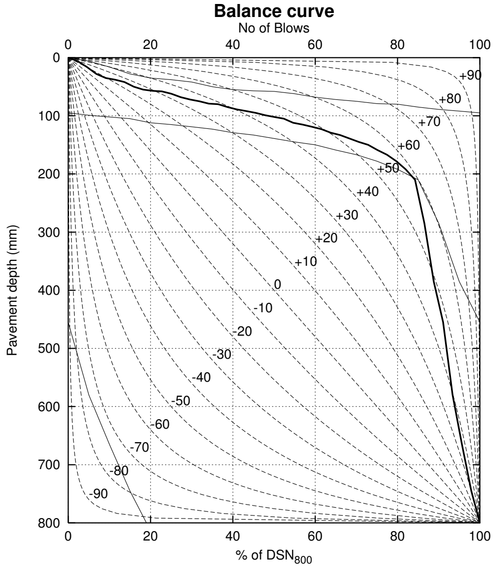

Normalized curve

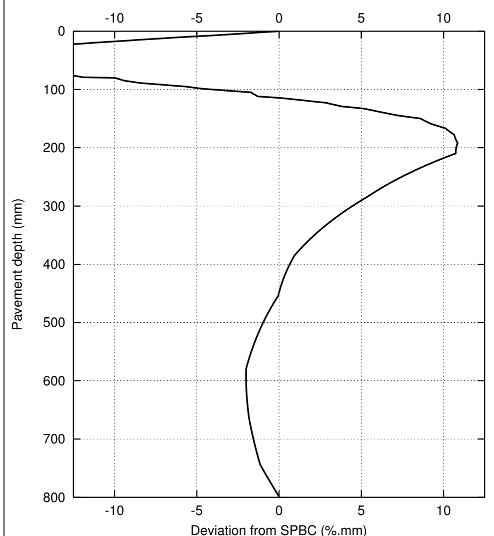

Layer strength diagram

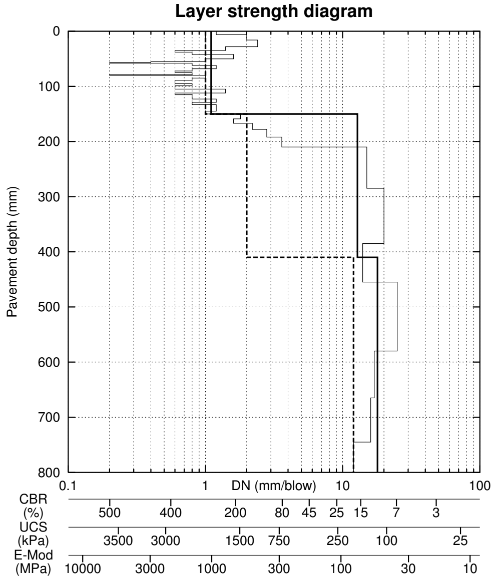

Redefined layer strength diagram

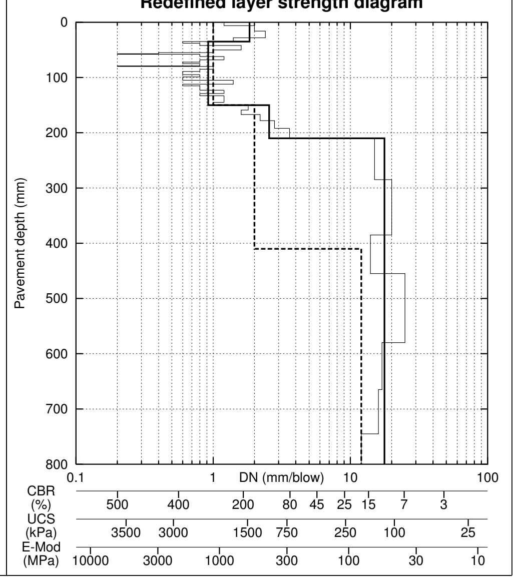

591RF#4 (Trafficked)

DCP summary

Area : RFS
Road : MB Road Distance : 4.00 km
Structure Number (DSN_{800}) : 178
B = 47 A = 3997

Moisture : Optimum
Position : Section
Base Type : Cemented
Category III: Poorly balanced shallow structure (PBS)

Category : 0
Test Date : 7/4/2007
Struct. Cap. (E80s) : $2.276x10^6$

User defined layer summary

From-To (mm)	Avg.DN (mm/blow)	Std.Dev. (mm/blow)	CBR (%)	Range 5% - 95%	UCS (kPa)	Range 5% - 95%	E-Mod (MPa)	Range 5% - 95%
0-150	1.52	0.32	216	129- 323	1701	1081- 2422	717	425- 1266
150-410	10.78	8.33	20	3- 212	209	40- 1673	89	19- 701
410-800	29.12	4.59	6	4- 9	69	45- 108	31	21- 48

Redefined layer summary

From-To (mm)	Avg.DN (mm/blow)	Std.Dev. (mm/blow)	CBR (%)	Range 5% - 95%	UCS (kPa)	Range 5% - 95%	E-Mod (MPa)	Range 5% - 95%
0-191	1.47	0.32	222	131- 332	1740	1093- 2483	739	429- 1336
191-244	4.01	1.12	70	31- 173	632	307- 1400	255	129- 549
244-524	18.78	1.13	10	8- 12	113	96- 133	50	42- 58
524-800	33.09	2.61	5	4- 6	60	48- 75	27	22- 34

Balance curve

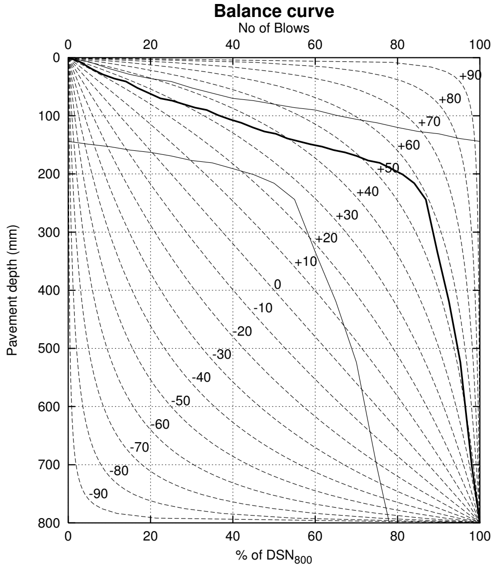

Normalized curve

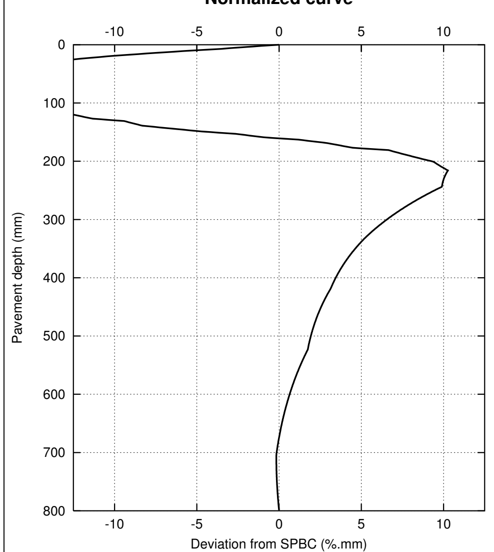

Layer strength diagram

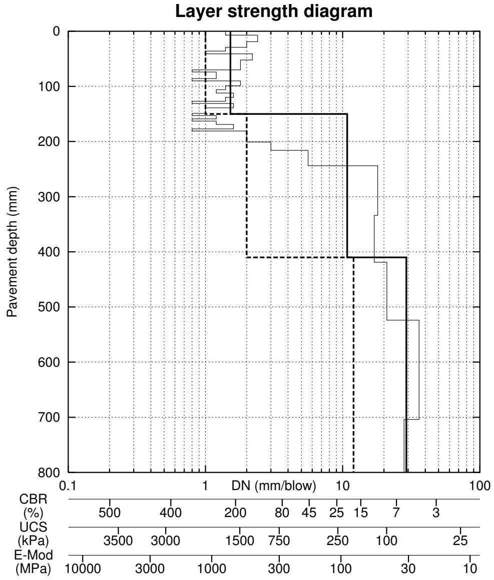

Redefined layer strength diagram

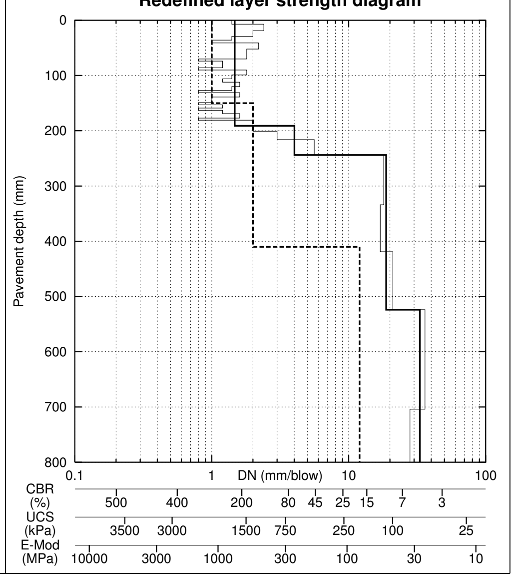

591RF#4 (Untrafficked)

DCP summary

Area : RFS
Road : MB Road Distance : 4.00 km
Structure Number (DSN_{800}) : 234
B = 46 A = 3616

Moisture : Optimum
Position : Traffic
Base Type : Cemented

Category : 0
Test Date : side
Struct. Cap. (E80s) : $5.896x10^6$

Category III: Poorly balanced shallow structure (PBS)

User defined layer summary

From-To (mm)	Avg.DN (mm/blow)	Std.Dev. (mm/blow)	CBR (%)	Range 5% - 95%	UCS (kPa)	Range 5% - 95%	E-Mod (MPa)	Range 5% - 95%
0-150	0.97	0.27	306	180- 423	2308	1449- 3071	1152	578- 2488
150-410	14.99	8.57	13	3- 85	145	39- 748	63	18- 299
410-800	14.62	3.04	14	7- 27	149	86- 271	65	38- 114

Redefined layer summary

From-To (mm)	Avg.DN (mm/blow)	Std.Dev. (mm/blow)	CBR (%)	Range 5% - 95%	UCS (kPa)	Range 5% - 95%	E-Mod (MPa)	Range 5% - 95%
0- 42	1.27	0.24	251	170- 345	1941	1380- 2567	863	537- 1440
42-137	0.76	0.15	351	260- 426	2603	2000- 3091	1489	903- 2556
137-215	3.20	0.96	94	39- 222	816	377- 1743	325	156- 741
215-620	19.45	1.40	9	8- 12	108	89- 133	48	40- 58
620-800	10.65	1.06	20	15- 28	212	162- 281	91	70- 118

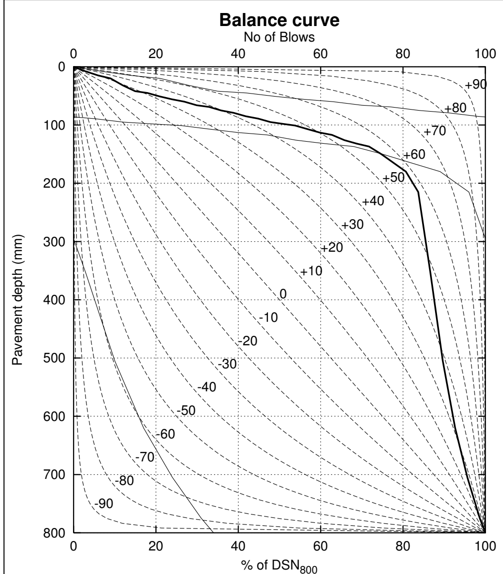

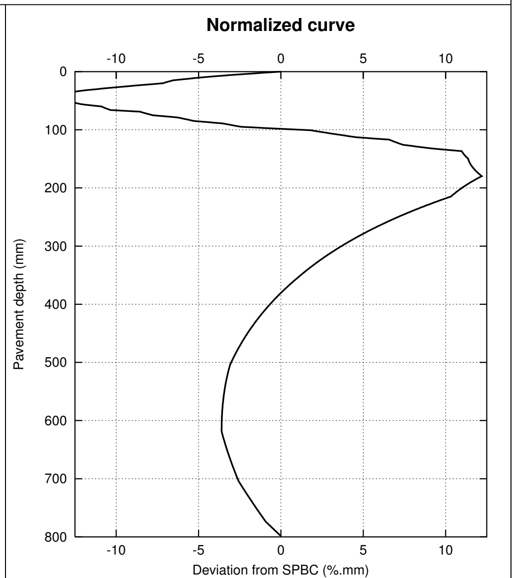

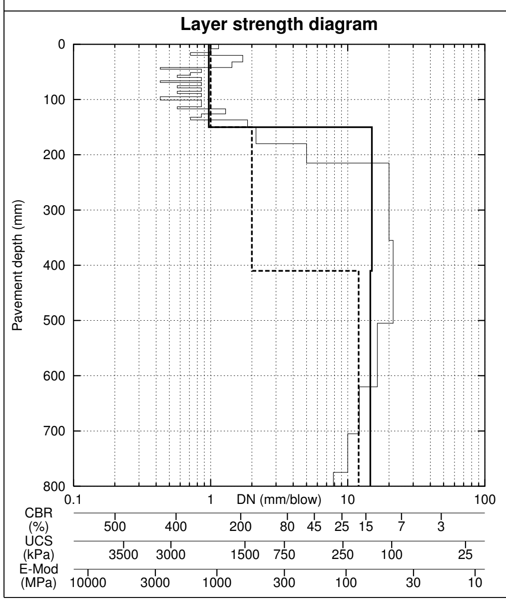

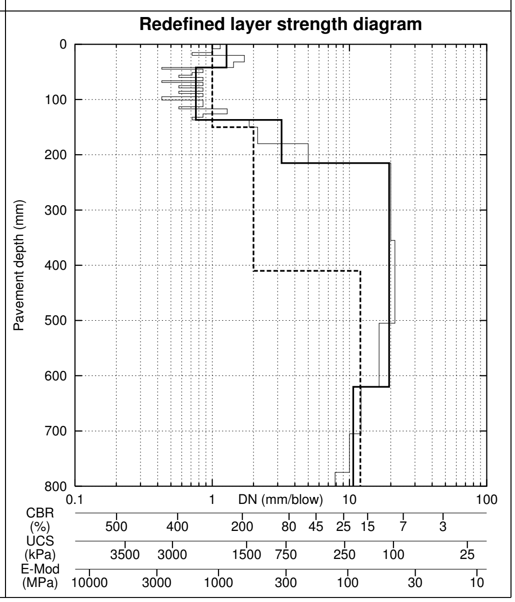

591RF#12 (Trafficked)

DCP summary

Area : RFS
Road : MB Road   Distance : 12.00 km
Structure Number (DSN_{800}) : 169
B = 43   A = 4272

Moisture : Optimum
Position : Section
Base Type : Cemented

Category : 0
Test Date : 7/4/2007
Struct. Cap. (E80s) : $1.882x10^6$

Category III: Poorly balanced shallow structure (PBS)

User defined layer summary

From-To (mm)	Avg.DN (mm/blow)	Std.Dev. (mm/blow)	CBR (%)	Range 5% - 95%	UCS (kPa)	Range 5% - 95%	E-Mod (MPa)	Range 5% - 95%
0-150	1.78	0.31	187	116- 273	1497	984- 2092	604	388- 970
150-410	8.58	6.35	27	4- 243	270	55- 1884	114	25- 826
410-800	26.56	3.45	6	4- 10	76	54- 111	34	25- 49

Redefined layer summary

From-To (mm)	Avg.DN (mm/blow)	Std.Dev. (mm/blow)	CBR (%)	Range 5% - 95%	UCS (kPa)	Range 5% - 95%	E-Mod (MPa)	Range 5% - 95%
0-270	2.21	0.76	149	56- 318	1229	515- 2390	480	210- 1233
270-800	23.46	4.48	7	4- 14	88	53- 152	39	24- 66

Balance curve

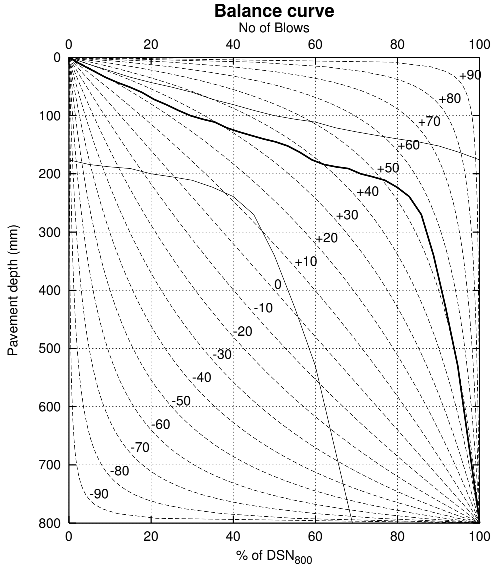

Normalized curve

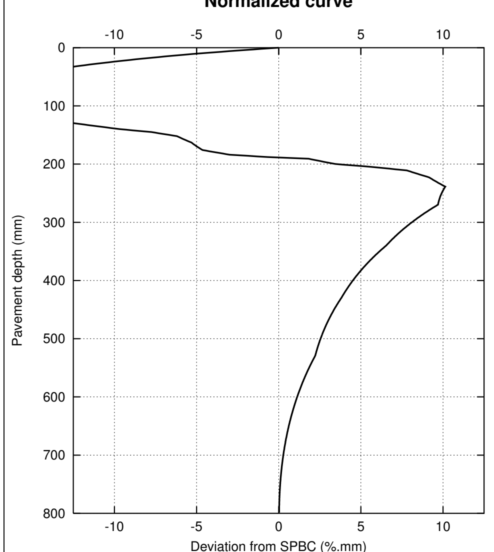

Layer strength diagram

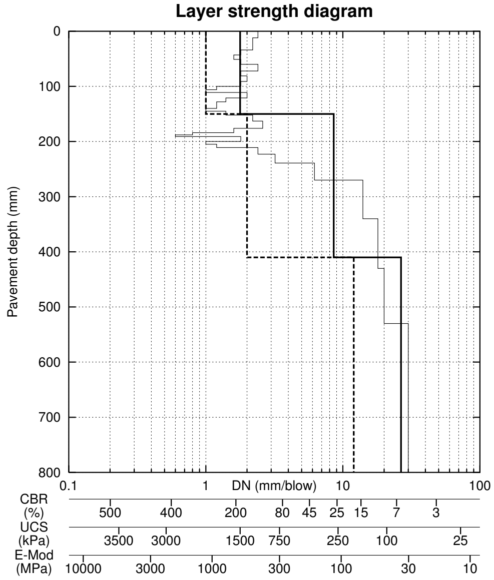

Redefined layer strength diagram

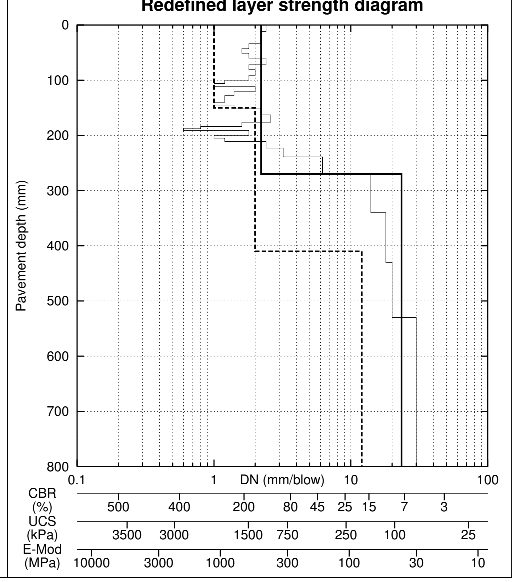

591RF#12 (Untrafficked)

DCP summary

Area : RFS
Road : MB Road Distance : 12.00 km
Structure Number (DSN_{800}) : 183
B = 48 A = 4144

Moisture : Optimum
Position : Caravan
Base Type : Cemented

Category : 0
Test Date : 7/4/2007
Struct. Cap. (E80s) : 2.499×10^6

Category III: Poorly balanced shallow structure (PBS)

User defined layer summary

From-To (mm)	Avg.DN (mm/blow)	Std.Dev. (mm/blow)	CBR (%)	Range 5% - 95%	UCS (kPa)	Range 5% - 95%	E-Mod (MPa)	Range 5% - 95%
0-150	1.60	0.34	206	118- 316	1629	1000- 2376	677	395- 1218
150-410	11.85	10.97	18	2- 260	189	30- 2001	81	14- 903
410-800	31.80	2.47	5	4- 7	63	51- 78	28	23- 35

Redefined layer summary

From-To (mm)	Avg.DN (mm/blow)	Std.Dev. (mm/blow)	CBR (%)	Range 5% - 95%	UCS (kPa)	Range 5% - 95%	E-Mod (MPa)	Range 5% - 95%
0-198	1.49	0.38	220	117- 347	1727	992- 2583	732	392- 1461
198-275	5.84	1.64	44	19- 110	416	201- 939	171	86- 371
275-800	29.45	3.54	6	4- 8	68	49- 96	31	23- 43

Balance curve

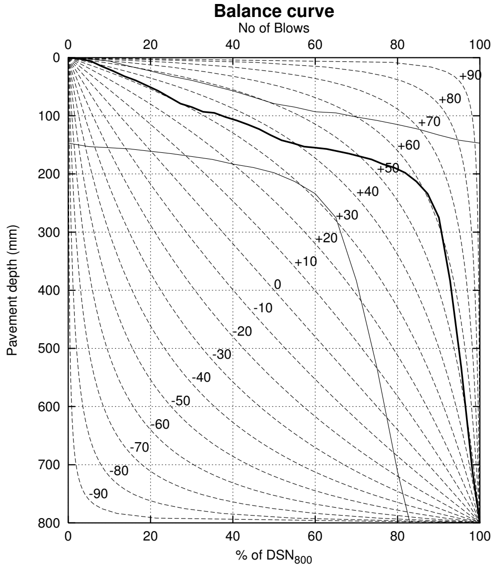

Normalized curve

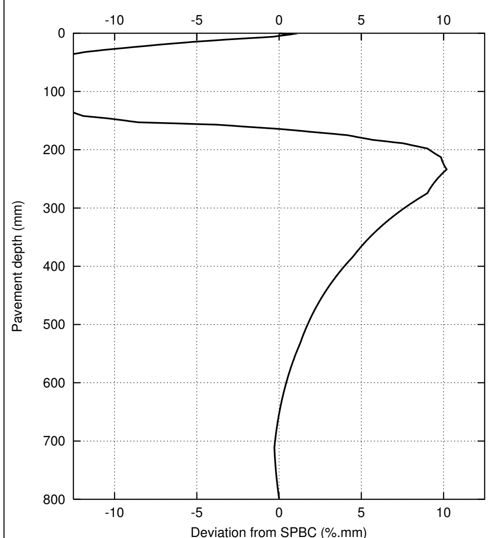

Layer strength diagram

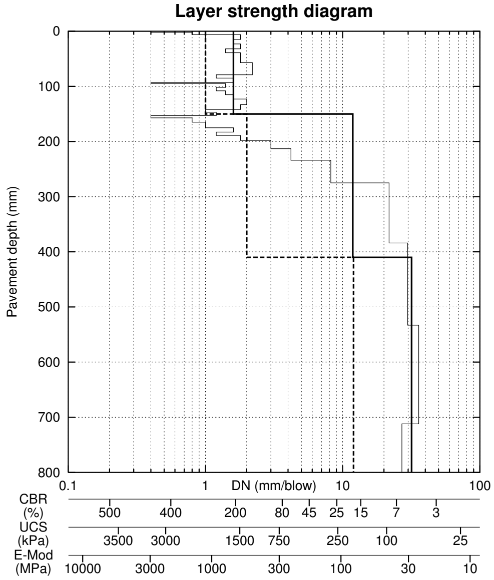

Redefined layer strength diagram